Aalborg Universitet

Turbulent Boyant Jets and Plumes in Flowing Ambient Environments

Chen, Hai-Bo

Publication date:
1991

Document Version
Publisher's PDF, also known as Version of record

[Link to publication from Aalborg University](#)

Department of Civil Engineering
University of Aalborg, Denmark
August 1991

TURBULENT BUOYANT JETS AND PLUMES IN FLOWING AMBIENT ENVIRONMENTS

Hai-Bo Chen

TURBULENT BUOYANT JETS AND PLUMES IN FLOWING AMBIENT ENVIRONMENTS

by

Hai-Bo Chen

August 1991

TURBULENT BUOYANT JETS AND PLUMES IN FLOWING AMBIENT ENVIRONMENTS

Hai-Bo Chen

Department of Civil Engineering
University of Aalborg, Denmark
August 1991

PREFACE

This thesis is to be submitted to the Department of Civil Engineering, the University of Aalborg, Denmark, in partial fulfilment of the requirements for the Ph.D. degree, according to the notice of February 18, 1981 from the Danish Ministry of Education.

Associate Professor Torben Larsen has acted as the supervisor during the study, which was carried out at the Departmet of Civil Engineering, the University of Aalborg. The author greatefully acknowledges for his excellent guidance and stimulating encouragement. Assistant Professor Ole Petersen has acted as the co-supervisor, his great helps and benificial discussions are highly appreciated. Dr. Jacob S. Møller from the Danish Hydraulic Institute acted as the external examiner, his constructive comments on the thesis are greatly acknowledged.

The author's thanks are due to Mr. Jørgen S. Sørensen and Mr. Werner Nielsen, the technicians, in the hydraulic laboratory at the University of Aalborg for their assistance during the laboratory experiments. Meanwhile, special gratitude goes to Ms. Birte Torstveit, the secretary in the hydraulics group, for her kindness and help during the study and to Ms. Lizzi Levin and Miss Marianne Jensen for their high quality drawings.

In addition, the author wishes to express his deep gratitude to Mr. Hans Schrøder, Mr. Tue Kell Nielsen and Mr. Poul Kronborg for their good advices and thoughtfull kindness when he was studying at the Danish Hydraulic Institute (October,1987 - October,1988) as a visiting fellow.

Aalborg, August, 1991

Hai-Bo Chen

SUMMARY

Turbulent buoyant jets and plumes in flowing ambient environments have been studied theoretically and experimentally.

The mechanics of turbulent buoyant jets and plumes in flowing ambients have been discussed. Dimensional analysis was employed to investigate the mean behavior of the turbulent buoyant jets and plumes, such as the jet trajectories and the dilutions. The basic physical processes for a submerged turbulent buoyant jet released from sea outfall have been outlined and divided into four primary stages, namely, the zone of flow establishment, the stage of jet, the stage of intermediate and the stage of plume. The stability criteria for the upstream wedge created by the submerged turbulent buoyant jet were established by applying the Bernoulli equations for a two-dimensional problem and by considering the front velocity driven by the buoyancy force for a three-dimensional problem.

Comprehensive laboratory experiments were conducted to study the mean behavior of turbulent buoyant jets and plumes in a flowing ambient by using both fresh and salt receiving waters. The experimental data on the jet trajectories and dilutions, for a horizontal jet in a coflowing ambient and for a vertical jet in a crossflowing environment, have been presented and successfully correlated using momentum and buoyancy fluxes and length scales. The analysis demonstrates that the experimental data on the jet trajectories and dilutions can be well correlated using the momentum or buoyancy fluxes and length scales, depending upon the types and regimes of the flows. The stability condition was verified using the experimental data and the flow regimes were categorized into three types regarding the formation of the upstream wedge, i.e. stable upstream wedge, unstable upstream wedge and no upstream wedge. In addition, the available field observed data on the initial dilutions for a horizontal jet issuing into a perpendicular crossflowing ambient have been presented and discussed.

Mathematical modelling of the turbulent buoyant jets and plumes has been carried out by using both an integral model and a turbulence model. The integral model was developed on the basis of the volume control method (for jets with two-dimensional trajectories) and the differential method (for jets with three-dimensional trajectories). The turbulence model adopted here was the $k - \varepsilon$ model based on Launder and Spalding. The mathematical models were used to predict the turbulent buoyant jets and plumes in flowing ambients. The predictions by the integral model and the turbulence model have been presented and compared with the available experimental data. The comparisons show good agreement between the model predictions and the laboratory measurements.

RESUME

Denne rapport omhandler fortynding i lette, turbulente stråler og faner i strømmende recipienter, som de ofte forekommer i forbindelse med udløbsledninger.

Med udgangspunkt i de styrende fysiske processer er fortyndingsprocessen inddelt i fire zoner : en initialzone, strålen, en overgangszone samt fanen. På baggrund af de grundlæggende fysiske love og dimensionsanalyser er der opstillet sammenhænge der belyser blandt andet strålebaner og fortynding. For overgangszonen er betingelserne for dannelsen af en opstrøms kile belyst.

De teoretiske analyser er understøttet af eksperimenter udført i laboratoriet, hvor fortyndingen i vandrette stråler med udløb i vand der strømmer parallelt med strålen er undersøgt. De opstillede betingelser for dannelse af en opstrøms kile er undersøgt i modelforsøgene. Disse er beskrevet ved hjælp af tre regimer : en stabil kile, en ustabil kile samt ingen opstrøms kile.

Der er endvidere lavet en omfattende gennemgang af litteraturen, hvor data fra både laboratorieforsøg og feltmålinger er inddraget i analysen.

Der er opstillet to typer numeriske modeller for fortyndingen. En en-dimensional integralmodel der ud fra bevarelse af masse og bevægelsesmængde, samt en medrivnings hypotese kan beskrive fortyndingen i idealiserede tilfælde. Der er endvidere anvendt en mere avanceret tredimensional $k - \varepsilon$ turbulensmodel der ud over bevarelse af masse og bevægelsesmængde i en lokal beskrivelse medtager massebalancer for den turbulente energi. Resultater fra begge modeller er sammenlignet med forsøgene.

Contents

Chapter 1

Introduction

1.1 Statement of the Problem

As the development of industrialization and urbanization, the releasing of pollutants into atomosphere and hydrosphere has become unfortunately inevitable. For example, industrial waste gas into atomosphere and waste water and pollutants into hydrosphere from industrial, agricultural and domestic sources.

The traditional means of discharging waste water is to release it at some depth below the surface and to some distance from the shore into large receiving water by a pipeline with single or multiport diffusers as seen in Fig.1.1.

Practically the waste gas is released through a chimney into the atomosphere as shown in Fig. 1.2.

The discharging of pollutants by sea outfall and chimney often leads to the formation of turbulent buoyant jets and plumes because of the fact that the sewage effluent and the waste gas are usually lighter than the receiving medium and with initial momentum and buoyancy.

Reliable knowlege on the consequence of releasing pollutants into the environment is indispensably needed concerning the environmental protection act on air and water quality standards and the optiminzation of discharging engineering system design. In other words, the spreading and mixing mechanics of the released pollutants should be predictable and the ecological consequences of discharging various pollutants into the environments should be assessable.
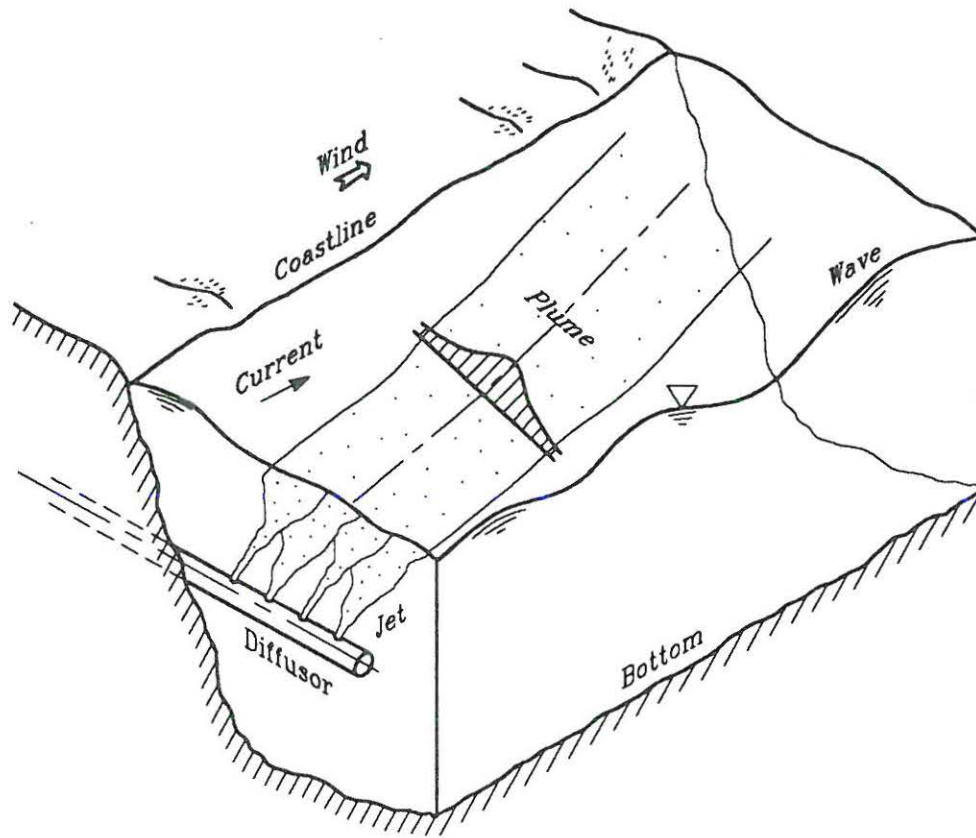
Figure 1.1: Example of Sea Outfall Practice
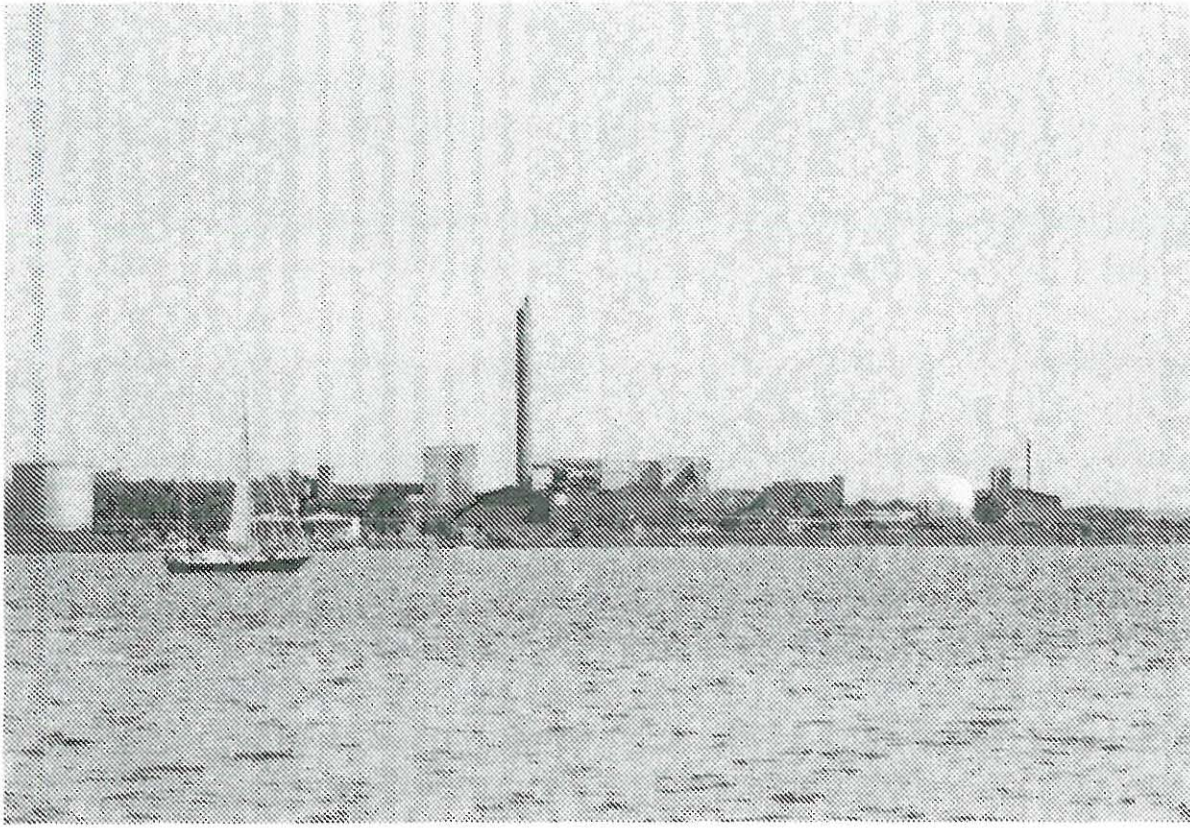
Figure 1.2: Example of Waste Gase Released from Chimney (Photo from Aalborg Harbour, Aalborg, Denmark)

1.2 Previous Studies

The problem of turbulent buoyant jets and plumes has been studied intensively since the early 1930's, both experimentally and theoretically.

The first systematic study was conducted by Rawn and Palmer (1930) from a raft carrying a fresh water tank and a vertical boom holding the nozzle at varying depth in the Los Angeles Harbor. An empirical formula was developed without using dimensional analysis and hydraulic similitude, and widely used for almost thirty years. The data were later reanalyzed using dimensionless parameters by Rawn, Bowerman and Brooks (1961).

Laboratory experiments on a simple momentum jet in a stagnant ambient fluid was carried out by Albertson, Dai, Jensen and Rouse (1950). The experimental results demonstrated that the velocity profiles were self-similar and held a Gaussian distribution after the zone of flow establishment. The length of the zone of flow establishment is approximately equal to 6.2 times of the initial jet nozzle diameter. The width of the jet and the gross volume flux were expended and increased both linearly with the distance.

In 1956, Morton, Taylor and Turner published their classic paper on the integral technique for solving buoyant plume problems in stratified environment and the well-known entrainment coefficent was firstly introduced. After that, the fluid mechanics of buoyant jets and plumes was investigated and the technique of the integral solution was elaborated on by different investigators for various cases in terms of jet parameters, geometrical factors and environment conditions.

A study of buoyant jets issuing vertically and horizontally into homogeneous ambient fluid was conducted by Abraham (1963). A new idear of entrainment hypothesis was presented and a set of diagrams for predicting the jet pathes and dilutions was provided, based on the theory of

integral analysis.

Fan (1967) studied the problem of turbulent buoyant jets on an in-clined round buoyant jet in a stagnant environmental fluid with linear density stratification and a circular vertical buoyant jet in a uniform cross-stream of homogenous density. The main contributions made by Fan were that firstly, the Morton, Talor and Turner's integral analysis was extented to cover the effect of initial angle of discharging. Secodly, an entrainment hypothesis based on the vector difference between the characteristic jet velocity and the ambient velocity was made. Thirdly, a gross drag force term was proposed to compensate the effect of the unbalance pressure term on the sides of the jet caused by the ambient current regarding the jet as a rigid body. Finally comprehensive laboratory experiments with sinking jets which are directly analogous to buoyant jets were performed.

All of the above mentioned integral models are developed on the basis of the volume control method by applying the principle of conservation of mass, concentration, density deficiency and momentum to a finite control volume, and obtain a set of equations which can be integrated and subsequently solved numerically. In contrast to the volume control method, a differential method based on the basic three-dimensional differential equations of fluid mechanics, to be integrated with the aid of some assumptions, was used by Hirst (1972), derivating the integral model to predict buoyant jets in flowing ambients with three-dimensional trajectories. In addition, an entrainment function including the effects of internal turbulence, buoyancy, jet orientation and cross flow was postulated.

A comprehensive experimental study on the mean behavior of buoyant jets in a crossflow was carried out by Wright (1977). The laboratory experimental data on trajectories and dilutions were successfully correlated by using momentum and buoyancy length scales. The experimental evidence reveals the fact that the jet trajectories and dilutions follow dif-

11

ferent power law relations, depending upon the magnitude of the ratio of momentum length scale and buoyancy length scale and the flow regimes.

Schatzmann (1978) published his paper on the integral equations for round buoyant jets in stratified crossflows using the differential method. Comparison of the derivated governing integral equations was made. Mathematical and methodological errors made by previous reserchers were pointed out.

The experimental data reported by Fan on buoyant jets in a crossflow were well correlated and presented in a simple manner by Chu (1979) using a set of dimensionless variables suggested by a line impulse model. The idear of the line impulse model was originally introducted by Priestly (1956) and Scorer (1958).

Available field observated data on initial dilutions of submerged horizontal round jets in perpendicular crossflow were interpreted using dimensionless length scales by Lee and Nevill-Jones (1987). The flow types were classified into momentum dominated and buoyancy dominated depending on the ratio of the momentum length scale and the buoyancy length scale greater or less than one. In addition, a correlation for the downstream location of the minimum dilution was given.

A numbers of review papers on the studies of turbulent buoyant jets and plumes has been published, for example, Fisher et al (1979), Chen and Rodi (1980), Jirka (1982) and List (1982).

As the development of turbulence models it becomes increasingly popular to use the turbulence model to predict the problem of turbulent buoyant jets, for examples,the buoyant jet into a stratified turbulent flows was predicted using turbulence model by Chen and Rodi(1975). McGuirk and Spalding (1975), using a standard $k - \varepsilon$ model, successfully predicted a three-dimensional thermal discharge.

1.3 Objective of the Study

Although the problems of turbulent buoyant jets and plumes have been studied for several decades, it still remains much work to be done. Firstly, the previous studies mostly focused on the buoyant jets and plumes in a stagnant ambient fluid. Since the ocean, like the atmosphere is seldom motionless. The effects of the ambient current on the behavior of jets and plumes, such as the mechanics of mixing, trajectory, width, drag force and ambient turbulence, are needed to be further understood. Secondly, not much effort has been devoted to the stage of intermediate located between the buoyant jet and the plume concerning the stability of the upstream wedge, the initial height and width of the plume and the dilution within the intermediate zone. Thirdly, the mathematical modelling of the turbulent buoyant jets and plume are remained to be further improved and verified, for example, the hypothesis of entrainment in a moving ambient, the pressure unbalance caused by the ambient current and the non-axisymmetrical distribution of the jet cross-section.

The objective of the present study is to investigate the turbulent buoyant jets and plumes in flowing ambient fluids, including both laboratory experiments and numerical modelling, in order to try to develop a more complete understanding of the foundemantal mechanics of the problem and to provide more reliable theoretical knowlege and practical tool for the purpose of engineering design and environment assessment. Specifically, the laboratory experiment is designed to study the mean behavior of the jets and plumes in flowing ambients and to verify the theory, including the jet trajectory and dilution in the jet stage and the stability of the upstream wedge, plume height and width in the intermediate stage. The numerical modelling is to try to develop mathemetical models in order to better predict the turbulent buoyant jets and plumes in flowing ambients.

1.4   Structure of the Thesis

This thesis consists of six chapters. In Chapter 2 some basic concepts of the buoyant jets and plumes are described, including the definitions and classifications of the problems. Meanwhile, the orders of the magnitudes in space and time for a typical turbulent buoyant jet in the ocean are given.

In Chapter 3 the mechanics of the turbulent buoyant jets and plumes in a flowing ambient are discussed by using the dimensional analysis and by dividing the basic physical processes into four primary stages. Emphasis has been put on the analyses of the jet trajectories and dilutions, and the discriptions and discussions of the mechanics in the four stages, including the important physical phenomene, such as the counter rotating vortex pairs, entrainment, pressure unbalance, stability criteria for upstream wedge and plume height and width.

In Chapter 4 the laboratory experiments and field investigations on the turbulent buoyant jets and plumes in coflows and crossflows have been dealt with. The experimental set-up and apparatus are described and the experimental data on the turbulent buoyant jets and plumes in flowing environments have been presented and analyzed.

In Chapter 5 mathematical models have been developed, including both integral and turbulence models. Predictions have been made and comparied to the available experimental data. In addition, the entrainment function in a flowing ambient has been discussed.

Finally the major conclusions of the study are given in Chapter 6.

Chapter 2

Basic Concepts of Jets and Plumes

2.1 Definition

A simple jet is defined as a flow from an orifice with pure momentum source, a plume is a pure buoyancy source and a buoyant jet is a flow from an orifice with both momentum and buoyancy source. Mathematically, one can define the problem by using the flow initial densimetrical Froude number $F_{\Delta o}$ that a simple jet ($F_{\Delta o} \to \infty$), a pure plume ($F_{\Delta o} \to 0$) and a buoyant jet ($0 < F_{\Delta o} < \infty$). The definition of the flow initial densimetrical Froude number is refered to Chapter 3.

2.2 Classification

Jets and plumes may be classfied according to three basic groups of parameters, i.e, jet parameters, ambient parameters and geometrical parameters, as shown in Fig.2.1. The figure was originally presented by Gu and Stefan (1988) and re-arranged by the present author since the term of combined factor proposed by them is mysterious and with some items missed or misplaced.

The first group, the jet parametres, includes the initial jet momentum flux, buoyancy flux, volume flux, tracer flux and turbulence level. The second group, the ambient parameters, contains the variables such as ambient turbulence level, current speed, current direction and density stratification. These factors play a significant role at some distance from the jet orifice. The geometrical factors mean the shape of the jet, jet orientation and the possible jet boundary.

The studies of jets and plumes are complicated because of the involment of the three groups of the parameters. In order to identifiy the problem, the jets will be classified according to the three groups. With respect to the first group, the jet parameters, the jets can be sorted into memontum jet, buoyant jet (negative or positive), turbulent jet and laminar jet. With refered to the second group, the ambient variables, the jets may be calssified into jets in stagnant environments with or without density stratifications, jets in flowing ambients with or without density stratifications, jets in turbulent environments or in laminar ambients. According to the third group, the geometrical factors, the jets can be divided into round jet, slot jet, vertical jet, horizontal jet, inclined jet, free jet or wall jet, surface jet and submerged jet, and so on. The general classification of the jets according to jet parameters, ambient variables and geometrical factors is shown in Fig. 2.1.

The studies of the jet problems involving all of the three groups of parameters are so complex that the investigations have to be undertaken step-by-step from simple configuration to more complex problmes. For instance, from simple jets in a stagnant ambient to buoyant jets in a stagnant environment, to buoyant jets in a motionless ambient fluid with density stratification, to buoyant jets in a flowing ambient etc.

The studies in this thesis are subject to turbulent bouyant jets and plumes from submerged sea outfalls into flowing environmental surroundings.

16

$$
\text{Jet}
\begin{cases}
\text{Momentum} \\
\text{Turbulence}
\begin{cases}
\text{Turbulent} \\
\text{Laminar}
\end{cases} \\
\text{Buoyancy}
\begin{cases}
\text{Nonbuoyant} \\
\text{Buoyant}
\begin{cases}
\text{Positive} \\
\text{Negative}
\end{cases}
\end{cases} \\
\text{Volume}
\end{cases}
$$

$$
\text{Ambient}
\begin{cases}
\text{Turbulence}
\begin{cases}
\text{Turbulent} \\
\text{Laminar}
\end{cases} \\
\text{Current}
\begin{cases}
\text{Stagnant} \\
\text{Flowing}
\begin{cases}
\text{Crossflow} \\
\text{Coflow} \\
\text{Counterflow}
\end{cases}
\end{cases} \\
\text{Stratification}
\begin{cases}
\text{Homogeneous} \\
\text{Stratified}
\end{cases}
\end{cases}
$$

$$
\text{Geometry}
\begin{cases}
\text{Shape}
\begin{cases}
\text{Round} \\
\text{Slot}
\end{cases} \\
\text{Dimension}
\begin{cases}
3-D \\
2-D
\end{cases} \\
\text{Orientation}
\begin{cases}
\text{Vertical} \\
\text{Inclined} \\
\text{Horizontal}
\end{cases} \\
\text{Submergence}
\begin{cases}
\text{Submerged} \\
\text{Surface}
\end{cases} \\
\text{Buondary}
\begin{cases}
\text{Free Jet} \\
\text{Wall Jet}
\end{cases} \\
\text{Instalation}
\begin{cases}
\text{Single} - \text{port} \\
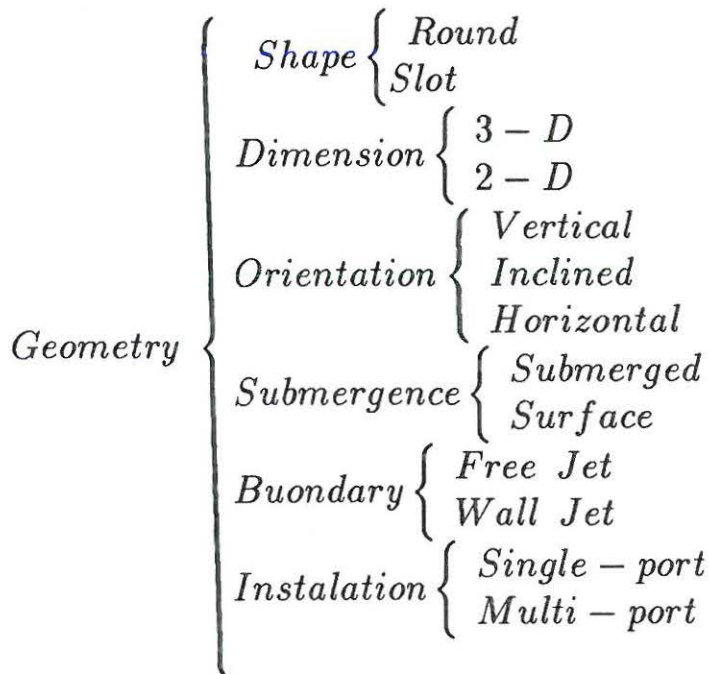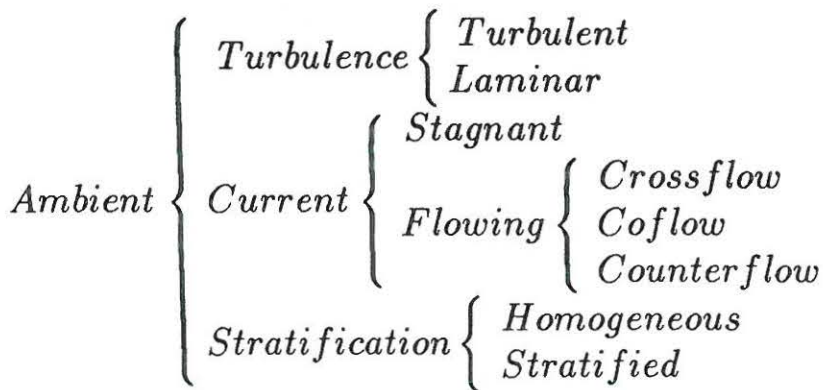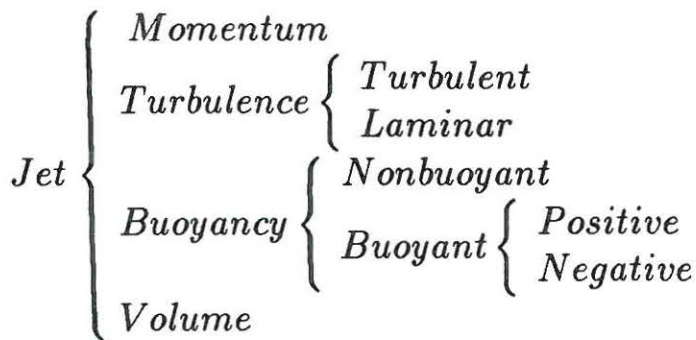\text{Multi} - \text{port}
\end{cases}
\end{cases}
$$

Figure 2.1: Jet Classification according to Jet Parameters, Ambient Parameters and Geometrical Factors.

17

2.3 Length in Space and Time

The turbulent buoyant jets and plumes from sea outfalls have a typical length and time scales with $10^1 \sim 10^6$ meters and $10^2 \sim 10^6$ seconds. The various processes and their approximate order of magnitude of length and time are summarized in Table 2.1. after Brooks (1980).

Table 2.1: Scales for Submerged Jets and Plumes

Phase	Phenomenon	Length Scale (m)	Time Scale (sec)
(1)	Initial jet mixing	$< 10^2$	$< 10^3$
(2)	Establishment of sewage field; Lateral gravitational spreading	$10^1 \sim 10^3$	$10^2 \sim 10^3$
(3)	Natural lateral diffusion and dispersion	$10^2 \sim 10^4$	$10^3 \sim 10^5$
(4)	Advection by currents	$10^3 \sim 10^5$	$10^3 \sim 10^6$
(5)	Large scale flushing up-/downwelling, sedimentation	$10^4 \sim 10^6$	$10^6 \sim 10^8$

Note: approximately, 1 day $= 10^5$ seconds; 1 month $= 10^{6.5}$ seconds and 1 year $= 10^{7.5}$ seconds.

As demonstrated in Table 2.1., macroscopically, the processes of releasing waste water into occean can be considered in five phases; microscopically, the first phase can be further divided into three stages, i.e. the zone of flow establishment, the stage of jet and the stage of intermediate, refere to Chapter 3 for detailed description.

In the initial mixing phase, the released sewage effulent is strongly mixed with and considerably diluted by ambient fluids, with an order of

10^2 meters in space and 10^3 seconds in time. Sewage field, e.g. surface plume in homogeneous ambient or submerged plume in density stratified environment will be established and lateral gravitational spreading will be occured immediately after the establishment owing to the density deficiency between the discharged flow and the the ambient flow, resulting in that the plume spreads laterally and becomes thinner. This stage will approximately have the order of $10^1 - 10^3$ meters in space and $10^2 - 10^3$ seconds in time. After the phase 2, the lateral and longitudinal dispersion of the waste fluids will be happened due to the ambient turbulence and stratification, in addition, the pollutants will be transported by ambient currents. The total impacted area by the sewage discharge could range up to 10 - 100 squre kilometers and the duration could last for months. In principle, the five phases can be subjected into two major fields, i.e. the near field (phase 1 and 2) and the far field (phase 3, 4, and 5), consequently, the studies of the problem can be carried out by considering the near and far fields and the combination of the near and far fields, Chen and Schrøder et al. (1989).

Chapter 3

Dimensional and Physical Analyses of Jets and Plumes

3.1 Dimensional Analysis

Physically, for a turbulent buoyant jet issued into a flowing ambient, it can be assumed that the pollutant concentration $c(x,y,z)$ is to be determined by the possibly relevant parameters (see Fig.3.1).
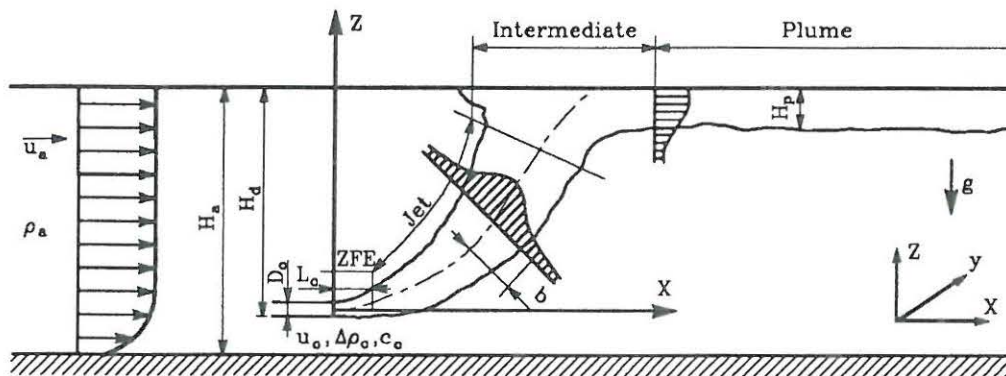
Figure 3.1: A Turbulent Buoyant Jet Discharged into a Flowing Ambient

20

$$c(x, y, z) = f_1\{g, \rho_o, \rho_a, H_d, D_o, u_o, u_a, \theta_o, \nu_o, c_o, x, y, z\} \tag{3.1}$$

By dimensional analysis, the following combinations are obtained:

$$\frac{c_o}{c(x, y, z)} = f_2\{\frac{H_d}{D_o}, F_{\Delta o}, \frac{u_o}{u_a}, R_e, \theta_o, \frac{x}{D_o}, \frac{y}{D_o}, \frac{z}{D_o}\} \tag{3.2}$$

where, $F_{\Delta o}$ is the jet initial densimetric Froude number, defined as $F_{\Delta o} = u_o/\sqrt{g\Delta\rho/\rho_a D_o}$, R_e is the jet Reynolds number, defined as $R_e = u_o D_o/\nu_o$.

In order to simplify the analysis and to reduce the number of independent variables to be considered, several necessary assumptions are made, i.e. (i) the jet flow is with adequately large Reynolds number; (ii) the initial discharging angle effect is deleted by considering only horizontal or vertical jets and (iii) Boussinesq approximation is introduced.

With the aforementioned assumptions, the turbulent buoyant jet can be defined as a source of mass, momentum and buoyancy. The basic independent fluxes characterizing the turbulent buoyant jet are defined as follows:

$$Q = \int_A u_o dA \tag{3.3}$$

$$M = \int_A u_o^2 dA \tag{3.4}$$

$$B = \int_A u_o \frac{\Delta\rho}{\rho_a} g dA \tag{3.5}$$

For a round jet, the volume flux $Q = u_o \pi D_o^2/4$; momentum flux $M = u_o^2 \pi D_o^2/4$; and buoyancy flux $B = Q\frac{\Delta\rho}{\rho_a}g$.

21

By using the volume flux Q, momentum flux M and buoyancy flux B, the dilution should be depended upon the following variables:

$$\frac{c_o}{c(x,y,z)} = f_3\{Q, M, B, u_a, x, y, z\} \tag{3.6}$$

By dimensional analysis, several length scales characterizing the jet can be formed from the fluxes Q, M and B, they are defined as

$$L_q = \frac{Q}{M^{1/2}} \tag{3.7}$$

$$L_m = \frac{M^{3/4}}{B^{1/2}} \quad or \quad L_m = \frac{M^{1/2}}{u_a} \tag{3.8}$$

$$L_b = \frac{B}{u^3_a} \tag{3.9}$$

For a circular jet in a flowing ambient, the volume length scale $L_q = \sqrt{\pi}D_o/2$, the momentum length scale $L_m = u_o(\pi D_o^2/4)^{1/4}/\sqrt{\Delta\rho/\rho_a g}$ or $L_m = \sqrt{\pi}D_o u_o/2u_a$ and the buoyancy length scale $L_b = u_o\pi D_o^2 \frac{\Delta\rho}{\rho_a}g/4u_a^3$.

L_q proportional to the jet diameter, is the appropriate length scale close to the jet orifice. For $z/L_q << 1$, the initial geometry will have a significant effect on the jet behavior; for $z/L_q >> 1$, the volume flux is of minor importance and the jet behavior is dominated by momentum close to the source, and by buoyancy at large distance from the source.

L_m is a measure of the distance at which buoyancy becomes more important than the jet momentum. Thus, for a horizontal jet in a coflowing environment, the momentum length scale is defined as $L_m = M^{3/4}/B^{1/2}$, since the jet direction is analogoue to the ambient current direction, it seems that the buoyancy force is more relevant than the ambient momentum in dominating the jet behavior, therfore it is more suitable to define the momentum length scale by taking the buoyancy flux into account. In the case of a vertical jet in a crossflow, the momentum length scale is

defined as $L_m = M^{1/2}/u_a$, because the jet direction is perpendicular to the ambient velocity direction then it appears that the ambient current velocity is more important than the buoyancy force in governing the jet structure. Thus it is more reasonable to consider the ambient momentum in the definition of the momentum length scale.

L_b, in the presence of ambient current, represents the vertical distance at which the velocity introduced by the buoyancy (proportional to $B^{1/3}z^{-1/3}$) has decayed to the ambient velocity, u_a.

Based on Eq.(3.6), a dimensionless grouping can be obtained as

$$S = \frac{c_o}{c(x,y,z)} = f_4\{\frac{L_m}{L_q}, \frac{L_m}{L_b}, (\frac{x}{L_b}, \frac{y}{L_b}, \frac{z}{L_b}) \text{ or } (\frac{x}{L_m}, \frac{y}{L_m}, \frac{z}{L_m})\}(3.10)$$

in which, S is the dilution at the point of (x,y,z) and $L_m/L_q = (4/\pi)^{1/4}F_{\Delta o}$. For $L_m/L_q = (4/\pi)^{1/2}$, $(F_{\Delta o} = 1.0)$, the discharge is like a pure plume and the jet orientation is unimportant to the flow behavior. For $L_m/L_q > (4/\pi)^{1/4}$, $(F_{\Delta o} > 1.0)$, the jet initial momentun is to advance the jet in the jet initial discharging direction before the jet starts to bend over and rise up as a buoyant plume.

The flows can be classified into two different types, namely buoyancy dominated flow and momentum dominated flow, depending on the ratio of L_m/L_b less or greater than unit. For $L_m/L_b < 1$ the flow is defined as buoyancy dominated; whereas for $L_m/L_b > 1$ the flow is regarded as momentum dominated flow. The third or fourth term in Eq.(3.10) is chosen in dimensional analysis according to the type of flows.

Trajectory Analysis

Dimensional analyses imply that the jet trajectory in the x-z plane can be expected to depend on the relation involving the momentum or buoyancy length scales, according to the types of flows. For momentum dominated flows, the jet trajectories are expected to be

$$\frac{z}{L_m} = C_1\left(\frac{x}{L_m}\right)^m \tag{3.11}$$

and for buoyancy dominated flows,

$$\frac{z}{L_b} = C_2\left(\frac{x}{L_b}\right)^n \tag{3.12}$$

The exponents of m and n, and the constants of C_1, C_2 and C_3 are to be determined by experimental data.

Dilution Analysis

In the analysis of dilution, the dilution can be defined in several ways, for examples, the ratio $S = c_o/c(x, y, z)$ gives the specified local dilution at point of (x,y,z); the ratio $S_o = Q_i/Q$ provides the average dilution of the jet fluid, where Q_i is the local volume flux. Alternatively, the reduced gravity $g' = \Delta\rho/\rho_a g$ is the appropriate variable giving the dilution of a buoyant plume since a pure plume has no initial discharge. Either variable S_o or g' can be used for buoyancy dominated flow and analogous results can be expected.

Dimensional considerations imply that, for momentum dominated flow, Wright (1977),

$$\frac{SQu_a}{M} = C_3\left(\frac{z}{L_m}\right)^p \tag{3.13}$$

and for buoyancy dominated flow

$$\frac{SQ}{u_a L_b^2} = C_4\left(\frac{z}{L_b}\right)^q \qquad or \qquad \frac{g'B}{u_a^5} = C_5\left(\frac{z}{L_b}\right)^r \tag{3.14}$$

The powers of p, q and r, and the constants of C_3, C_4 and C_5 are to be determined by laboratory data.

24

3.2 Physical Analysis

A turbulent buoyant jet discharged from submerged sea outfall into a large flowing receiving water, the sketch of the processes is outlined in Fig.3.1. Due to the buoyancy force the jet will reach either the sea surface in a uniform or a weakly-stratified ambient environment or a trapped-height in a stratified receiving water. For a turbulent buoyant jet issuing into a homogeneous flowing ambient, the physical processes, basically can be divided into four primary stages, namely:

- Zone of Flow Establishment;

- Stage of Jet;

- Stage of Intermediate;

- Stage of Plume.

3.2.1 Zone of Flow Establishment

For a momentum jet, it is observated in the experiments that there is a short region existing from the nozzle to where the jet flow is fully developed. The region is called zone of flow establishment, see Fig. 3.2. It shows that strong shear stresses are introduced near the orifice due to the discontinuity of the velocity.

Experimental results by Albertson, Dai, et al (1950) demonstrated that in the zone of flow establishment the profiles of concentration and velocity are changed from uniform at the outlet to Gaussain distribution at the end of the zone of flow establishment. In the zone of flow establishment, the distribution of velocity and concentration can be written as:

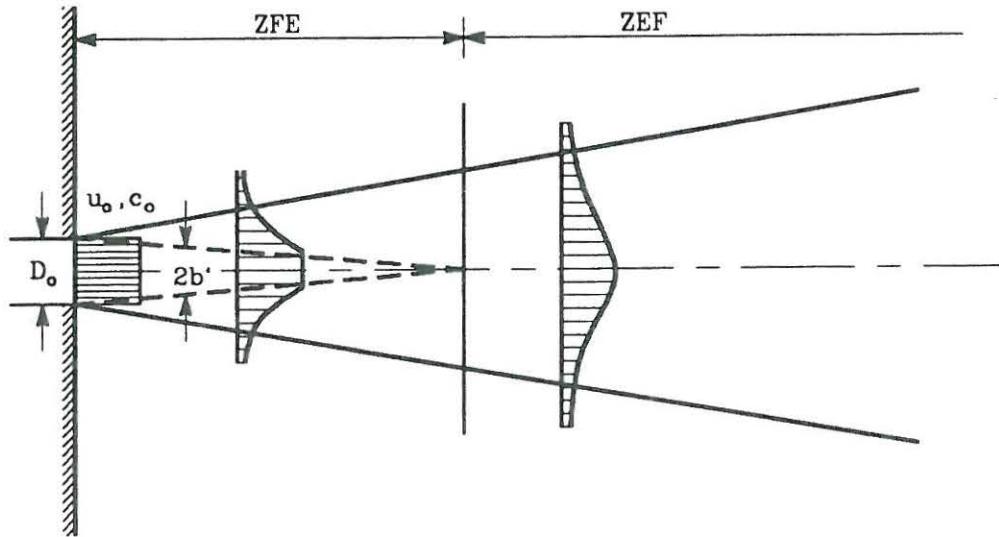$$\left.\begin{array}{l} u = u_o \\ c = c_o \end{array}\right\} r < b' \qquad (3.15)$$

Figure 3.2: Zone of Flow Establishment(ZFE)

$$\left.\begin{array}{l} u = u_o exp\{-\frac{(r-b')^2}{b^2}\} \\ c = c_o exp\{-\frac{(r-b')^2}{\lambda^2 b^2}\} \end{array}\right\} \quad r > b' \qquad (3.16)$$

It is shown by experiments that the length of the zone of flow establishment is approximately equal to 6.2 times of D_o, where D_o is the diameter of orifice.

A turbulent buoyant jet is the turbulent flow generated by a source with initial momentum and buoyancy fluxes. The basic mechanics of the buoyant jet is in principle the same as a momentum jet in the zone of flow establishment. However there is one point interesting here to point out that the length of the zone of flow establishment for buoyant jet is considerably shorter than that generally assumed to occur in the case of a momentum jet, see chapter 4 for explanations.

26

3.2.2 Stage of jet

The stage of jet starts at the end of the zone of flow establishment and ends at the beginning of the stage of intermediate. In the stage of jet, the discharged flow is fully developed and mainly dominated by the jet momentum in which the buoyancy is comparatively unimportant. In a flowing ambient as jet raising up and mixing with ambient fluid, the jet will be bend-over due to the ambient current drag force. During the jet stage, ambient fluid is entrained into the jet flow due to the turbulece, resulting in a considerable dilution of the jet flow.
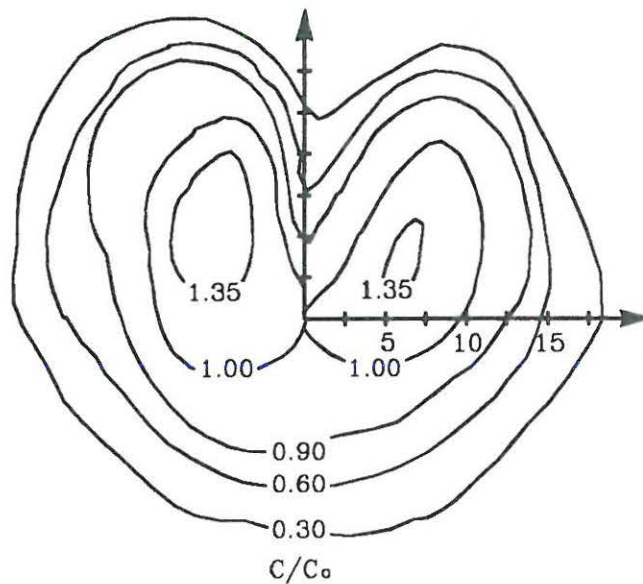

Figure 3.3: Measured Jet Cross Section Concentration Contours, after Wright (1977)

In addition, it is observed that the distribution of velocity and concentration is clearly distored since the fact that the dilutions are higher at the edges of the jet than that in the core of the jet flow, which results in the buoyancy at the edges are smaller, consequently the out edges of the jet are moving towards inside of the jet fluid to forme a horse shaped distribution showing a pair of counter rotating eddies.

27

Fig. 3.3 is measured jet cross section concentration contours in a crossflowing ambient, by Wright(1977), a similar result was reported by Fan (1967). It is clearly shown that the maximun concentration is not located at the center of the cross section but existing two peak values on both sides of the symmetric plane. The maximun value is somewhat $60 - 80\%$ higher than the central concentration. However, if the analysis is to estimate the gross behavior of the jet flow but not the detailed structure, it is reasonable enough to assume Guassain distribution ingnoing the fact of the horese-shaped, Hoult(1963), Fan(1967), Abraham(1970) and Hirst(1972), therefore the integral technique is still applicable to turbulent buoyant jet in flowing environment.

In the stage of jet, there are two key physical phenomena to be concerned, i.e. the turbulent entrainment and the unbalanced pressure field on both sides of the jet flow caused by the ambient current.

The entrainment is the physical phenomenon which the flow entrained from a non-turbulent or low turbulent region into a turbulent or high turbulent region. In the situation of a turbulent buoyant jet in a flowing environment, it is the ambient flow (with low turbulence lever) into the jet (with high turbulence lever). The turbulent buoyant jet discharged into a flowing ambient forms a pair of counter rotating vortices at which the entrainment occuring, see Fig. 3.4.

Because the entrainment is closely related to the turbulence it seems unlikely to describe the entrainment function in detailed, but a great effort has been devoted to relate the entrainment velocity to the jet local mean characteristics such as the jet centerline excess velocity and the characteristic width, etc. Different entrainment hypotheses have been made, refer to Chapter 5, section 5.1.5 for detailed discussion.

Because of the presence of the ambient current, the pressures on both sides of the jet is unbalanced and so complex that it seems to be al-
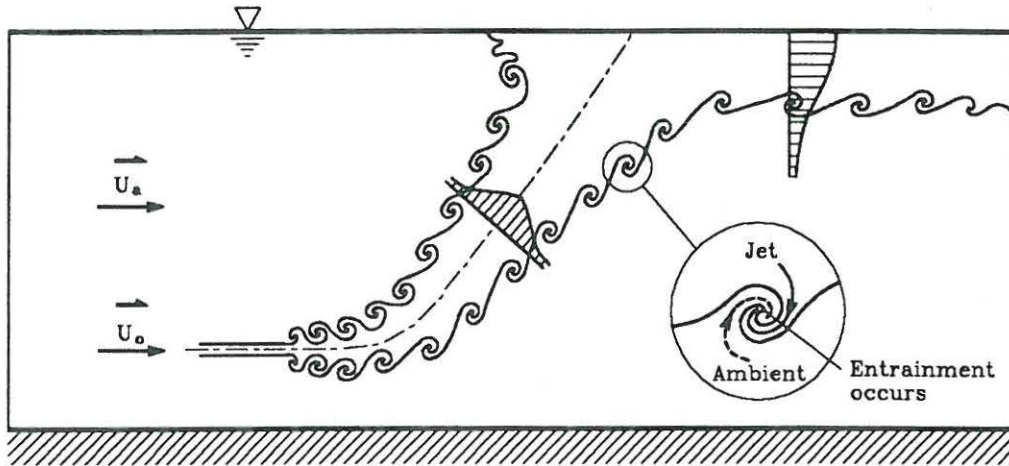
Figure 3.4: Entrainment and Counter Rotating Vortices

most impossible to propose a function to describe the pressure unbalance around the bend-over jet in a flowing ambient. Therefore it becomes a good idear to introduce a gross drag force acting on the jet by considering the jet as a rigid body. See Chapter 5, section 5.1.5 for further discussion.

The ambient turbulence effect on the jet devolopment in the jet stage remains unclear because no sufficent laboratory data exist. But it is beleived that the ambient turbulence infulence on the jet in the jet stage is unimportant in comparison to the jet self-generated turbulence. It can be expected that the ambient turbulence plays a more and more important role as the jet travelling away from the orifice, and eventually dominates the movement of the discharged flow. Attempt has been tried to evaluate the ambient turbulence effects on the jet in the present project by changing the bed roughness, but unfortunetely, this part of the programme has to be given up due to lack of sufficently accurate equipment to distinguish the ambient turbulece effects on the jet development. But it is generally believed that the ambient turbulece will not decrease the dilution of the effluent, Fisher et al (1979).

3.2.3   Stage of Intermediate

In the stage of intermediate, the discharged flow is governed by both momentum and buoyancy. It appears to be very difficult to describe the distribution of velocity and concentration in the intermediate stage because the fact that both buoyancy and remained momentum will cause the jet to move horizontally with radial velocities as soon as the jet reaches the water free surface. In the stage of intermediate, two main aspects are of interests to be discussed here. Firstly, the stability criterion for the upstream wedge introduced by a turbulent submerged buoyant jet; secondly the initial plume height and width for the plume stage and thirdly the dilution in the intermediate zone. In order to carry out the study in the intermediate zone, it is assumed that the density distribution for the plume stage is Gaussian, shown in Figs. 3.5 and 3.6, as:

$$\Delta \rho = \Delta \rho_m exp\{-\frac{y^2}{B^2}\}exp\{-\frac{z^2}{H_p^2}\} \tag{3.17}$$

in which, $\Delta \rho_m$: excess centerline density deficit;
$\quad\quad\quad\quad B$: plume width;
$\quad\quad\quad\quad H_p$: plume height;

Stability Criteria for Upstream Wedge

An upstream wedge created by a submerged turbulent buoyant jet in a homogenous flowing ambient is formed on the water surface and sketched in Fig. 3.5.

It is assumed that the Bernoulli equation applies to a surface and a bottom streamline on Fig. 3.5, the following equations are obtained immediately, Hansen(1978).
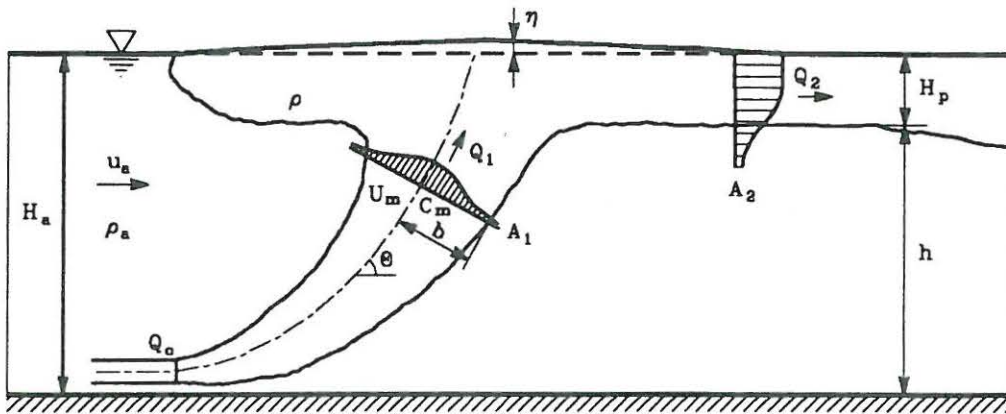
$$\eta = \frac{u_a^2}{2g} \tag{3.18}$$

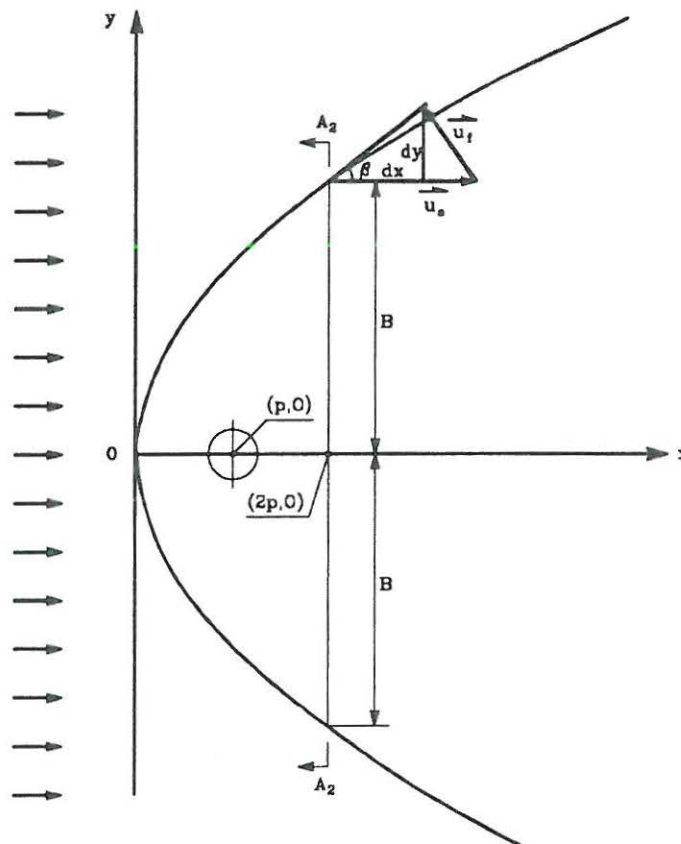Figure 3.5: Schametic Diagram of Upstream Wedge

Figure 3.6: Definition Schetch of Surface Plume

31

$$H_a + \frac{u_a^2}{2g} = h + \rho\frac{H_p}{\rho_a} + \frac{u_a^2}{2g}\left(\frac{H_a}{h}\right)^2 \tag{3.19}$$

in which, η : surface excess water lever;
    u_a : ambient current velocity;
    H_a : ambient water depth;
    h : water depth under the plume;
    ρ_a : ambient density;
    ρ : plume density;
    g : gravitational acceleration;

With the geometric relation:

$$H_a + \eta = h + H_p \tag{3.20}$$

From Eqs.(3.18) $\sim$ (3.20), it can be obtained

$$\frac{\rho_a - \rho}{\rho_a}H_p - \frac{u_a^2}{2g}\left(\frac{H_a}{h}\right)^2 = 0 \tag{3.21}$$

Since $\eta/H_a \ll 1$, the following approximation is valid,

$$\frac{h}{H_a} = 1 - \frac{H_p}{H_a} \tag{3.22}$$

thus, the Bernoulli equation finally yields:

$$2\left(1 - \frac{H_p}{H_a}\right)^2\frac{H_p}{H_a} = \frac{u_a^2}{\frac{\Delta\rho}{\rho_a}gH_a} \tag{3.23}$$

In fact the right hand side of Eq.(3.23) is a densimetrical Froude number, the maximun value of the left hand side of Eq.(3.23) is 0.296 for H_p/H_a in the range of 0.0 $\sim$ 1.0, therefore, the criterion to form a stable upstream wedge depends on the value of the densimetrical Froude number, a stable upstream wedge may be established if

32

$$F_{\Delta s} = \frac{u_a^2}{\frac{\Delta\rho}{\rho_a}gH_a} \leq 0.296 \approx 0.30 \tag{3.24}$$

The analysis of stability condition for the upstream wedge is based on the two-layer flow system sketched in Fig. 3.5. without taking the shape or the width of the surface plume into account.

Another approch to establish the stability criterion for the upstream wedge and to find the height of the plume is to consider the front velocity on the surface, Schrøder(1990), see Fig. 3.6.

$$tg\beta = \frac{u_f}{\sqrt{u_a^2 - u_f^2}} \tag{3.25}$$

in which, the front velocity u_f can be expressed as

$$u_f = (1 - \frac{H_p}{H_a})\sqrt{\frac{\Delta\rho}{\rho_a}gH_p} \tag{3.26}$$

substituting Eq.(3.26) into Eq.(3.25), we have

$$tg^2\beta[u_a^2 - (1 - \frac{H_p}{H_a})^2\frac{\Delta\rho}{\rho_a}gH_p] = (1 - \frac{H_p}{H_a})^2\frac{\Delta\rho}{\rho_a}gH_p \tag{3.27}$$

the plume height can be found from Eq.(3.27) as

$$H_p = \frac{1}{\frac{1}{tg^2\beta}+1}\frac{u_a^2}{(1 - \frac{H_p}{H_a})^2\frac{\Delta\rho}{\rho_a}g} \tag{3.28}$$

Assuming the shape of the surface plume as a parabolic and written as

33

$$y^2 = 4px \tag{3.29}$$

By defining the location of the width of the plume at $x = 2p$, where p is the focal distance of the parabolic, then

$$tg\beta = \frac{dy}{dx}\big|_{x=2p} = \sqrt{\frac{p}{x}}\big|_{x=2p} = \frac{\sqrt{2}}{2} \tag{3.30}$$

By substituting Eq.(3.30) into Eq.(3.28), it yields

$$3(1 - \frac{H_p}{H_a})^2 \frac{H_p}{H_a} = \frac{u_a{}^2}{\frac{\Delta\rho}{\rho_a}gH_a} \tag{3.31}$$

This leads to a similar equation to Eq.(3.23) with a different factor of 3 instead of 2. Hence, the criterion for a stable upstream intrusion created by a submerged buoyant jet states that

$$F_{\Delta s} = \frac{u_a^2}{\frac{\Delta\rho}{\rho_a}gH_a} \leq \frac{3}{2} \times 0.296 \approx 0.45 \tag{3.32}$$

Plume Height and Width

From Eq.(3.31) in the stability condition section, the plume height is found as

$$H_p = \frac{u_a^2}{3(1 - \frac{H_p}{H_a})^2 \frac{\Delta\rho}{\rho_a}g} \tag{3.33}$$

The relation between the plume height and width can be derived by applying the continuity equation of mass in the intermediate zone, the continuity equation of mass reads:

34

$$\frac{dQ}{ds} = 0 \tag{3.34}$$

By substituting the Guassian profile of velocity and integrating across the sections A_1 and A_2,

$$\int_{A_1} [u_m + u_a cos\theta] dA = \int_{A_2} u_a dA \tag{3.35}$$

$$\tag{3.36}$$

After the integration, it yields,

$$\pi b^2 (u_m + 2u_a cos\theta) = 2u_a B H_p \tag{3.37}$$

Finally, the half width of the plume is found to be

$$B = \frac{\pi b^2 (u_m + 2u_a cos\theta)}{2u_a H_p} = \frac{S_o Q_o}{2u_a H_p} \tag{3.38}$$

in which, S_o is the initial dilution defined at the end of the jet stage and Q_o is the initial jet discharge rate.

Dilution in Intermediate Stage

By considering the conservation equation of density deficiency in the intermediate stage, it reads:

$$\frac{d}{ds} [\int_A u \Delta \rho dA] = 0 \tag{3.39}$$

Substituting the Guassian profiles of velocity and density, then integrating across the sections A_1 and A_2, (Fig.3.5) it yields:

35

$$\frac{\pi b^2}{2}[u_m + 2(\lambda^2 + 1)u_a cos\theta]\Delta\rho_{m1} = \frac{\pi}{2}u_a\Delta\rho_{m2}BH_p \qquad (3.40)$$

Finally, the dilution S_2 in the intermediate stage reads:

$$S_2 = \frac{\Delta\rho_{m1}}{\Delta\rho_{m2}} = \frac{u_a H_p B}{b^2[u_m + 2(\lambda^2 + 1)u_a cos\theta]} \qquad (3.41)$$

Eq.(3.41) states the fact that the dilution in the intermediate stage is depended on the ambient velocity, plume height and width, jet radius, spreading coefficent, jet excess velocity and the deflected angle at the end of the jet stage. It is believed that the excess jet velocity, u_m, is neglectable and the angle θ is less than 20 degrees in the presence of the ambient current. Therefore it is reasonable to assume that $u_m \approx 0$ and $cos\theta \approx 1.0$, then Eq.(3.41) can be rewritten as

$$S_2 = \frac{\Delta\rho_{m1}}{\Delta\rho_{m2}} = \frac{u_a H_p B}{2b^2(\lambda^2 + 1)u_a} \approx \frac{1}{5}\frac{H_p B}{b^2} \qquad (3.42)$$

by taking $\lambda = 1.16$. Eq.(3.42) implys that the dilution in the intermediate stage is mainly determined by the geometric parameters. The dilution can be estimated in the order of $1 \sim 2$ times due to the fact that the plume height H_p has the same order as the jet radius b and the plume width B is about $5 \sim 10$ times of b.

3.2.4 Stage of Plume

In the plume stage, the surface plume will be governed by the ambient parameters such as the ambient velocity, ambient turbulence, wave and wind velocity etc. The physical processes of the surface plume are subject to transport due to the ambient current and dispersion owing to the ambient turbulence. The parameters characterizing the plume are the width of the plume, the height of the plume and the density deficiency or concentration difference between the plume and the ambient.

Chapter 4

Laboratory Experiments and Field Investigations

Many investigators, for examples, Fan (1967), Ayoub (1971),Chu (1975), Wright (1977), Holley and Jirka (1985), Lee and Cheung (1986), Lee and Neville-Jones (1987) as well as Knudsen and Wood (1988), have studied the problem of turbulent buoyant jets and plumes in a flowing ambient by means of laboratory experiments and field investigations. Basically, the studies can be classified into three categories, namely, (i) horizontal turbulent buoyant jets and plumes in a coflowing current, (ii) vertical turbulent buoyant jets and plumes in a crossflowing ambient and (iii) horizontal jet in a perpendicular crossflowing environment.

In this chapter the experimental set-up and apparatus will be firstly described, secondly the laboratory experimental data in association with the data by Fan and Wright and the field observated results reported by Lee and Neville-Jones will be presented and analyzed, and finally, a brief summary of the experimental studies and field investigations will be given.

4.1 Experimental Set-up and Apparatus

The experimental facilities consist of a water flume, a water barrel, a submerged diffusor, a propeller velocity measuremet instrument and a personal computer control temperature measurement system. In addition, the photographic technique was used by a photo camera and a video camera to determine the instantaneous and continuous pictures of the turbulent buoyant jets and plumes in order to investigate the jet trajectories and the development and the mechanism of the turbulent buoyant jets and plumes in a flowing ambient.

4.1.1 Flume and Flow Discharging System

The experiments were conducted in the water flume with a dimension of 20 meter long, 1.5 meter wide and 0.8 meter deep in the hydraulic laboratory at the University of Aalborg. In order to increase the density difference between the discharged water and the ambient water, the experiments were carried out by means of both fresh and salt ambient receiving water. Schematic diagram of the flume for the fresh and salt water experiment is shown in Fig. 4.1.

For the fresh water experiments the water in the flume was recirculated through an approximately 20 m^3 reservoir. In most of the experiments the water depth in the flume was 30 cm equivalent to about 10 m^3 total water volume in the flume. For the salt water experiments the salt water was stored and recirculated directly in the flume without going though any reservoir. The salinity of the salt water was approximatly 20 - 25 ppt and the density of the salt water was in the range of 1010 - 1020 kg/m^3.

The water barrel with a volume of 180 litters, constant head can be filled with water at desired temperature. The discharged water flows from the barrel through an adjustable valve and a flowmeter to a deareator, consisting of a closed box with an air bleeder where the air bubbles

influnce can be eliminated, and finally to a submerged nozzle and releases into ambient fluid. The sketch of the discharging system is illustrated in Fig. 4.1
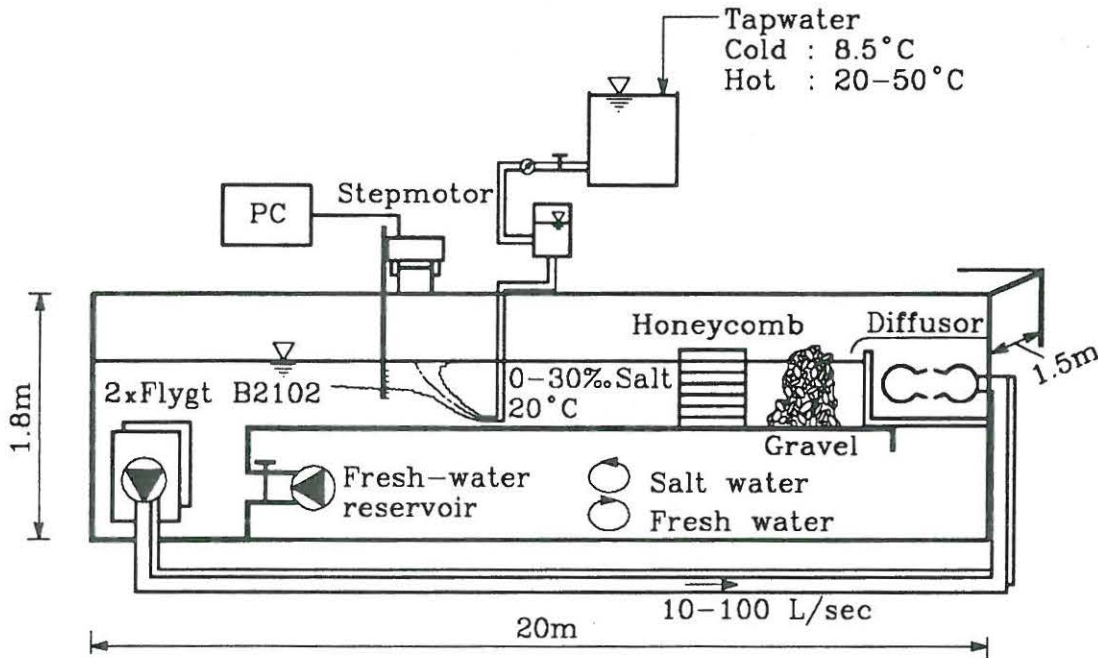

Figure 4.1: Experimental Flume Set-up and Flow Discharging System

4.1.2 Temperature Measurement

The temperature was measured by means of eight copper-constantan thermocouples with a reference temperature bottle mounted on a metal rod which is fixed on a transversing waggon controlled by a PC system, Petersen, O. (1987), as shown in Fig. 4.2

The principle of the thermocouple is that a temperature difference between the two solderings produces a voltage, proportional to the temperature difference. The constant of the proportionality for each thermocouple is found by measuring voltage and temperature in a range covering
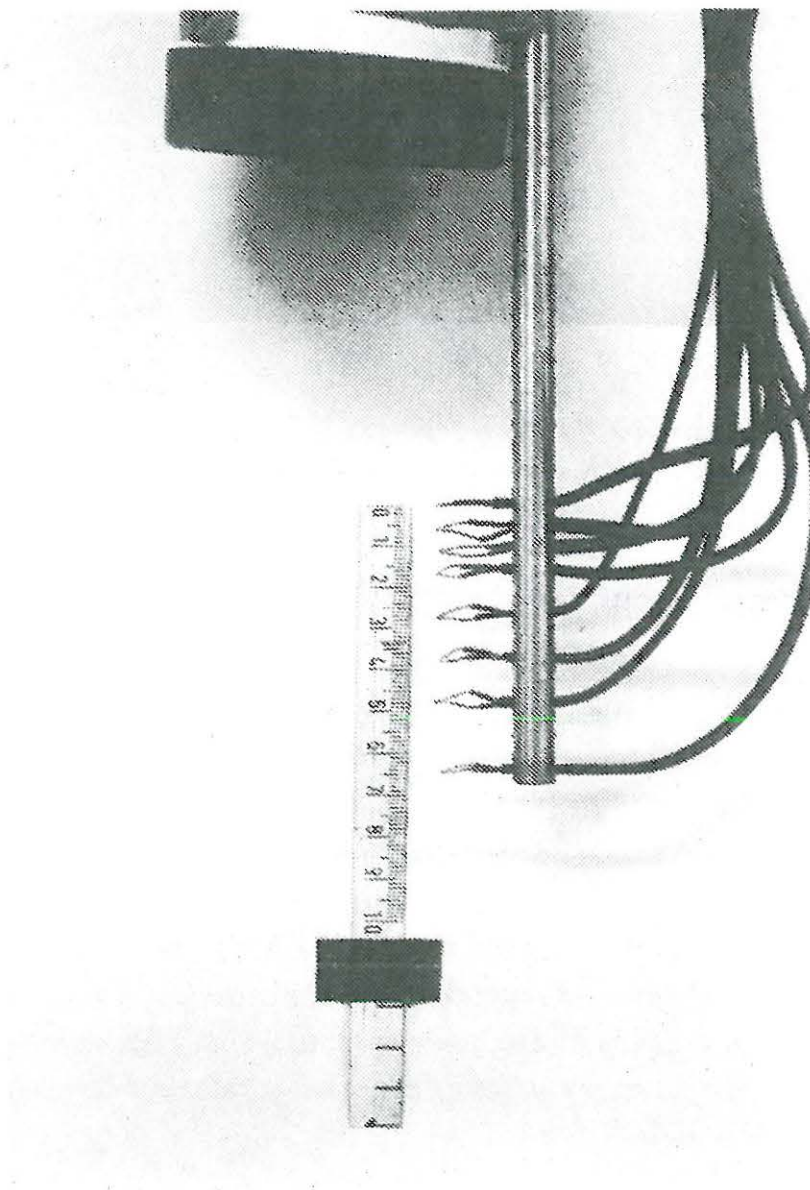
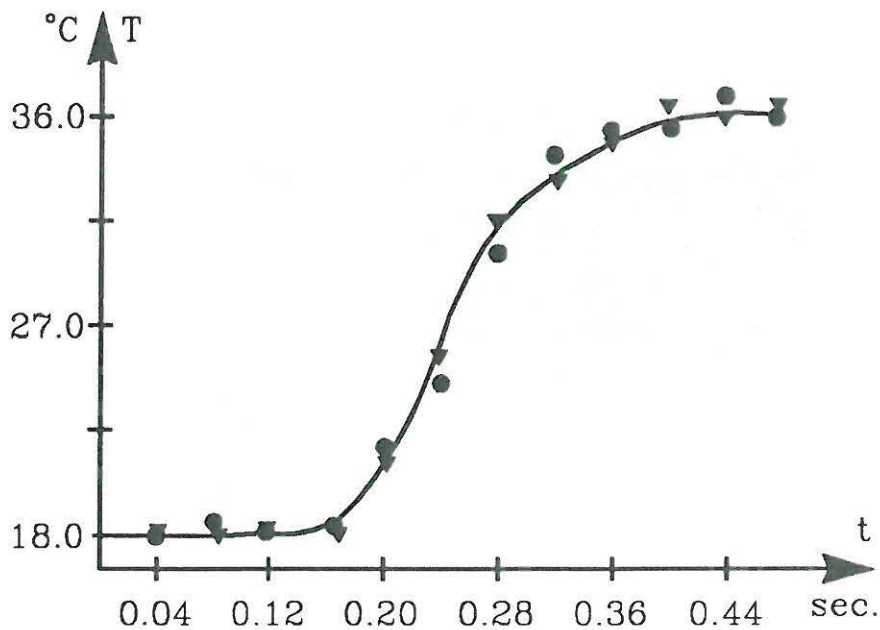Figure 4.2: Thermocouple Mounting

41

Figure 4.3: Step Response of Thermocouple

the expected temperatures in the experiments. The voltage from each thermocouple is amplified 5000 times and registrated on a digital volt-meter with a smallest increment of 10 mV.

The measured parameter in the experiments is the temperature difference between the jet and the ambient water. The zero of the thermocouples is set to the temperature of the ambient water before each measurement. This procedure accounts for the drift in the electronic equipment and the change in ambient temperature. The sensitivity of the thermocouples is $0.05°$ C.

Since the temperature flunctuation, it is essential to know the time constant of the thermocouple. This has been estimated by simulating a temperature step function. As shown in Fig. 4.4 the registrated temperature as a function of time, while the thermocouple is dropped down right in the water. The time constant is very important when dynamic

measurements are undertaken, for example., fluctuation etc.

By using an energy balance for the soldering one can express the time constant K as

$$T_2 - T = (T_2 - T_1)exp\{-\frac{t}{K}\} \qquad (4.1)$$

where T_1 and T_2 are ambient temperatures before and after the step; T is the temperature of the soldering and t is the time. K is found to be 0.05 seconds from the experiments.

4.1.3 Density Determination

In the fresh receiving water experiments, the water density was calculated from the measured water temperature using a density-temperature function, $\rho = f(T)$.

In salt receiving water experiments the ambient water density was determined each time before starting the experiment by weighting the water sample in a pycnometer. The salinity of the ambient water was found by the density and temperature. The salinity of the measured jet and plume fluid was found by the concept of dilution. It is assumed that the dilutions of temperature and salinity are equal in the measurements, therefore the salinity of the measured fluid can be found from the measured temperature as $S = S_a + (S_o - S_a)/D_T$, in which, S is the measured salinity; S_o and S_a are the salinities of the discharged water and the ambient water respectively; D_T is the dilution of temperature defined as $D_T = (T_o - T_a)/(T - T_a)$, in which, T, T_o and T_a are the measured, discharged and ambient water temperatures, respectively.

Finally, the density of the measured jet fluid was calculated from the function of $\rho = f(T, S)$, based on Fisher's (1979) table. However, it should be pointed out that the density of sodium chloride water is different from the density of sea water, Weast (1978), and this difference has not been taken in to account.

43

4.1.4 Velocity Measurement

The velocity was measured by using a propeller velocity measurment instrument. The propeller is 1.0 cm in diameter and mounted on a needle which was fixed on the waggon. The calibration curves were obtained by calibrating the propeller in the flume with known velocities. The absolute error in the velocity measurments is approximately 0.1 - 0.2 cm/s and the minimum possibly measured velocity by the propeller is about 4.0 $\sim$ 5.0 cm/s. The velocity under 4.0 cm/s was measured by a floater and a stop watch.

4.1.5 Photographic Techniques

The released water was mixed with red colour dye, potassium permanganate in order to determine the jet trajectories photographically. The influnce of the dye concentration on the discharged fluid density was ignored. Both an ordinary camera and a video camera were placed in front of the water flume to take insitantaneous and continuous pictures of the turbulent buoyant jets and plumes in flowing ambients. Light was projected on the free water surface from the top of the flume. Kodak ASA 100 and 200 colour films were used in the experiments. Grids were marked on the glass wall so as to measure the jet travelling distance and the distortion of the image was not taken into account.

4.2 Laboratory Experimental Results

Totally thirty-four runs of experiments on buoyant jets and plumes in coflowing ambients were performened, nineteen of them with fresh receiving water and fifteen of them with salt ambient water. The experiments were determined to measure the jet trajectories (24 runs), dilutions (10 runs), velocities (3 runs) and stability conditions for upstream wedge (25 runs), and plume heights and widths (10 runs).

The experiments on buoyant jets in coflowing ambients are summarized in Table 4.1. The original measurements on jet trajectories, dilutions and velocities are summarized in Tables 4.2 ~ 4.4. The experiments cover a rather wide range of initial and ambient conditions with the initial densimetrical Froude number $F_{\Delta o} = 1.0 \sim 35.0$; the velocity ratio between the initial velocity and the ambient velocity, $u_o/u_a = 1.0 \sim 50.$; and the ratio between the momentum and buoyancy length scales, $L_m/L_b = 0.001 \sim 12.0$.

The symbols used in Table 4.1 - 4.4 are refered to Fig. 3.1 in Chapter 3.

Table 4.1: Summary of Experiments on Horizontal Buoyant Jets in Coflows

exp. no.	u_o	D_o	T_o	$\Delta\rho_o/\rho_a$	u_a	H_a	T_a	u_o/u_a	$F_{\Delta o}$	L_m/L_b
(-)	(cm/s)	(cm)	(c)	(10^3)	(cm/s)	(cm)	(c)	(-)	(-)	(-)
1	75.0	1.0	42.9	7.184	2.2	30.0	19.8	34.1	28.3	0.682
2	75.0	1.0	42.1	6.738	2.2	30.0	20.4	34.1	29.2	0.751
3	75.0	1.0	43.6	7.260	2.2	30.0	20.8	34.1	28.1	0.671
4	75.0	1.0	44.2	7.568	2.2	30.0	20.5	34.1	27.5	0.661
5	75.0	1.0	42.4	6.817	1.7	30.0	20.6	44.1	29.0	0.335
6	85.0	1.0	40.1	5.741	1.7	30.0	21.4	50.0	35.8	0.441
7	78.6	1.0	40.5	5.983	1.7	30.0	21.0	46.2	32.4	0.435
8	40.0	1.0	40.9	6.224	1.7	30.0	20.6	23.5	16.2	0.410
9	78.6	1.0	40.5	6.048	1.7	30.0	20.7	46.2	32.2	0.408
10	40.0	1.0	40.5	6.087	1.7	30.0	20.5	23.5	16.4	0.404
11	7.5	1.0	42.4	7.023	2.2	29.0	19.6	3.4	2.9	0.706
12	15.5	1.0	38.8	5.378	1.3	30.0	20.8	11.9	6.7	0.213
13	15.5	1.0	38.8	5.421	1.3	30.0	20.6	11.9	6.7	0.215
14	18.5	1.0	38.8	5.039	1.0	29.0	21.0	18.5	8.3	0.101
15	10.0	1.0	38.4	5.357	1.0	30.0	20.2	10.0	4.4	0.113
16	10.0	1.0	36.5	4.748	0.8	29.0	19.8	12.5	4.6	0.062
17	75.0	1.0	40.5	6.335	2.0	29.0	19.3	37.5	30.1	0.076
18	60.0	1.0	41.5	7.978	6.0	30.0	11.0	10.0	21.5	11.825
19	18.5	1.0	39.0	6.156	5.0	30.0	17.2	3.7	7.5	9.648
S-1	8.5	2.0	12.8	13.773	2.0	28.0	22.2	4.3	1.6	0.067
S-2	8.5	2.0	13.5	13.764	2.0	29.0	22.5	4.3	1.6	0.068
S-3	8.5	2.0	12.5	13.639	3.5	29.0	22.5	1.3	1.6	0.391
S-4	8.5	2.0	12.4	13.075	8.3	30.0	22.8	1.0	1.7	5.275
S-5	8.5	2.0	13.2	12.046	3.5	30.0	25.0	2.4	1.7	0.391
S-6	8.5	2.0	12.7	12.825	0.5	30.0	22.0	17.0	1.7	0.001
S-7	8.5	2.0	12.7	12.757	6.8	30.0	22.3	1.3	1.7	2.986
S-8	8.5	2.0	13.0	12.762	0.5	30.0	22.5	17.0	1.7	0.001
S-9	8.5	2.0	12.9	12.576	5.8	30.0	23.2	1.5	1.7	1.872
S-10	8.5	2.0	12.8	12.576	5.8	30.0	23.2	1.5	1.7	2.635
S-11	18.0	2.0	12.5	12.801	7.9	31.0	22.0	2.3	3.6	4.677
S-12	18.0	2.0	12.8	12.849	7.5	31.0	22.0	2.4	3.6	3.995
S-13	18.0	2.0	12.9	12.861	4.4	31.0	22.0	4.1	3.6	0.811
S-14	18.0	2.0	13.9	12.300	2.8	31.0	23.4	8.2	3.7	0.215
S-15	18.0	2.0	14.0	12.302	0.9	31.0	23.4	20.0	3.7	0.008

Table 4.2: (a) Summary of Measurements of Jet Trajectories in Coflows

exp. no.	7	8	12	13	14	15	16	17	18	19
x/D_o					z/D_o					
5	0.0		2.0	1.0	1.1	3.0	0.6	0.0	0.0	0.5
10	0.0	0.05	5.0	3.0	2.8	6.2	2.0	0.5	0.0	1.5
15	0.6	1.0	8.5	8.5	5.3	12.0	5.0		0.1	
20	1.0	1.5	13.0	10.0	9.0	21.0	21.0	1.0	0.5	2.8
25	1.5	3.0		20.0	15.0			2.5		
30		4.0	21.0					3.5	1.5	4.5
35	3.5	6.0								
40		8.0						5.8	2.8	7.0
45	6.3	10.5								
50		13.0						9.0	4.7	10.0
55	9.5	16.5								
60		21.0						13.7	6.7	16.5
65	14.5									
70								19.5		21.0
75	21.0								10.7	

Table.4.2: (b) Summary of Measurements of Jet Trajectories in Coflows

S-2		S-3		S-4		S-5		S-6		S-7		S-8	
x	z	x	z	x	z	x	z	x	z	x	z	x	z
(cm)		(cm)		(cm)		(cm)		(cm)		(cm)		(cm)	
3.3	2.0	6.7	1.3	3.8	0.5	4.7	1.3	2.6	0.4	2.6	0.5	2.6	0.5
10.0	4.6	12.0	4.0	4.6	0.7	10.0	3.7	12.6	1.9	7.6	1.8	12.6	3.75
17.3	10.0	21.3	6.0	7.6	1.5	12.6	9.3	22.6	5.6	12.6	3.2	22.6	9.0
21.3	15.0	26.0	7.7	14.6	3.3	24.7	13.3	32.6	15.0	17.6	4.3	32.6	18.0
24.7	20.0	35.3	11.3	17.6	4.8	28.7	17.3	43.0	18.8	22.6	5.9	34.0	19.5
		44.7	16.0	24.6	6.0					32.6	9.4		
		48.0	18.0	34.6	10.0					42.6	13.1		
				44.6	10.7					52.6	17.3		
				54.6	14.7					55.6	18.8		
				64.0	20.0								

Table.4.2: (c) Summary of Measurements of Jet Trajectories in Coflows

S-9		S-10		S-11		S-12		S-13		S-14		S-15	
x	z	x	z	x	z	x	z	x	z	x	z	x	z
(cm)		(cm)		(cm)		(cm)		(cm)		(cm)		(cm)	
2.6	0.8	2.6	0.5	4.6	0.4	4.6	0.4	4.6	1.2	4.6	2.4	4.6	0.8
7.6	1.1	7.6	0.8	9.6	1.7	9.6	1.3	14.6	3.9	14.6	8.2	14.6	6.4
12.6	1.8	12.6	0.9	14.6	2.4	14.6	2.3	24.6	6.9	24.6	16.6	24.6	15.8
17.6	5.3	17.6	1.1	19.6	3.8	24.7	4.6	34.6	9.8	27.8	19.6	27.0	19.2
22.6	4.1	22.6	2.6	24.6	4.8	34.6	7.6	44.6	13.6				
32.6	6.4	32.6	4.6	34.6	7.6	44.6	10.8	53.5	17.6				
42.6	9.0	42.6	7.5	44.6	10.8	54.6	14.4						
52.6	12.6	52.6	10.4	54.6	14.0	63.4	17.6						
62.6	17.3	62.6	13.7	60.4	16.8								
68.0	19.9	72.6	17.3										
		75.5	19.0										

Table 4.3: Summary of Measurements of Dilutions in Coflows

exp. no.	7	8	12	13	14	15	16	17	18	19
x/D_o	$\Delta\rho_m/\Delta\rho_o$									
5	0.68		0.32	0.31	0.41	0.25	0.26	0.33	0.38	0.55
10	0.29	0.32		0.15	0.23	0.10	0.09	0.26	0.13	0.15
15	0.22		0.09	0.08	0.05	0.08	0.07			
20		0.11	0.06	0.06		0.03	0.04	0.15	0.08	0.07
25	0.12									
30		0.09	0.03	0.03		0.02		0.10	0.06	0.04
35	0.09									
40		0.07						0.07		
45	0.07									
50		0.05						0.04	0.04	0.02
55	0.05									
60		0.04						0.03		
65	0.05									
70								0.03	0.03	
75	0.03									

Table 4.4: Summary of Measurements of Centerline Velocities in Coflows

exp. no.	x/D_o	5	10	20	30	40	50	60	70
7	u_m/u_o	0.80	0.49	0.21	0.13	0.10	0.07	0.06	0.05
10	u_m/u_o	0.84	0.48	0.24	0.14	0.08			
18	u_m/u_o	0.82	0.44	0.21	0.14	0.10	0.08	0.07	0.06

Some of the photographies on the jet trajectories from the present experiments are reproduced in Fig. 4.4. The measured jet trajectories, centerline densities, centerline velocities, and density contours in the y-z plane are plotted and compared with mathematical models' predictions in Chapter 5, section 5.3. For the sake of convinence and simplification, the measurements will not be plotted separately in this chapter.
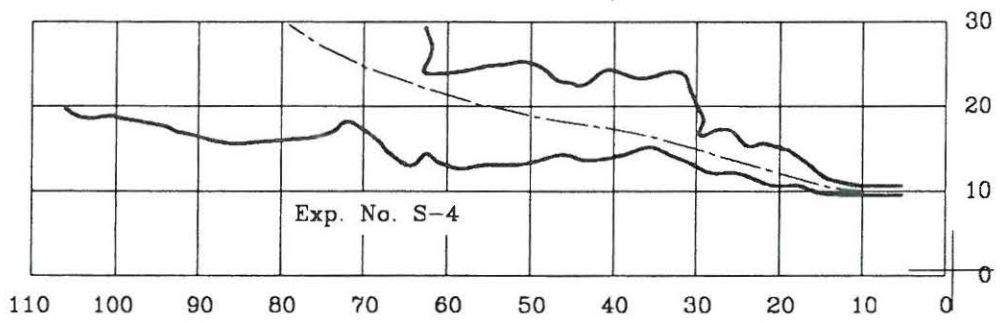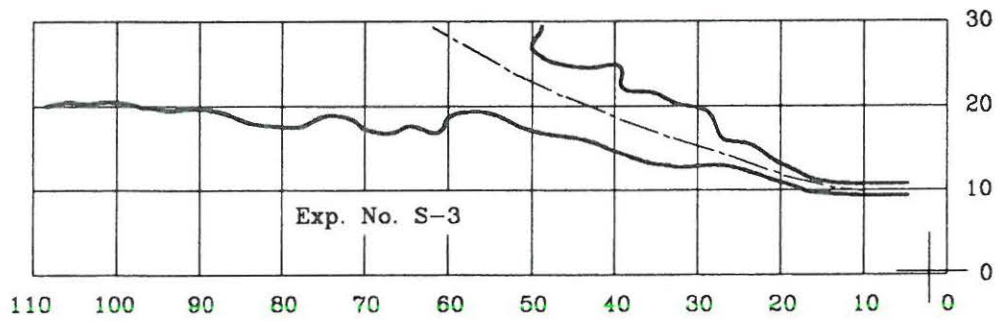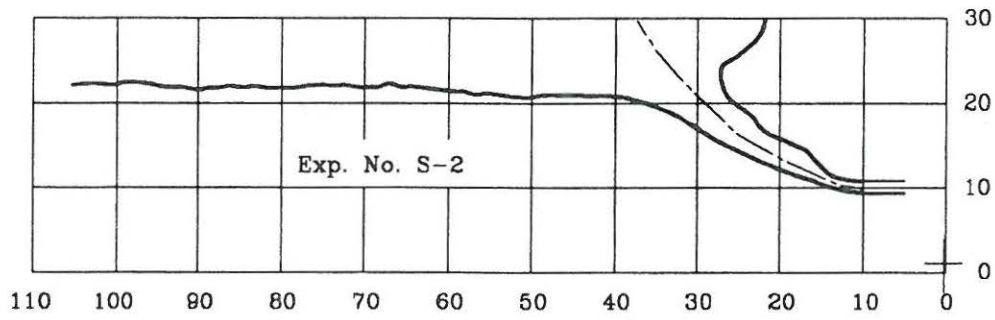
Figure 4.4: (a) Reproduced Photographies for Jet Trajectories in Coflows (unit: cm)

50
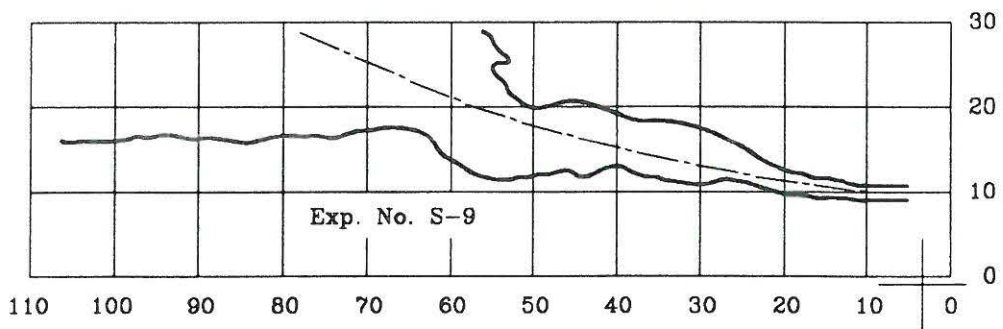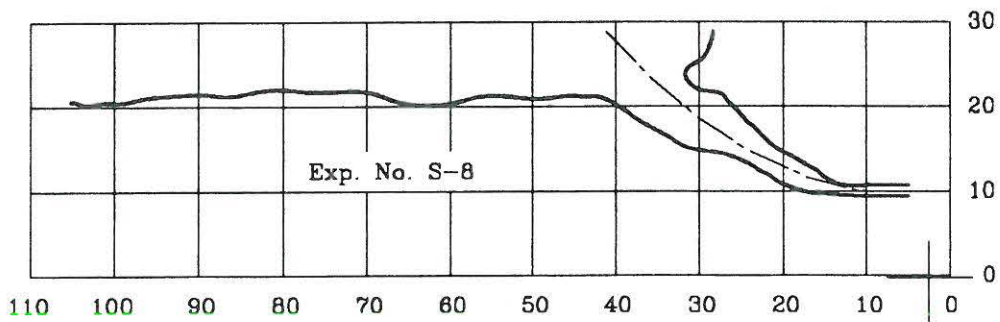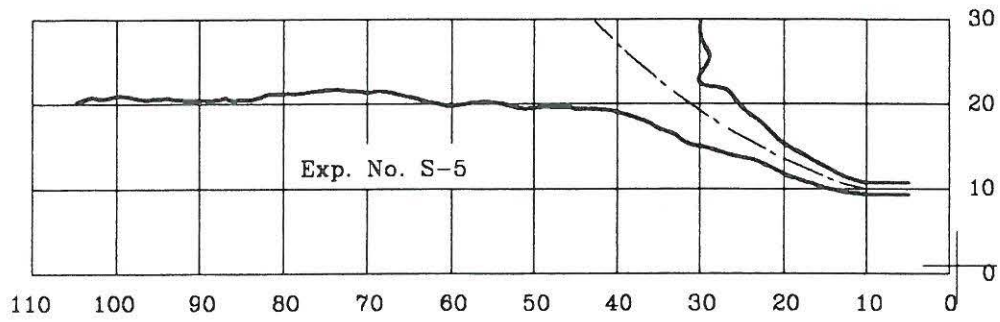
Figure 4.4: (b) Reproduced Photographies for Jet Trajectories in Coflows (unit: cm)
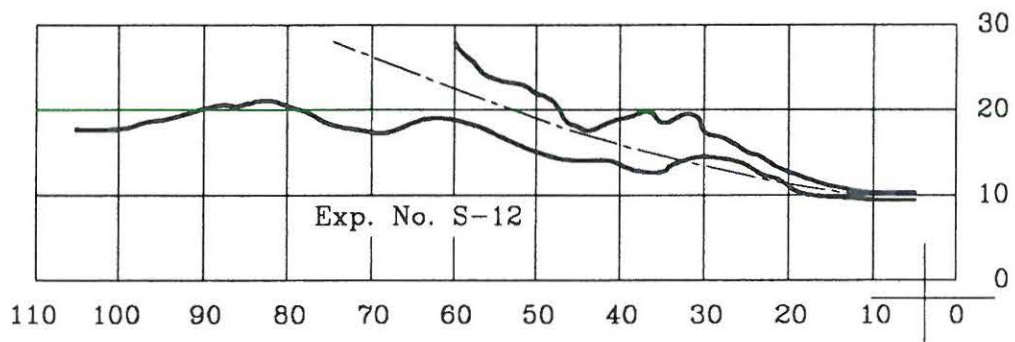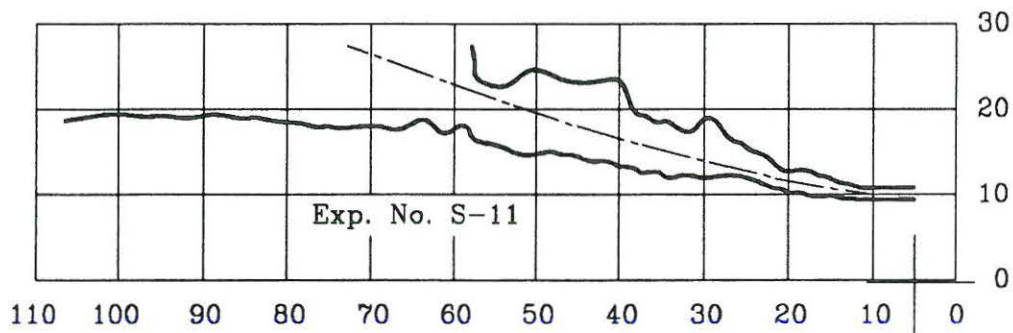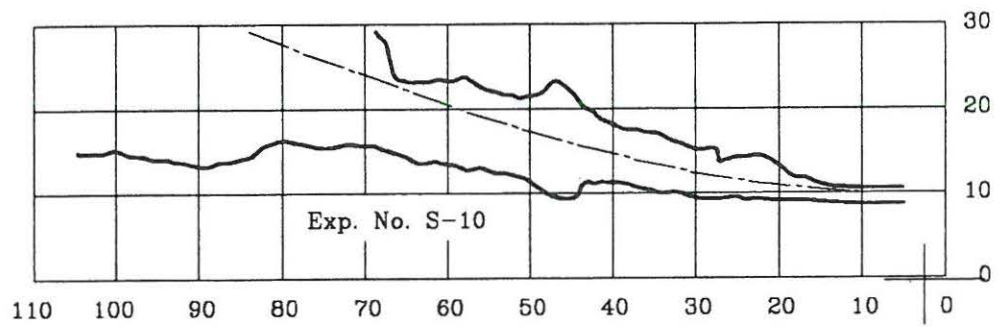
Figure 4.4: (c) Reproduced Photographies for Jet Trajectories in Coflows (unit: cm)
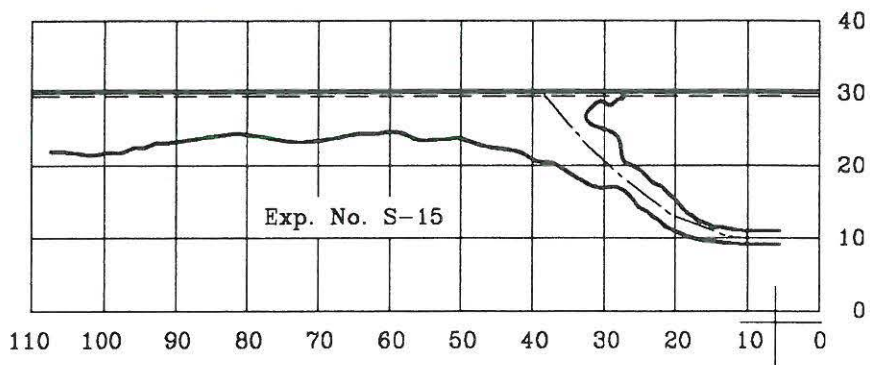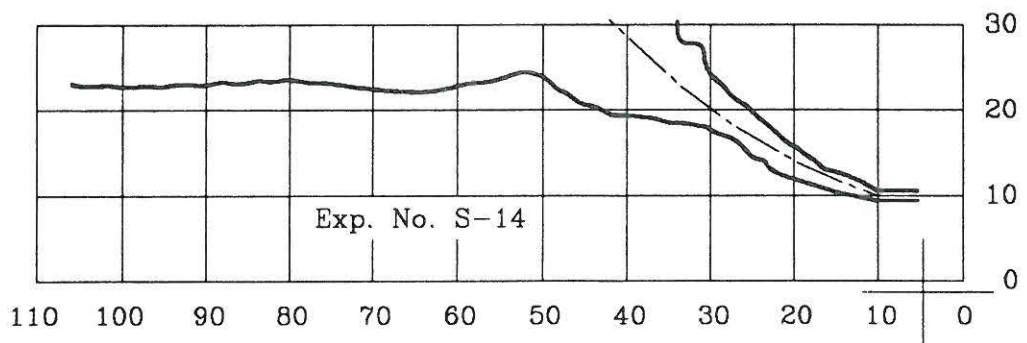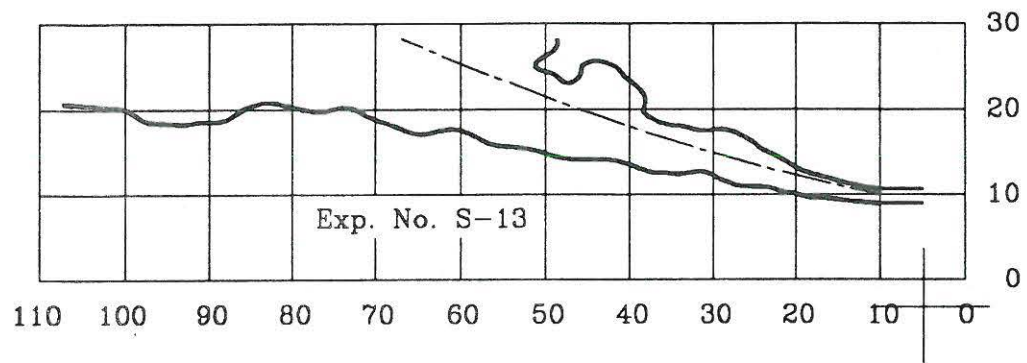
52

Figure 4.4: (d) Reproduced Photographies for Jet Trajectories in Coflows
(unit: cm)

53

4.3 Analyses of Experimental Data

The present experiment results will be analysized and presented in association with the available data by previous researchers in terms of length of zone of flow establishment, jet trajectory, dilution, stability criterion for upstream wedge, and plume height and width.

4.3.1 Length of Zone of Flow Establishment

A simple jet is the turbulent flow generated by a continuous source of pure momentum definded in chapter.3. It is observed in the experiment, Albertson, Dai, et al (1950), that the length of the zone of flow establishment is approximately equal to 6.2 times of the diameter of the jet nozzle and was adopted to buoyant jet by Fan (1967) and commenly accepted by many other researchers.

However, a turbulent buoyant jet is the turbulent flow generated by a source of both momentum and buoyancy. The basic mechanics of the flow in the vicinity of the nozzle is in principle the same as a simple jet flow. There is also a zone of flow establishment exsiting and the velocity and concentration profiles are developed from uniform to Gaussian distributions as well. But it is interesting to point out that the length of the zone of flow establishment for a buoyant jet is shorter than that generally assumed to occur for a simple jet. It is found in the experiments that the length of the zone of flow establishment is approximately equal to (4.0 - 4.5) Do, where the Do is the diameter of the jet nozzle as shown in Fig. 4.5.

It seems that there are different possible explanations for the shorter length of the zone of flow establishment for the buoyant jet. One of the possible reasons could be that the discharge pipe and the nozzle in the present experiment probably introduced considerable turbulence in the jet, resulting in a greater mixing with the ambient fluid than that would be presented for a jet though a smooth nozzle (see Fig. 4.6).
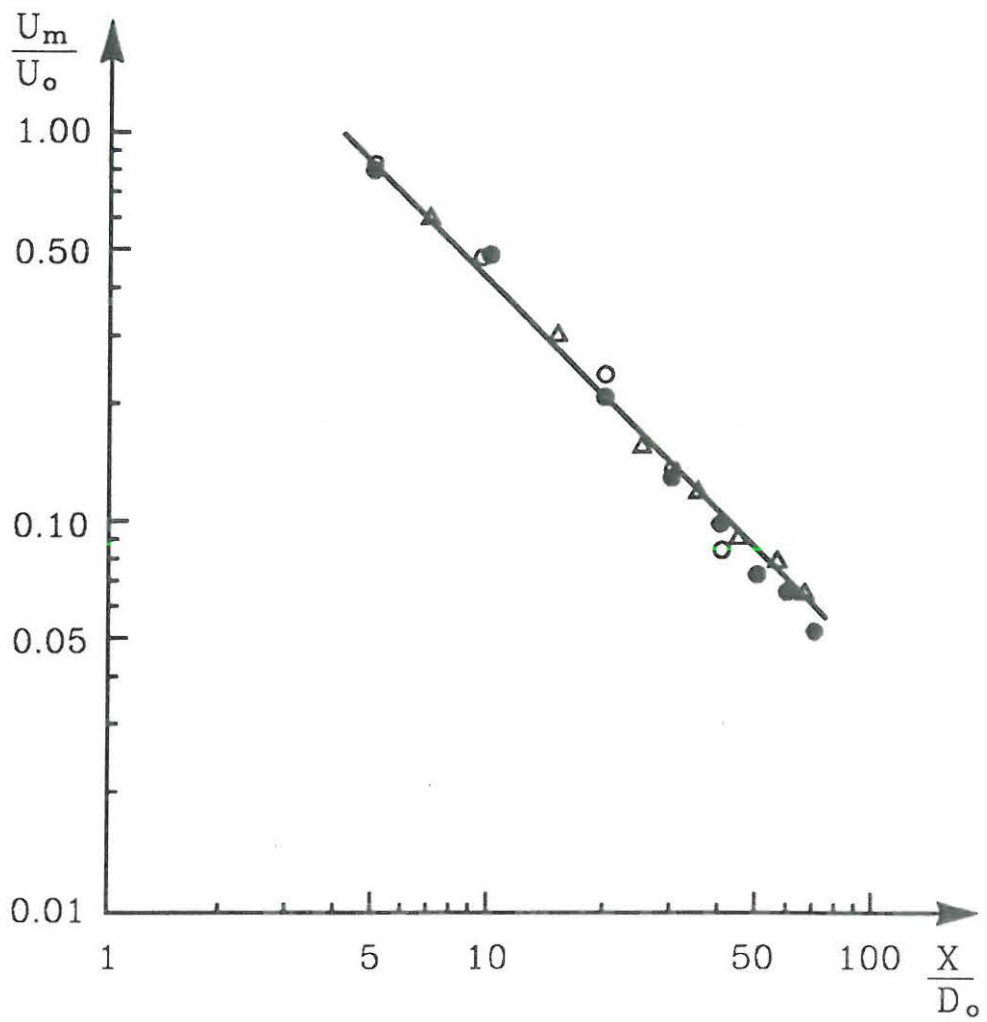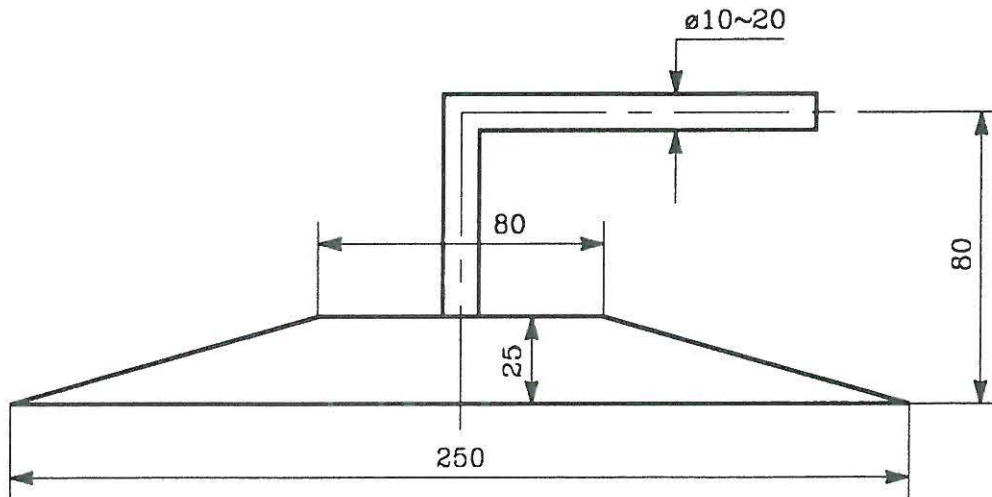
Figure 4.5: Length of Zone of Flow Establishment

Figure 4.6: The Nozzle of the Discharge (unit: mm)

The second reason for the shorter length of the zone of flow establishmet may be that the entrainment within the zone of flow establishment is stronger in the presence of ambient flow than the entrainment in a stagnant flow. The third explanation for the shorter length of the zone of the flow establishment observated in the buoyant jet experiments would be that most of the previous experimental results have been obtained from the experimental medium with air but not water. The two experimetal medium have different properties.

4.3.2 Jet Trajectories

Horizontal Jets in Coflowing Ambients

In the analysis of jet trajectories, the turbulent buoyant jets in a coflowing fluid have been classified into momentum dominated flow and buoyancy dominated flow according to the ratio between the momentum length scale L_m and the buoyancy lenghth scale L_b. For $L_m/L_b > 1.0$, the jets are subject to momentum dominated flow, contradictorily, for $L_m/L_b < 1.0$, the jets are defined as buoyancy dominated flow. In addition, the buoyancy dominated flows are further divided into strongly and weakly buoyancy dominated flows, depending upon either $L_m/L_b < 0.25$ or $L_m/L_b > 0.25$ in the present experimental analysis since the fact that the constants in the jet trajectory correlations are found to be a function of L_m/L_b.

The measured jet trajectories in coflows are normalized by either momentum length scale L_m or buoyancy length scale L_b, depending on the ratio of L_m/L_b greater or less than unit. The present laboratory data on jet trajectories in coflows are plotted in Fig. 4.7 for momentum dominated flows and in Fig. 4.8 for buoyancy dominated flows.

It is evident from the experimental results that the trajectories of either momentum or buoyance dominated flow can be successfully correlated using the momentum or buoyancy length scales. It appears that the jet trajectories for momentum dominated flow follows a power law of 3/2 and for the buoyancy dominated flow obeys a power law of 5/3 with different constants. The power exponents and constants are obtained using the least square method on the basis of analyzing the experimental data.

For Momentum Dominated Flow

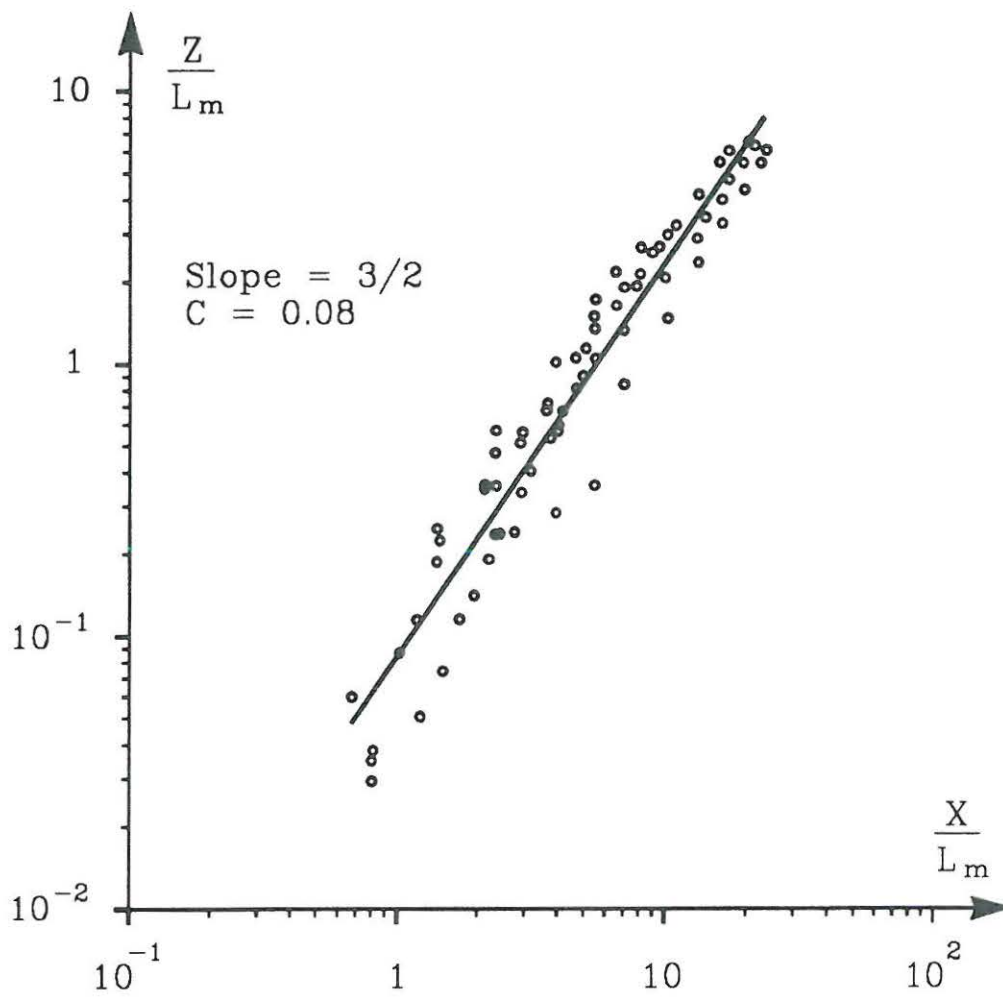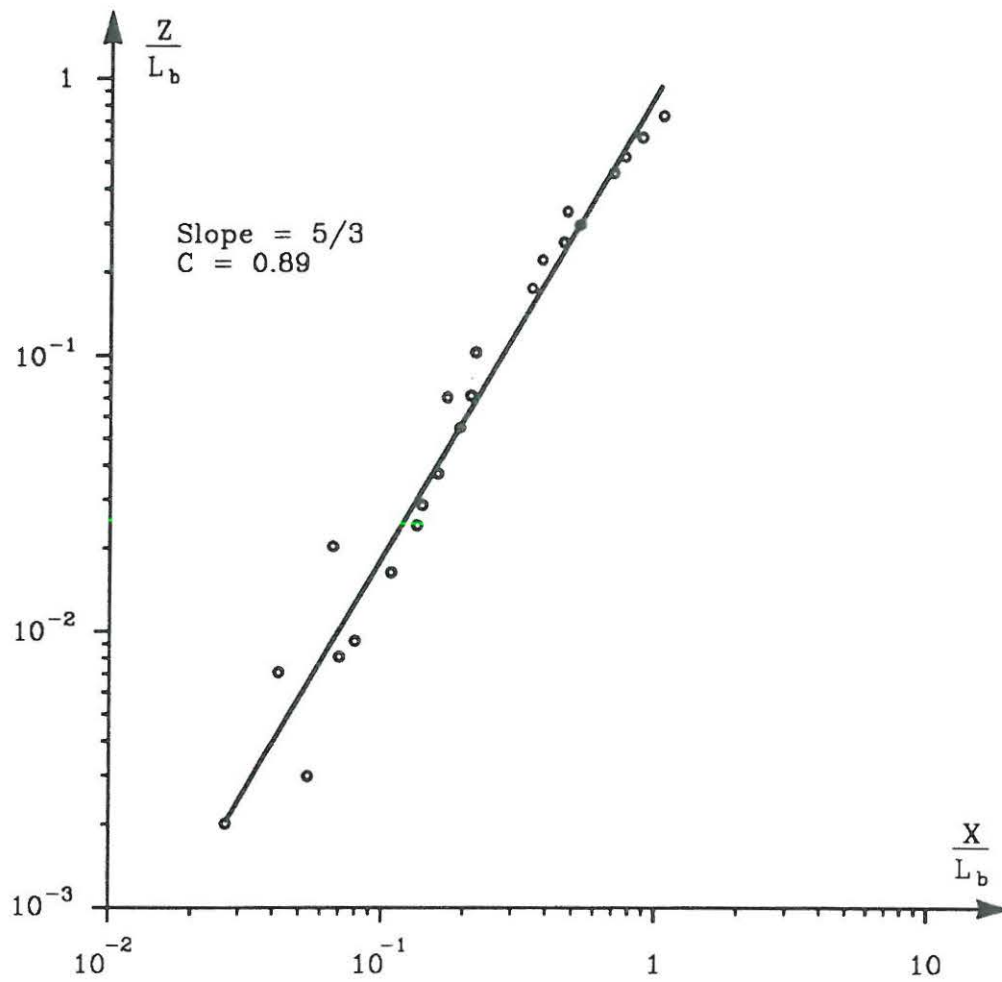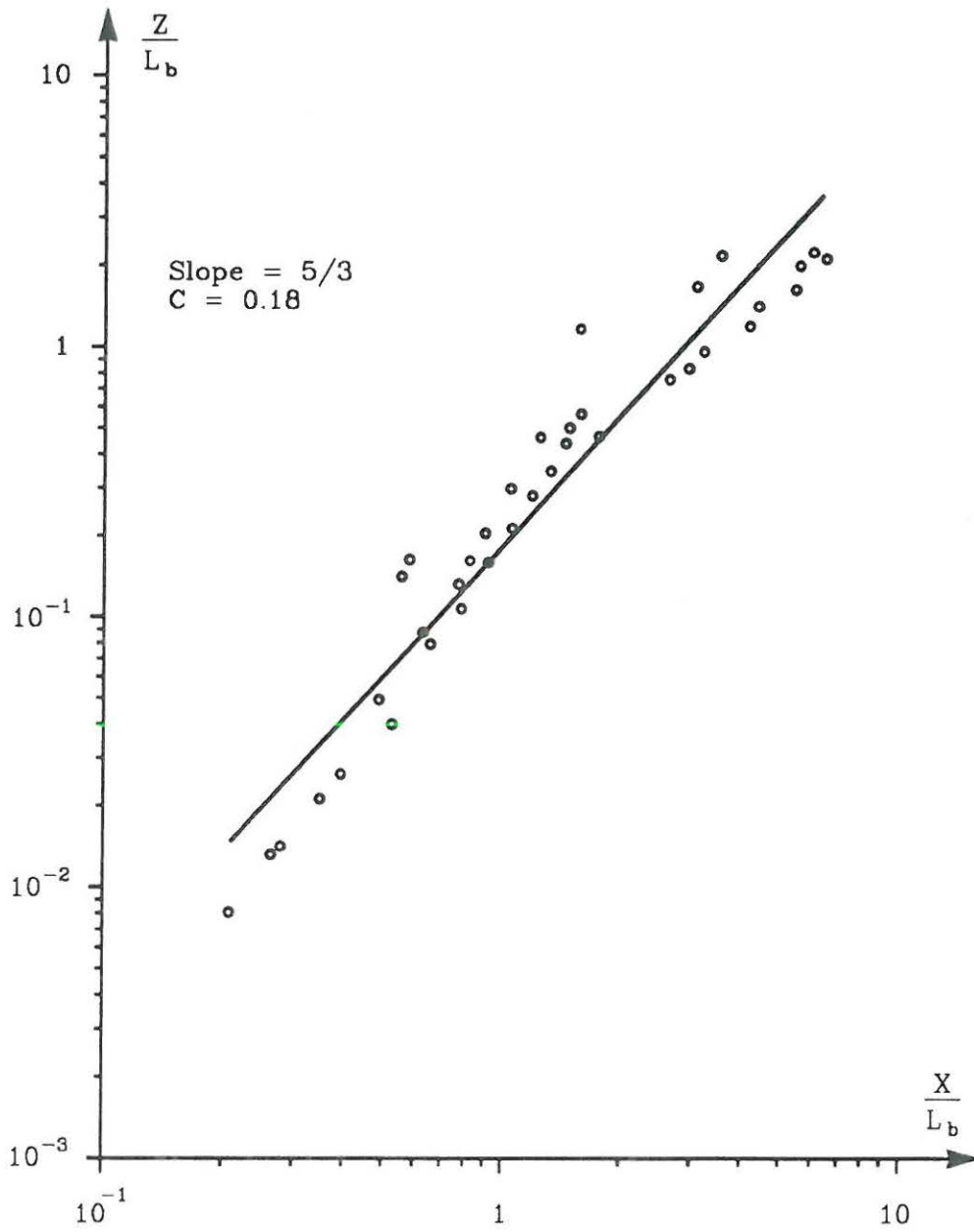$$\frac{z}{L_m} = C_1 \left(\frac{x}{L_m} \right)^m \tag{4.2}$$

57

Figure 4.7: Jet Trajectories for Momentum Dominated Flow in Coflows

58

Strongly Buoyancy Dominated Flow ($L_m/L_b < 0.25$)

Figure 4.8: (a) Jet Trajectories for Buoyancy Dominated Flow in Coflows

Weakly Buoyancy Dominated Flow ($L_m/L_b > 0.25$)

Figure 4.8: (b) Jet Trajectories for Buoyancy Dominated Flow in Coflows

in which, m = 3/2 and C_1 is a function of L_m/L_b. From the experimental results, it shows that $C_1 = 0.08$ for $L_m/L_b > 1.0$.

For Buoyancy Dominated Flow

$$\frac{z}{L_b} = C_2(\frac{x}{L_b})^n \tag{4.3}$$

in which, n = 5/3 and C_2 is a function of L_m/L_b . From the experimental results, it has been found that $C_2 = 0.89$ for $L_m/L_b < 0.25$ (strongly buoyancy dominated flow) and $C_2 = 0.18$ for $0.25 < L_m/L_b < 1.00$ (weakly buoyancy dominated flow).

Vertical Jets in Crossflowing Currents

The vertical buoyant jets and plumes in a crossflow have been studied by various investigators, for example, Fan(1967), Chu(1975), Wright(1977), Holly and Jirka(1985),as well as Knudsen and Wood(1988). The availabe data from two comprehensive experimental studies conducted by Fan and Wright are used here to analyze the vertical jet trajectories in a cross-flowing ambient.

The jet trajectories for both momentum and buoyancy dominated flows are correlated using the momentum and buoyancy length scales and shown in Fig. 4.9 and Fig. 4.10, respectively.

It is found from the experimental studies that the jet trajectories of either momentum or buoyance dominated flow can be well correlated using the momentum or buoyancy length scales. It demonstrates that the trajectories for momentum dominated flow follows a power law of 1/2 in the near field and 1/3 in the far field. For buoyancy dominated flow, it obeys a power law of 3/4 in the near field and 2/3 in the far field with different constants. The power exponents and constants are visually obtained by fiting the experimental data.
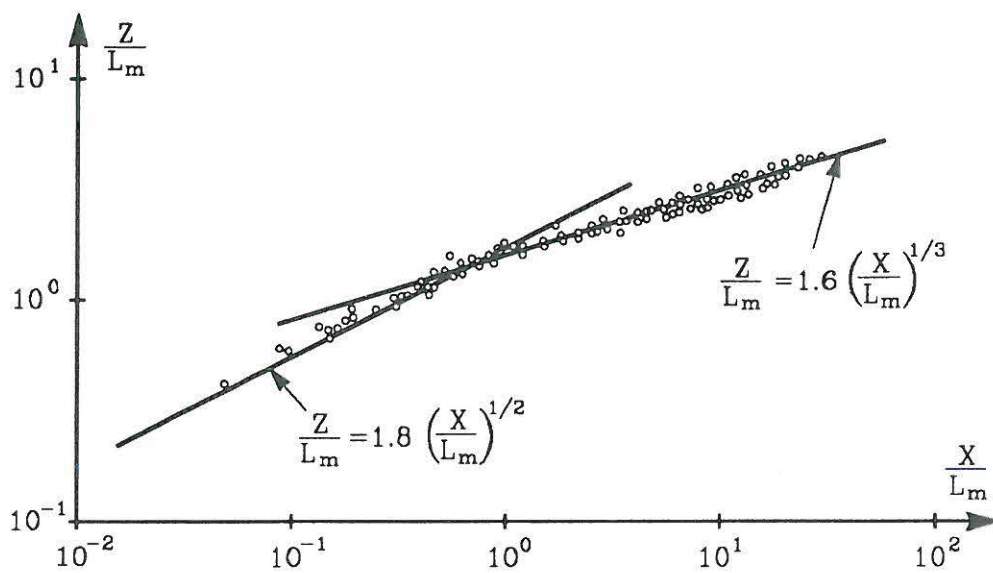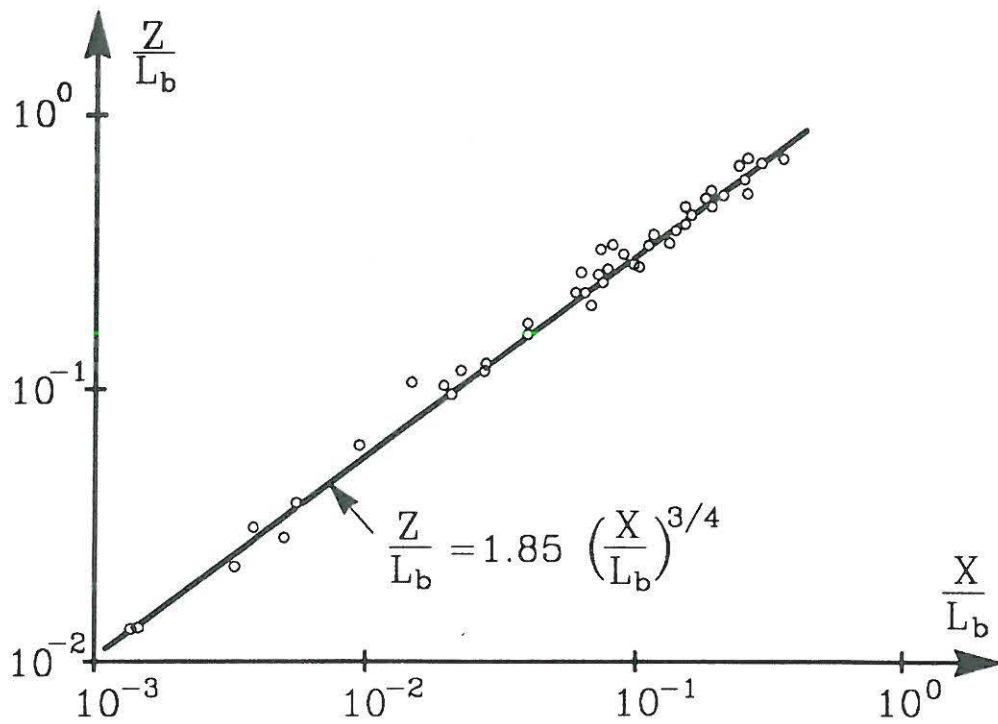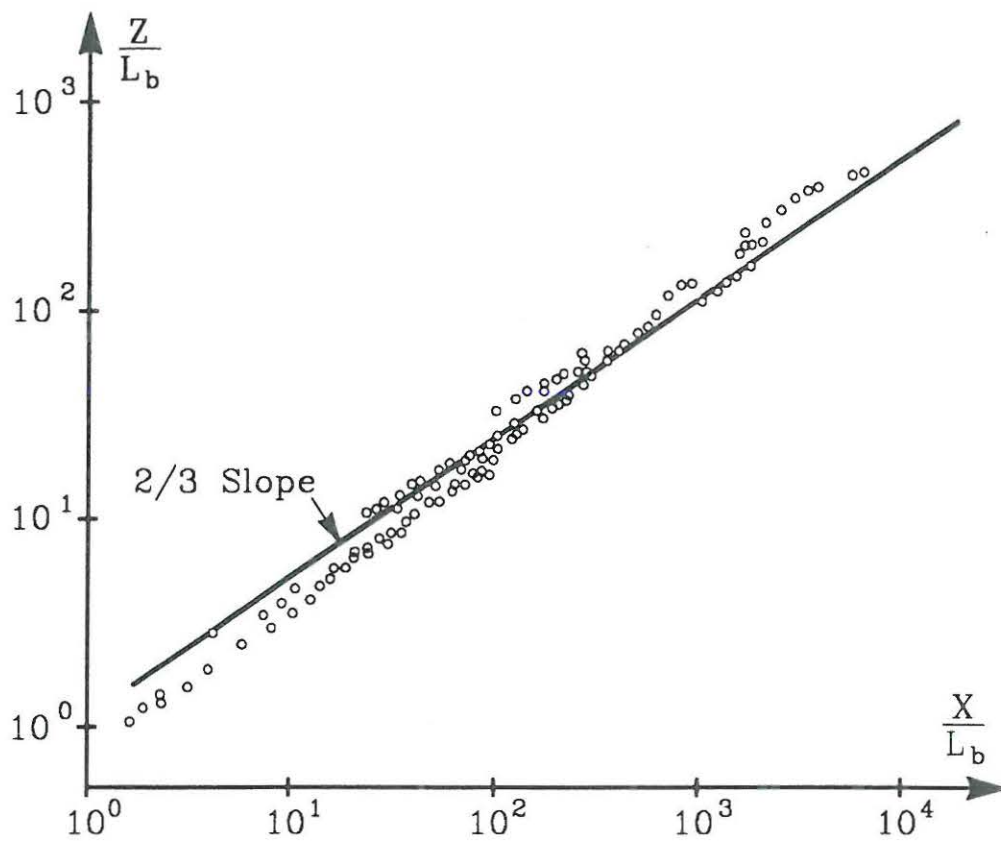
61

Figure 4.9: Jet Trajectories for Momentum Dominated Flow in Cross-flows, after Wright(1977)

$$\frac{Z}{L_b} = 1.85 \left(\frac{X}{L_b}\right)^{3/4}$$

(a) Near Field

Figure 4.10: (a) Jet Trajectories for Buoyancy Dominated Flow in Cross-flows, after Wright(1977)

63

(b) Far Field

Figure 4.10: (b) Jet Trajectories for Buoyancy Dominated Flow in Cross-flows, after Wright(1977)

For Momentum Dominated Flow

$$\frac{z}{L_m} = C_3 \left(\frac{x}{L_m}\right)^p \qquad (4.4)$$

in which, for the momentum dominated near filed, p = 1/2 and for the momentum dominated far field, p = 1/3 and the constant C_3 is a function of L_m/L_b. From the experimental results, it has been found that $C_3 = 1.8 \sim 2.3$ in the near field and $C_3 = 1.6 \sim 2.1$ in the far field, respectively.

For Buoyancy Dominated Flow

$$\frac{z}{L_b} = C_4 \left(\frac{x}{L_b}\right)^k \qquad (4.5)$$

in which, k = 3/4 and 2/3 for buoyancy dominated near and far fields respectively, and C_4 is a function of L_m/L_b as well. From the experimental results, it seems that

$$
\begin{aligned}
C_4 &= 1.35 \sim 1.8 && (\ near\ field\ ) \\
C_4 &= (0.85 \sim 1.40)\left(\tfrac{L_m}{L_b}\right)^{1/6} && (\ far\ field\ )
\end{aligned}
$$

Summary of Jet Trajectories

As a matter of fact, the basic configurations of the jet trajectories can be outlined as two-dimensional and three-dimensional ones. The situations of horizontal jet in a coflow and vertical jet in a crossflow are with two-dimensional trajectories and horizontal jet in a perpendicular crossflow is an example with three-dimensional trajectory.

It has been found that the jet trajectories for both momentum and buoyancy dominated flows can be successfully correlated using the momentum and buoyancy length scales. The correlations of jet trajectories for horizontal jet in coflows and vertical jet in crossflows found from the experimental studies are summarized in Table 4.5.

Table 4.5: Summary of Jet Trajectory Relations

Type and Regime	Relation	Exponent	Constant
Horizontal Jet in Coflow			
MDF	$(z/L_m) = C_1(x/L_m)^m$	$m = 3/2$	$C_1 = 0.08$
BDF			
Strongly BDF	$(z/L_b) = C_2(x/L_b)^n$	$n = 5/3$	$C_2 = 0.89$
Weakly BDF		$n = 5/3$	$C_2 = 0.18$
Vertical Jet in Crossflow			
MDNF		$p = 1/2$	$C_3 = 1.8 \sim 2.3$
MDFF	$(z/L_m) = C_3(x/L_m)^p$	$p = 1/3$	$C_3 = 1.6 \sim 2.1$
BDNF		$k = 3/4$	$C_4 = 1.35 \sim 1.8$
BDFF	$(z/L_b) = C_4(x/L_b)^k$	$k = 2/3$	$C_4 = (0.85 \sim 1.4)(\frac{L_m}{L_b})^{1/6}$

Note:
1) For horizontal jet in coflow: $L_m = M^{3/4}/B^{1/2}$;
2) For vertical jet in crossflow: $L_m = M^{1/2}/u_a$;
3) Abrivations:

        MDF: Momentum Dominated Flow;
        BDF: Buoyancy Dominated Flow;
        MDFF: Momentum Dominated Far Field;
        MDNF: Momentum Dominated Near Field;
        BDFF: Buoyancy Dominated Far Field;
        BDNF: Buoyancy Dominated Near Field;

4.3.3 Jet Dilutions

The dilution is one of the most important parameters to be determined in the experiments because it is necessary to predict the concentration at some specified locations from the outlet in the engineering design of sea outfalls and in the water quality standard requirenment for the sake of environmental protection.

Following the same idear as indicated in determination of the jet trajectories, the turbulent buoyant jets and plumes are categorized into buoyancy dominated flow and momentum dominated flow. The dimensionless dilution parameters are, for the momentun dominated flow, SQu_a/M, and for the buoyancy domenated flow, $g'B/u_a^5$ and $SQ/L_b u_a^2$. The reasons for selecting these dimensionless variables are refered to Chapter. 3, section 3.1. Dimensional Analysis.

Horizontal Jets in Coflowing Environments

The experimental data on jet dilutions are correlated by using of the previously mentioned dimensionless parameters against the normalized dimensionless water depth z/L_b or z/L_m upon to the types of the flows. The dilution for the momentum dominated flow dominated flow is presented in Fig. 4.11 and the dilution for buoyancy dominated flow is shown in Fig. 4.12 (a),(b) by defining the dilution for buoyancy dominated flow in Eq.(4.7) and Eq.(4.8), respectively.

It is demonstrated in Fig. 4.11 and 4.12 that the dilutions for both momentum and buoyancy dominated flows can be reasonably well correlated by using the fluxes Q, M, B and the length scales of L_m and L_b.

For Momentum Dominated Flow

$$\frac{SQu_a}{M} = C_5 \left(\frac{z}{L_m}\right)^r \tag{4.6}$$

67

in which, $r = 2/3, C_5 = 8.28$.

For Buoyancy Dominated Flow

$$g'B/u_a^5 = C_6(\frac{z}{L_b})^q \qquad (4.7)$$

or

$$\frac{SQ}{L_b^2 u_a} = C_7(\frac{z}{L_b})^l \qquad (4.8)$$

in which, $q = -4/5, l = 4/5$; and $C_6 = 2.59, C_7 = 0.38$.

Vertical Jets in Crossflowing Ambients

The experimental data by Wright and Fan on the jet dilutions are correlated by using of the previously mentioned dimensionless dilution parameter against the normalized dimensionless water depth z/L_b or z/L_m upon to the types of the flows. The dilutions for the momentum dominated flow and buoyancy dominated flow are shown in Fig. 4.13 and 4.14, respectively.

It is demonstrated in Fig. 4.13 and 4.14 that the dilutions can be successfully correlated by using the fluxes Q, M, B and the length scales of L_m and L_b.

For Momentum Dominated Flow

$$\frac{SQu_a}{M} = C_8(\frac{z}{L_m})^i \qquad (4.9)$$

in which, i = 1 and $C_8 = 0.35$ in the near field and i = 2, and $C_8 = 0.14$ in the far field.
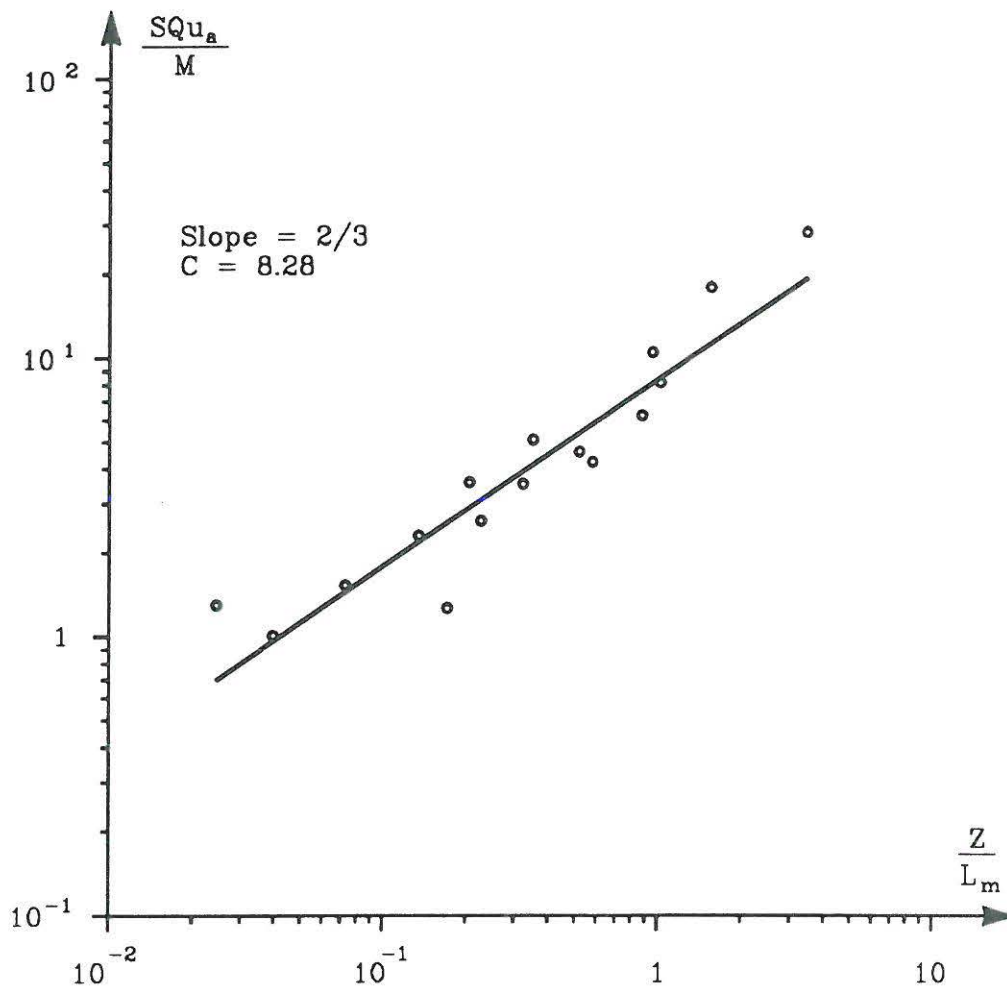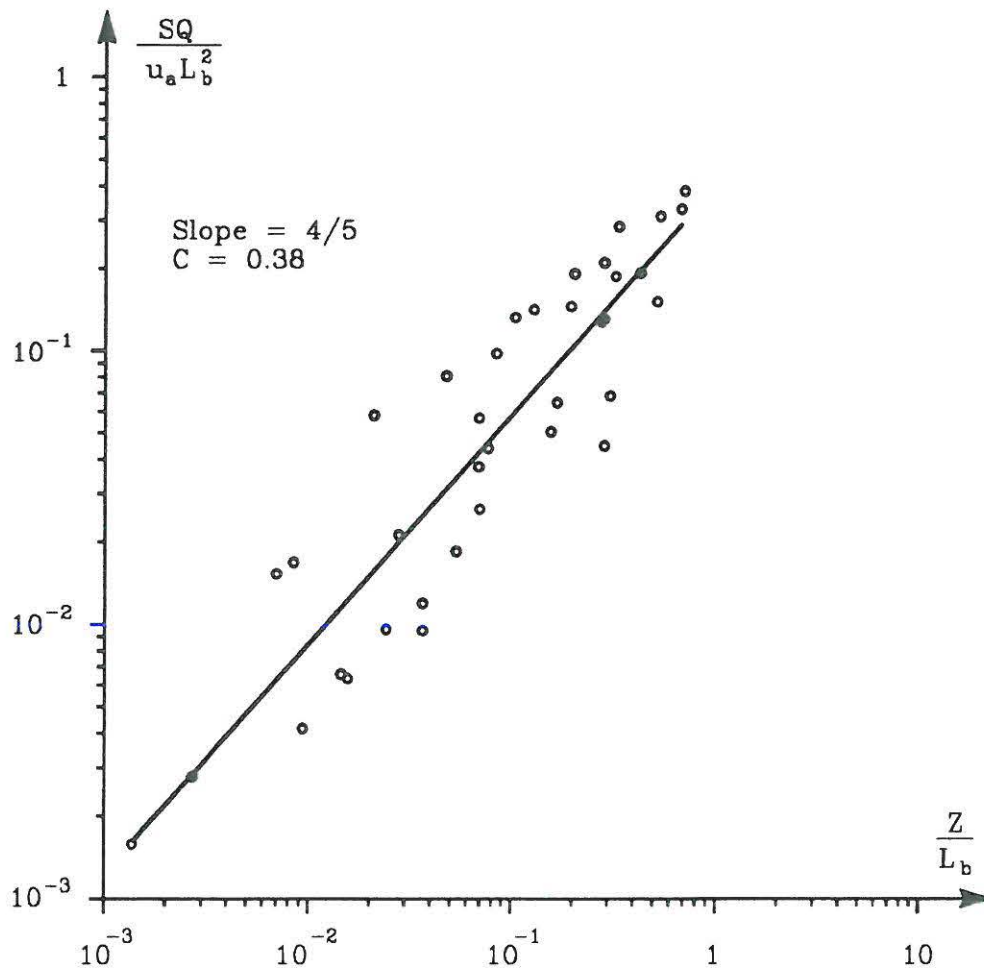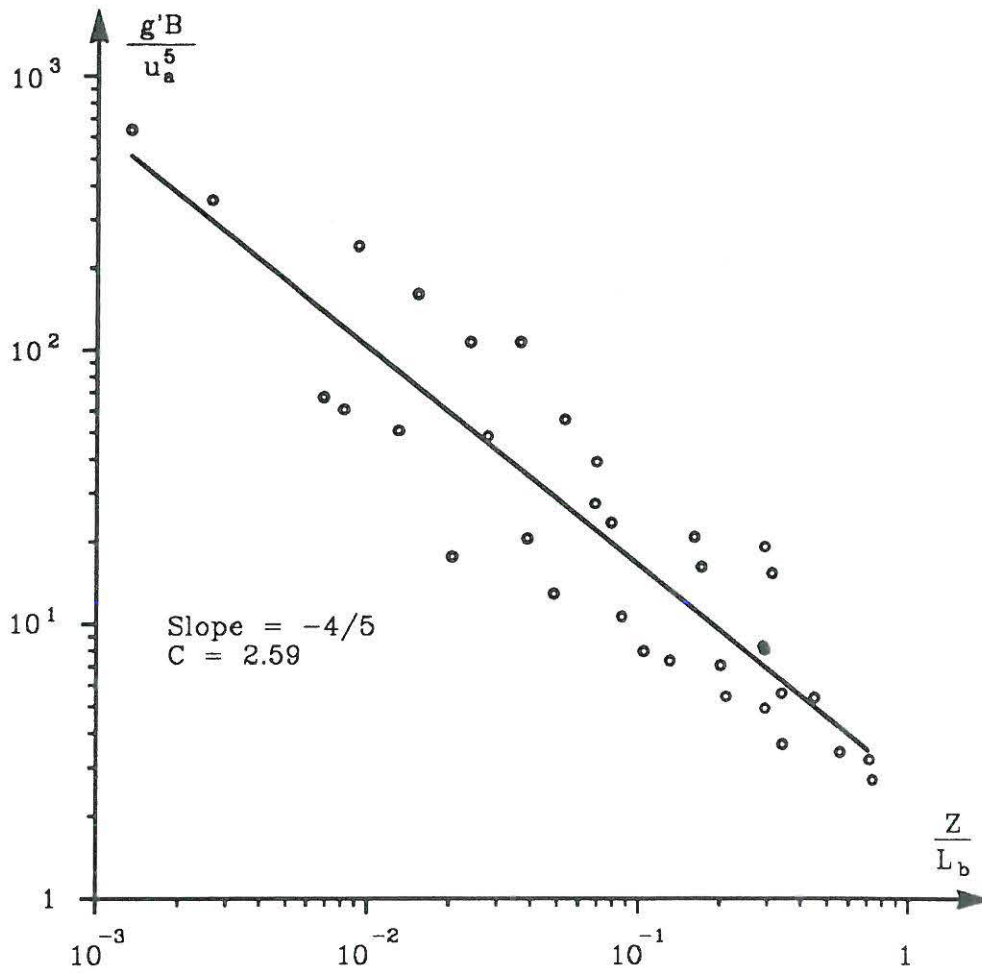
Figure 4.11: Dilutions for Momentum Dominated Flow in Coflows

(a) Dilution in Term of $SQ/u_a L_b^2$

Figure 4.12: (a) Dilutions for Buoyancy Dominated Flow in Coflows

(b) Dilution in Term of $g'B/u_a^5$

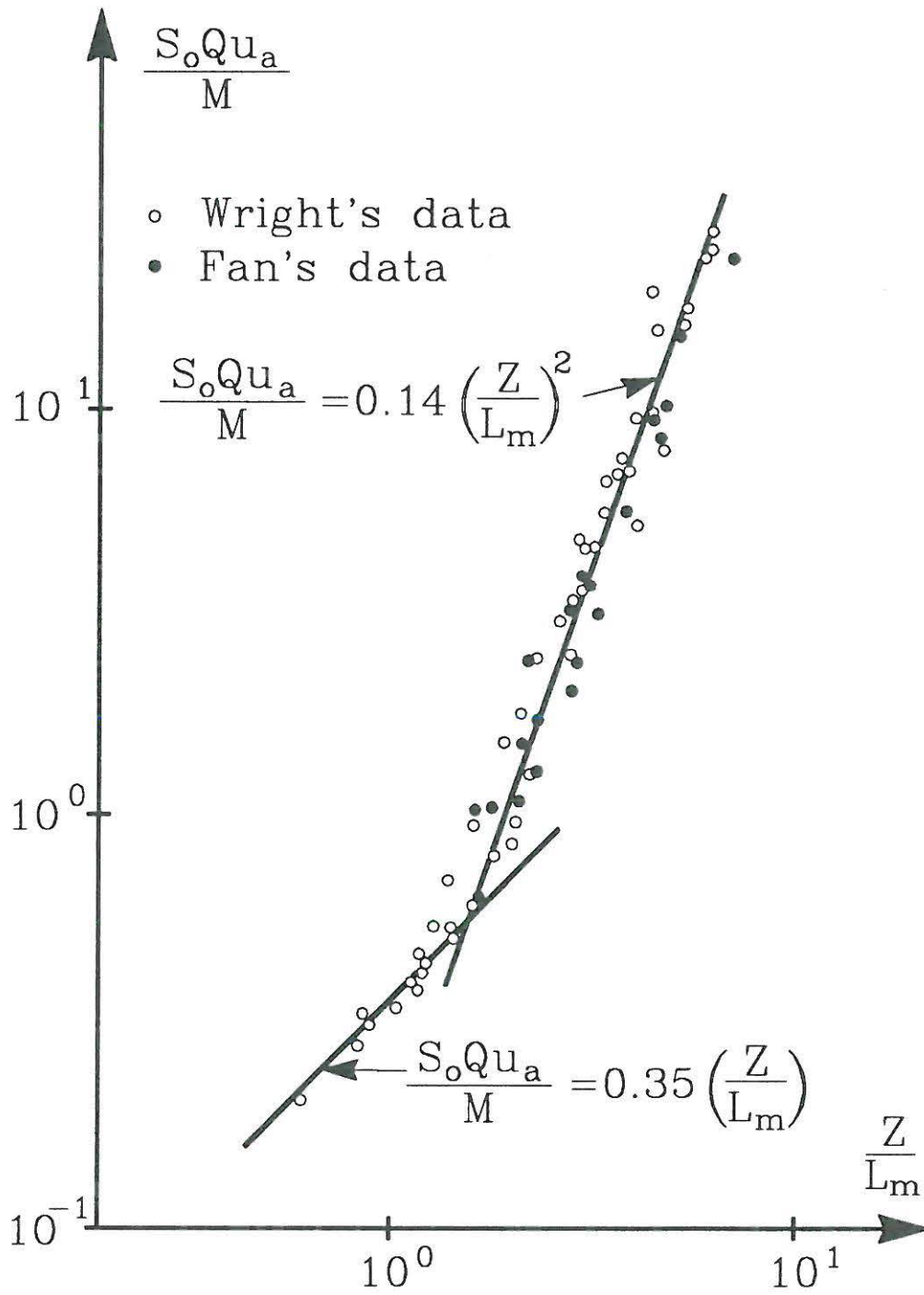Figure 4.12: (b) Dilutions for Buoyancy Dominated Flow in Coflows

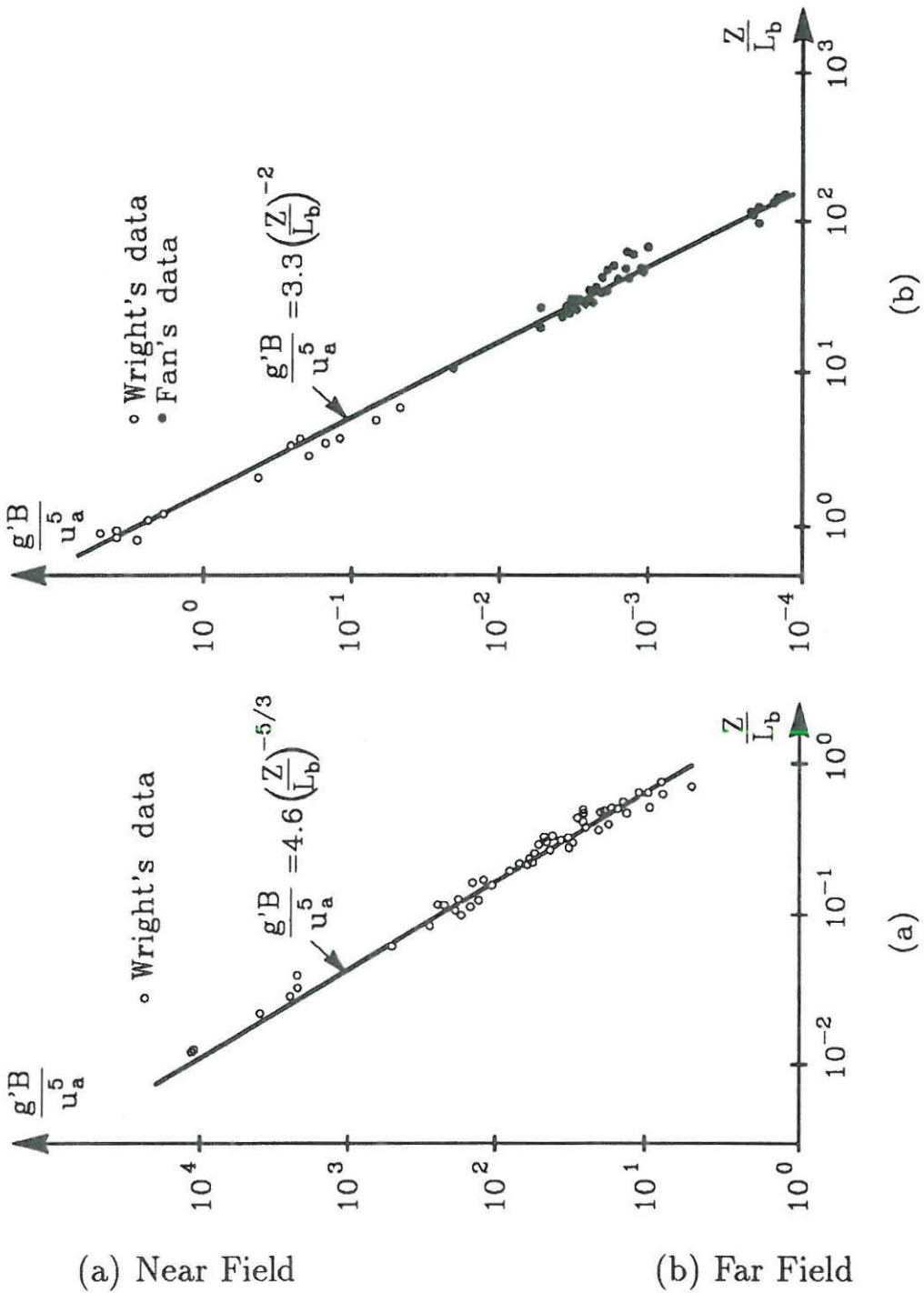Figure 4.13: Dilutions for Momentum Dominated Flow in Crossflows

72

Figure 4.14: Dilutions for Buoyancy Dominated Flow in Crossfolws

73

Types and Regime	Relation	Exponent	Constant
Horizontal jets in coflows			
MDNF	$SQu_a/M = C_5(z/L_m)^r$	$r = 2/3$	$C_5 = 8.28$
BDNF	$g'B/u_a^5 = C_6(z/L_b)^q$	$q = -4/5$	$C_6 = 2.59$
Vertical jets in crossflows			
MDNF	$SQu_a/M = C_8(z/L_m)^q$	$i = 1$	$C_8 = 0.35$
MDFF		$q = 2$	$C_8 = 0.14$
BDNF	$g'B/u_a^5 = C_9(z/L_b)^j$	$j = -5/3$	$C_9 = 4.6$
BDFF		$j = -2$	$C_9 = 3.3$
Horizontal jets in crossflows			
BDNF	$SQ/u_a L_b^2 = C_{10}(z/L_b)^t$	$t = 5/3$	$C_{10} = 0.31$
BDFF		$t = 2$	$C_{10} = 0.32$

Note: Table 4.6 caption "Table 4.6: Summary of Jet Dilution Relations" appears above the table.

<u>For Buoyancy Dominated Flow</u>

$$g'B/u_a^5 = C_9(\frac{z}{L_b})^j \qquad (4.10)$$

in which, $j = -5/3, C_9 = 4.6$ in the near field and $j = -2, C_9 = 3.3$ in the far field.

Summary of Jet Dilutions

It seems that the jet dilutions may be defined by different ways and follow different power laws depending on the types of flows and the jet dilutions can be reasonably well correlated using the mometum and buoyancy fluxes and length scales.

The dilution relations for horizontal jets in coflowing ambients, for vertical jets in crossflowing environments and for horizontal jets in perpendicular crossflowing currents are summarized in Table. 4.6.

4.3.4 Stability of Upstream Wedge

A series of experiments were performed in order to verify the theoretical stability criteria derivated in chapter. 3 for the upstream wedge. It has been found in the present laboratory studies that a stable upstream wedge is formed under the condition of surface plume densimetrical Froude number $F_{\Delta s} = u_a{}^2 / \Delta\rho / \rho_a g H_a \leq 0.3 \sim 0.4$, in which, H_a is the total ambient water depth. The upstream wedge created by the submerged turbulent buoyant jet will be completely expired if $F_{\Delta s} \geq 1.0$ and an unstable upstream wedge will be likely to appear when the densimetrical Froude number is in the range of $0.4 \sim 1.0$. The flow regimes found in the experiment can be categorized into three types with stable, unstable and no upstream wedges. The experimental results are summarized in Table. 4.7. and plotted in Fig. 4.15.

Table 4.7: Stability of Upstream Wedge

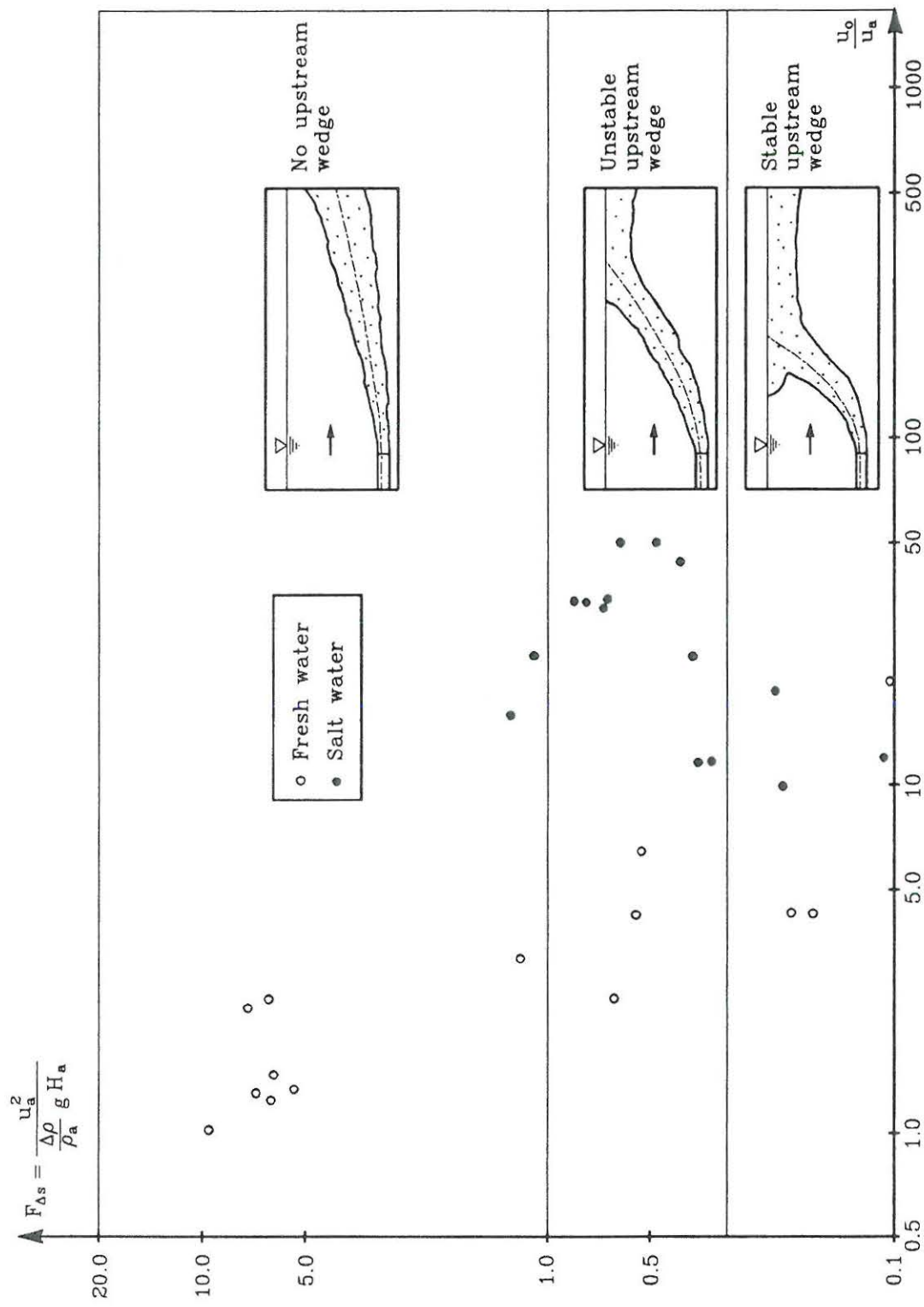| Stability Condition	Flow Regimes
$F_{\Delta s} \leq 0.3 \sim 0.4$	Stable upstream wedge
$0.4 \leq F_{\Delta s} < 1.0$	Unstable upstream wedge
$F_{\Delta s} \geq 1.0$	No upstream wedge

Figure 4.15: Stabilities of Upstream Wedges

76

4.3.5 Plume Height and Width

The experimental data on plume heights and widths are analyzed by calculating the variances of the measured cross-sections:

$$\sigma_y^2 = \frac{\sum_{i=1}^{m} \sum_{j=1}^{n} (y - \bar{y})^2 \Delta\rho_{ij} \Delta y_i \Delta z_j}{M_o} \tag{4.11}$$

$$\sigma_z^2 = \frac{\sum_{i=1}^{m} \sum_{j=1}^{n} z^2 \Delta\rho_{ij} \Delta y_i \Delta z_j}{M_o} \tag{4.12}$$

in which,

$$M_o = \sum_{i=1}^{m} \sum_{j=1}^{n} \Delta\rho_{ij} \Delta y_i \Delta z_j$$

$$\bar{y} = \sum_{i=1}^{m} \sum_{j=1}^{n} y_i \Delta\rho_{ij} \Delta y_i \Delta z_j$$

In order to ensure the measurements correct the total mass budget is checked against the initial discharged mass by comparing the terms of $\int\int_{A_o} \Delta\rho_o u_o dA$ and the zeroth mememnt M_o. Theoretically, the following equation should be valid:

$$\int\int_{A_o} \Delta\rho_o u_o dA = \int\int_A \Delta\rho u_a dy dz \tag{4.13}$$

based on the assumption that the temperature and density difference obey a linear relation, i.e. $\Delta\rho = \beta\Delta T$, where, β is a constant.

Using the calculated variances and assuming Gaussain profiles the measured data on the center profiles both in vertical and horizontal directions can be well fit with the assumed curve. Examples are shown in
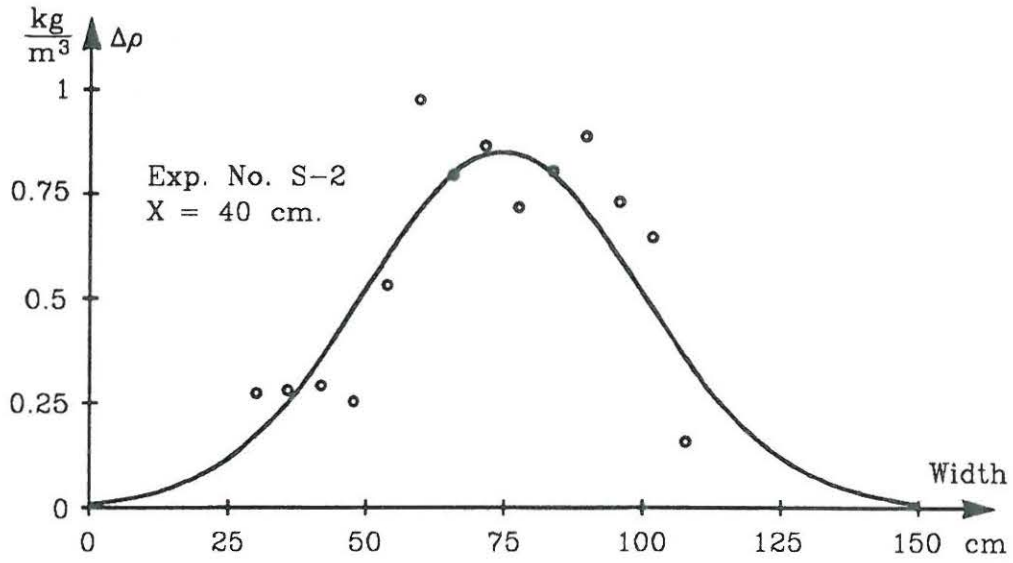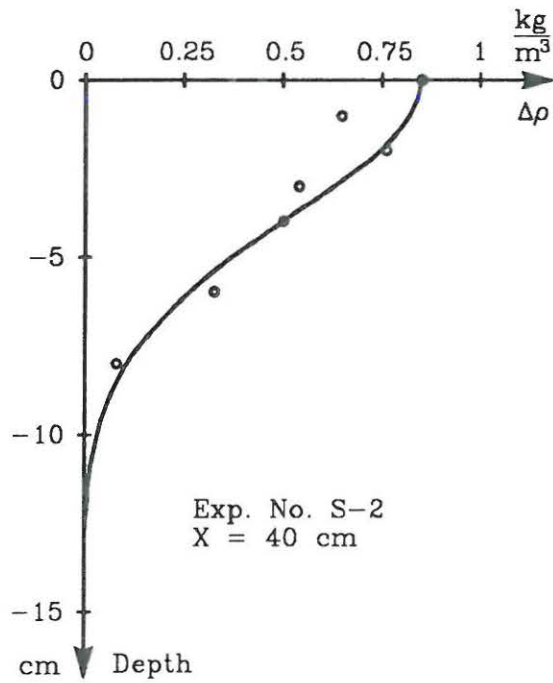
77
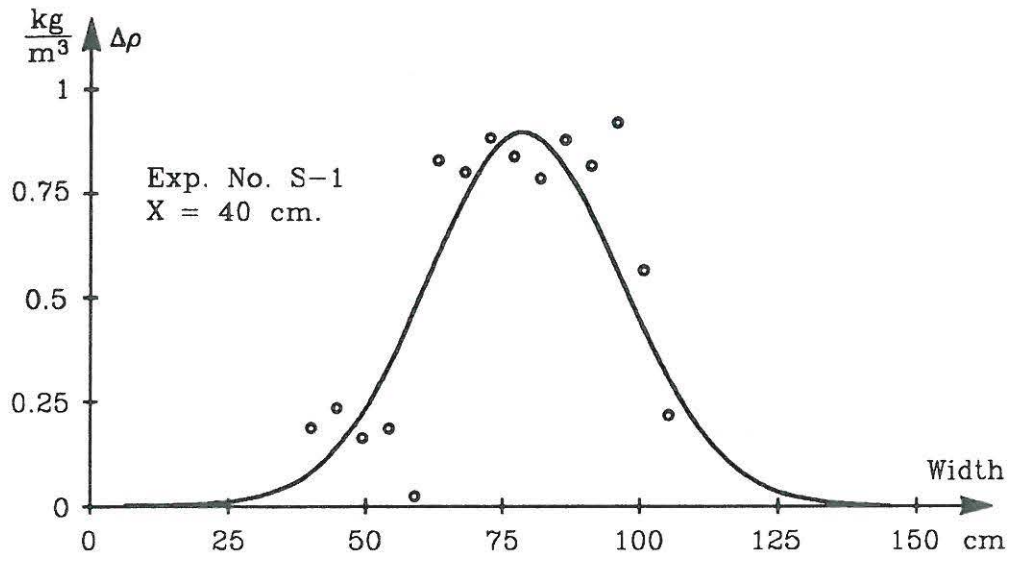
(a) Horizontal Profile
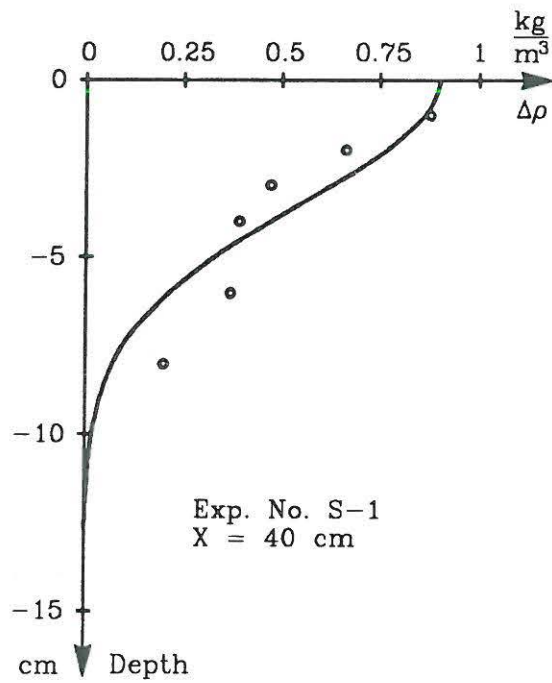
(b) Vertical Profile

Figure 4.16: (A) Measured Profiles Data fit with Gaussain Curve

78

(a) Horizontal Profile

(b) Vertical Profile

Figure 4.16: (B) Measured Profiles Data fit with Gaussain Curve

Fig. 4.16.

The height of the surface plume introduced by the submerged buoy-ant jet is found to be related to the densimetrical Froude number $F_{\Delta s} = u_a{}^2/\Delta\rho/\rho_a g H_a$. The experimental data on the plume heights are plotted in Fig. 4.17 and compared with the theory. It shows that the experi-mental data agree fairly well with the theory derivated by applying the front velocity driven by the buoyant force, see chapter 3, section 3.2.3.

The experimental data on plume width are domenstrated in Fig. 4.18 and comparied with the theory in Chapter 3. It should be pointed out that the dilution in the theory is the average dilution defined as $S_o = Q/Q_o$ but in the analysis of the experimental data on the plume width the minimun centerline dilution $S_{min} = \Delta\rho_o/\Delta\rho_m$ is used instead.

In fact, the plume width is closely related to the ambient current velocity, the residual jet mometum and the front velocity driven by the buoyancy force. It is observed in the experiments that the plume will be suddenly expended while the jet hits the free water surface and carried downstream by the ambient current. The phenomene of bifurcation of the plume was sometime found in the experiemnts as described by Fisher et al (1979).
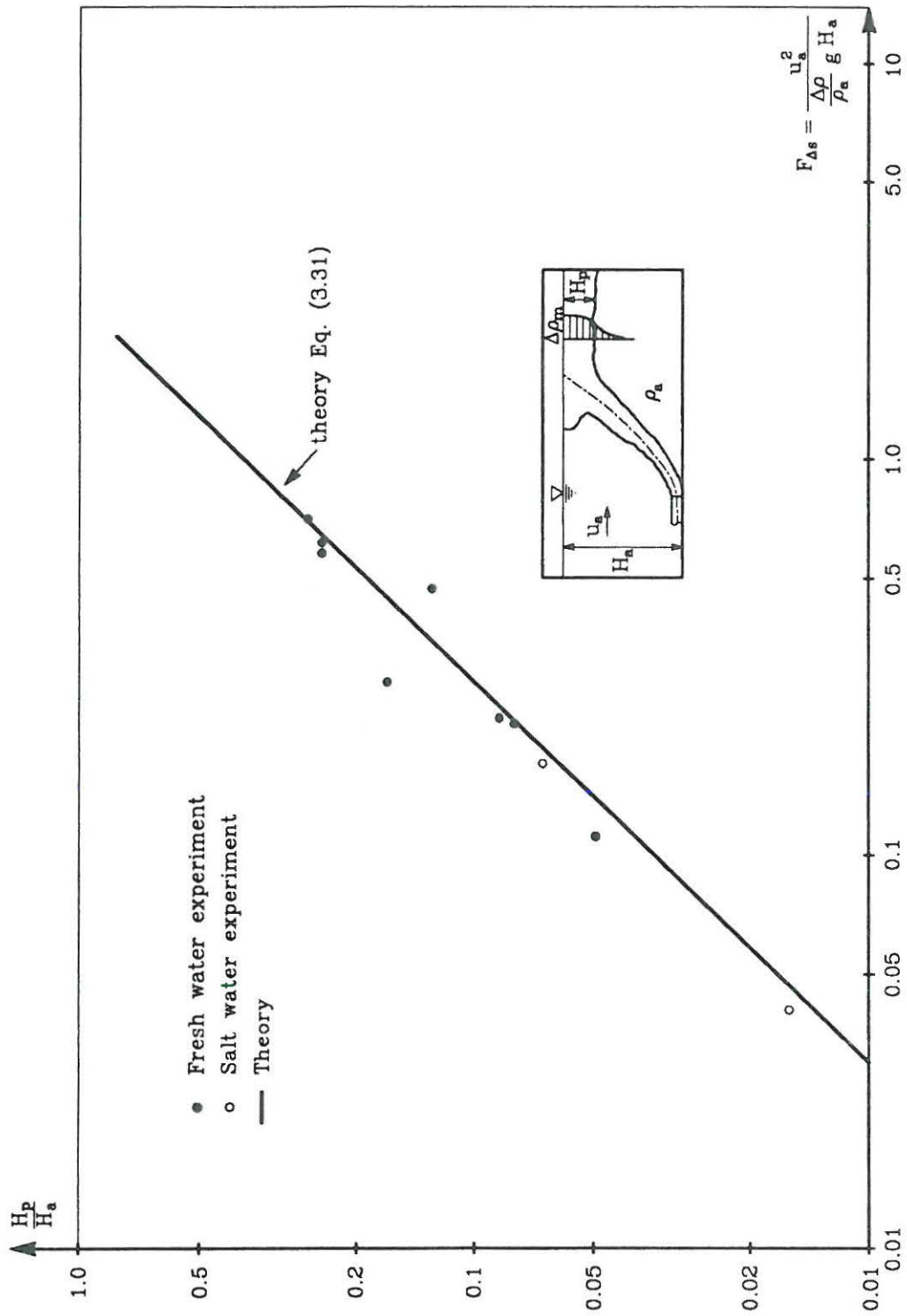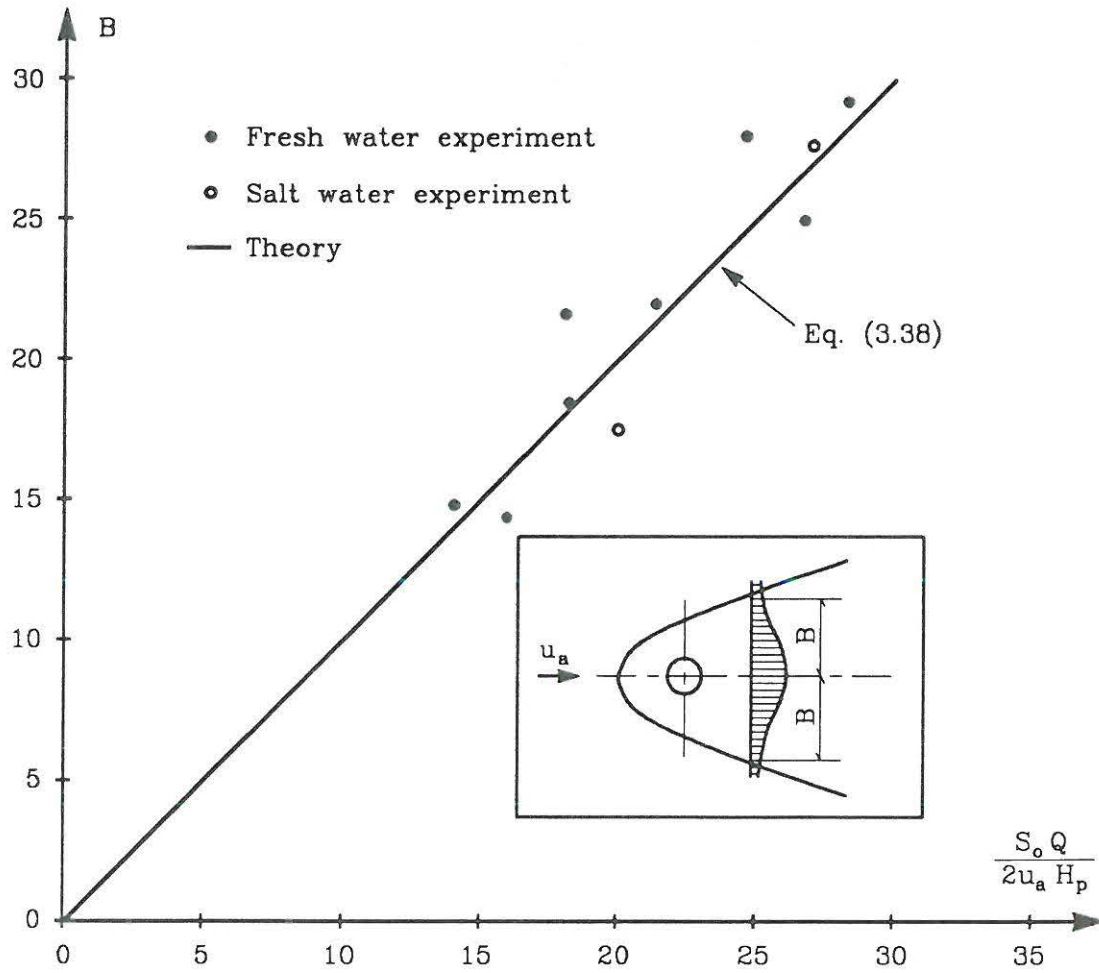
Figure 4.17: Experimental Data on Plume Heights

81

Figure 4.18: Experimental Data on Plume Widths

4.4 Field Investigations

4.4.1 Data Sources

Comprehensive field investigations were undertaken by the Water Research Centre at six outfall sites (1969-70, 1981), Ref.[3] and at the Hastings sea outfall by the South Water Authority(1979-80),Ref.[7,8] in U.K. The observated data on initial dilutions of horizontal jets in a perpendicular crossflow are summarized by Lee and Neville-Jones(1987), as shown in Table 4.8 and Table 4.9.

Table 4.8: Reduced Field Data Used in Empirical Correlation of Initial Dilution. Gosport and Bridport Outfalls, Ref.[3]

Gosport Outfall ($D_o = 0.91$ m)					
Experiment number	Data sample size	Tidal mean velocity (m/s)	Jet velocity (m/s)	Depth/diameter ratio (H/D_o)	Mean dilution at sewage boil
1	6	0.30	0.42	17.5	79
2	8	0.70	0.46	17.0	246
3	10	0.81	0.41	17.0	184
4	20	0.76	0.45	16.8	151
5	24	0.66	0.41	16.8	109
6	16	0.74	0.43	16.9	289
7	24	0.33	0.42	16.7	32
8	20	0.11	0.42	17.0	17
Bridport outfall C ($D_o = 0.38$ m)					
Experiment number	Data sample size	Tidal mean velocity (m/s)	Jet velocity (m/s)	Depth/diameter ratio (H/D_o)	Mean dilution at sewage boil
1	8	0.10	0.36	20.0	46
2	19	0.22	0.36	20.0	170
3	12	0.25	0.40	17.0	226
4	20	0.22	0.37	16.0	93
4	8	0.29	0.37	16.7	208
5	20	0.26	0.39	20.5	155
5	8	0.18	0.39	20.0	88
6	16	0.25	0.45	21.5	179
6	8	0.23	0.45	20.0	133

Table 4.9: Summary of Relevant Parameters for Outfall Dilution Data

Outfall site and diameter	Water Depth over diffuser (m)	Ambient velocity u_a (m/s)	Jet velocity u_o (m/s)	Measured minimum dilution (time)
Sidmouth ($D_o = 0.91$ m)	3.7 - 6.8	0.07 - 0.23	0.11 - 0.14	6 - 21
Gosport ($D_o = 0.9$ m)	15.2 - 15.9	0.11 - 0.81	0.41 - 0.46	14 - 183
Bridport ($D_o = 0.38$ m)	6.1 - 8.2	0.10 - 0.29	0.36 - 0.45	41 - 225
Jaywick ($D_o = 0.305$ m)	2.2 - 4.3	0.28 - 0.95	0.50 - 1.33	23 - 521
Hastings 1979 ($D_o = 0.158$ m)	9.0 - 15.6	0.05 - 0.4	0.53 - 1.36	185 -1765
Hastings 1980 ($D_o = 0.158$ m)	6.1 - 14.6	0.03 - 0.42	0.21 - 2.79	39 -2275

4.4.2 Initial Dilutions

The observated data on initial dilutions were correlated by introducing the momentum and buoyancy fluxes by Lee and Neville-Jones(1987). It seems that the initial dilution for a horizontal jet in a perpendicular cross-flowing ambient follows a power law of 5/3 in the buoyancy dominated near field and of 2 in the buoyancy dominated far field, respectively, as shown in Fig. 4.19.
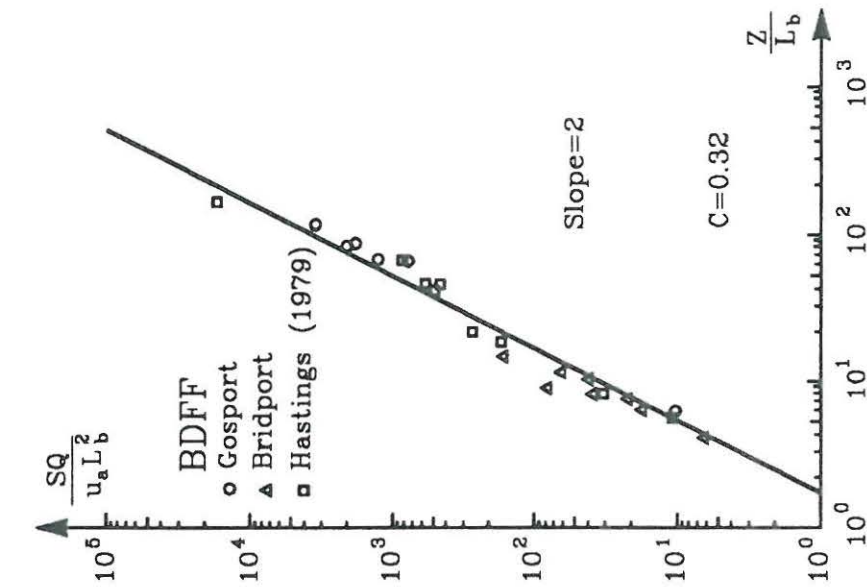
For Buoyancy Dominated Flow

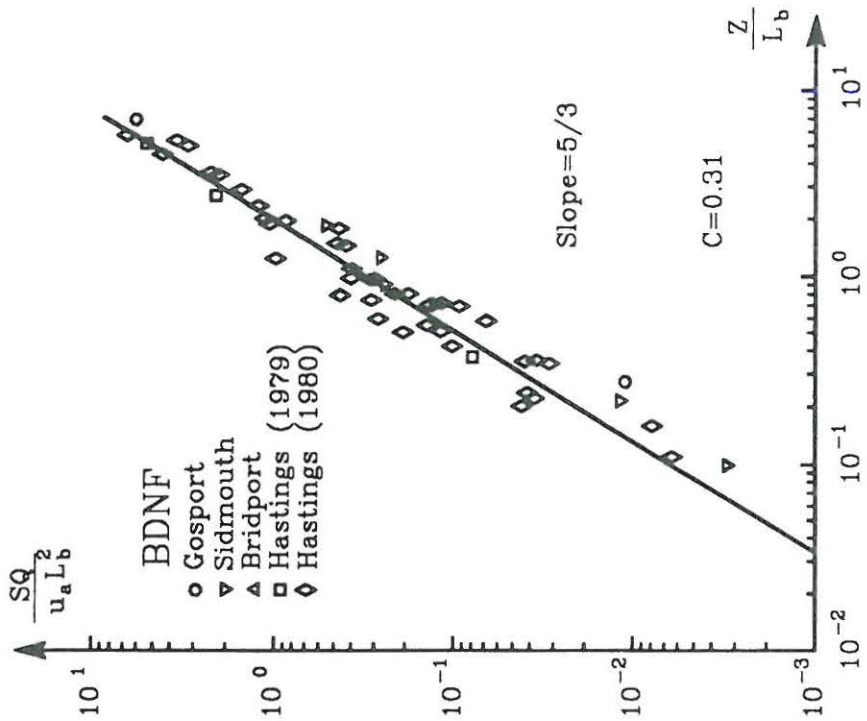$$\frac{SQ}{u_a L_b^2} = C_{11}\left(\frac{z}{L_b}\right)^t \tag{4.14}$$

in which, t = 5/3, $C_{11} = 0.31$ in the near field and t = 2, $C_{11} = 0.32$ in the far field.

After studying the field observed data and limited laboratory data, Lee and Nevill-Jones (1987) finally suggested an empirical formula for the minimum initial dilution of a horizontal buoyant jet in a perpendicular crossflow, it holds

$$S = 0.31\frac{B^{1/3}H^{5/3}}{Q}; \qquad y < 5\frac{B}{u_a^3} \qquad (near\ field) \tag{4.15}$$

84

Figure 4.19: Initial Dilutions for Buoyancy Dominated Flow in Perpendicular Crossflow

85

$$S = 0.32 \frac{u_a H^2}{Q}; \qquad y \geq 5 \frac{B}{u_a^3} \qquad (far\ field) \qquad (4.16)$$

The minimum time-averaged surface dilution S in the buoyancy dominated far field and its location X_m downstream can be estimated:

$$S = 1.1 \frac{u_a H^2}{Q} \qquad (4.17)$$

$$X_m = 1.1 \frac{H^{3/2} u_a^{3/2}}{B^{1/2}} \qquad (4.18)$$

in which, H is the water depth over the diffuser.

4.5 Comparative Disscusion of Laboratory and Field Studies

Laboratory experiment and field investigation are two basic means to study hydraulic problems. The first method is easy to handle and educate the investigator about various phenomena. The later means is costly and difficult to carry out and with greater uncertaincy due to the complex situations in the reality.

It seems to be difficult to compare the laboratory experimental results reported here directly to the field investigation data reported by Lee and Neville-Jones because of the fact that, first of all, the laboratory experiments are subject to horizontal jets in coflows and vertical jets in crossflows but the field studies were focued on horizontal jets in a perpendicular crossflow; secondly. the measured dilutions are different in the two studies, that is, the laboratory experiment is to measure the minimun dilution alongthe jet centerline but the field investigation was to study the initial dilution at the sea boil on the surface because it is almost impossible to measure the dilutions along the jet centerline under the water surface in the field.

86

Neverthless, it is still possible to see some meaningful hints from the two studies. It seems that optimal mixing of the waste effulent can be achieved by incresing the distance of travel and the interaction of the jet flow with the ambient flow for a given ambient water depth over the diffusor. Obviously, the vertical jets in crossflow has the shortes travel distance and subsequently has the lowest dilution. One can expect that a jet in a counter flowing ambient has much higher dilution comparied to jet in a coflowing environment because the interaction between the jet flow and ambient current is much stronger.

4.6 Summary

The laboratory experiments and field investigations are presented in this chapter. The results on length of zone of flow establishment, jet trajectories, dilutions, plume heights and widths, and stability of upstream wedge have been analyzed and successfully correlated using momentum and buoyancy fluxes and length scales. The conclusions are summarized as follows:

- The length of the zone of flow establishment for a buoyant jet is approximately equal to $4.0 \sim 4.5$ time of the orifice diameter, which is shorter than the length of the zone of flow establishment for a simple jet with pure momentum source.

- The horizontal jet trajectories and dilutions in a coflowing current for mometum dominated flow follows a power law of $3/2$ and $2/3$, and for buoyancy dominated flow obeys a power law of $5/3$ and $-4/5$, respectively.

- The vertical jet trajectories and dilutions in a crossflows for momentum dominated flow shows a power law of $1/2$ and 1 in the near field and of $1/3$ and 2 in the far field. It follows a power law of $3/4$ and $-5/3$ for buoyancy dominated flow in the near field and obeys a power law of $-2/3$ and -2 in the far field.

- A stabe upstream wedge created by submerged buoyant jet in flowing ambient is formed under the condition that the surface densimetrical Froude number $F_{\Delta s}$ is less than $0.3 \sim 0.4$. An unstable upstream wedge is likely to appear under the circustance that $0.4 \geq F_{\Delta s} \leq 1.0$ and the upstream wedge will be completely expired if $F_{\Delta s} \geq 1.0$.

- The height of the surface plume created by submerged jet is found to be in relation with the surface densimetrical Froude number. The width of the surface plume introduced by submerged jet is believed to be closely related to the ambient current velocity, the residual jet

momentum and the front velocity driven by the buoyancy force. A suddenly expended plume width and the phenomenon of bifucation can be expected in a flowing ambient.

Chapter 5

Mathematical Models

Generally speaking there are three basic mathematical models availabe to approach the problem of turbulent buoyant jets and plumes in a flowing ambient, i.e. empirical formula method,integral model and turbulence model.

The simple empirical formula method is to correlate experimental data according to theoretical considerations such as dimensional analysis as demonstrated in Chapter 4. The empirical correlations are used to determine the jet trajectory and dilution and may be useful guidance for practical problems in the primary stage.

The integral model is developed on the basis of the conservation laws of mass, momentum and density deficiency with the aid of profile and entrainment assumption to integrate and close the governing equations. The integral model is widely used today to describe turbulent buoyant jets and plumes because of its simplicity and economy, Chen, Schrøder et al (1989).

The turbulence model has become increasingly popular as a tool to predict turbulent buoyant jet problems since the fact that the integral model is difficult to be extended to more complex flows with boundary

effects. The turbulence model is to calculate the mean velocity and temperature at each grid point and does not employ profile and entrainment assumptions but obtain them as a part of the solutions.

5.1 The Integral Model

The steady integral technique is the classic and still one of the most popular method used today to predict the turbulent buoyant jets and plumes. Morton, Taylor and Turner(1956) published their classic paper on the integral technique for solving buoyant plume problem in stratified environments. The technique was soon elabrated on by several investigators for various cases. Solutions for horizontal round buoyant jets were published by Abraham(1963) and Fan and Brooks(1966). For buoyant jet into linearly stratified ambients, solutions were given by Brooks and Koh(1965) and a general compilation of solutions for two-dimensional and three-dimensional problems, with and without density stratification was published by Fan and Brooks(1969),Hirst(1972),Brooks(1973) and Schatzmann(1978).

Basic Equations in Vector Forms

By using the conservation law of mass, momentum and concentration, the following equations of vector forms for a fully turbulent flow are obtained.

Continuity equation of mass

$$\vec{V} \; grad \; \rho + \rho \; div \; \vec{V} = 0 \tag{5.1}$$

Continuity equation of momentum

$$\rho(\frac{1}{2} \; grad \; \vec{V}^2 - \vec{V} \times rot \; \vec{V}) = (\rho - \rho_a) \; \vec{g} \; grad \; \vec{P_d} \tag{5.2}$$

91

Continuity equation of scalar

$$\vec{V} \, grad \, c = 0 \tag{5.3}$$

Basic Equations in Natural Coordinates

In order to solve the Eqs. (5.1) - (5.3) an appropriate coordinate system must be defined in which to express these equations. Hirst (1972) Selected a curvilinear coordinates (s, r, φ) with the unit vectors ($\vec{I_s}, \vec{I_r}, \vec{I_\varphi}$) which moves with the jet axis (see Fig.5.4). Variables (x, y, z) are the Cartesian coordinates which situated in the following manner: y is set parallel to the ambient velocity and z opposite to the gravitational force direction. The two systems are related to each other by θ_1 and θ_2, where θ_1 is the angle between the projection of the jet axis onto the x-y plane and the x-axis; θ_2 is the angle between the jet axis and the x-y plane.

Using the defined coordinate system the vector forms of Eqs. (5.1) $\sim$ (5.2) can be written as a set of five non-linearly coupled partial differential equations with the three independent variables (s, r, φ), See Schatzmann (1978).

In order to simplify these equations the jet flow is assumed to be axisymmetric, that is

$$w = 0 \tag{5.4}$$

$$\frac{\partial (\quad)}{\partial \varphi} = 0 \tag{5.5}$$

in which, w is the tangential velocity componet. The dependent variables for a fully turbulent flow are then written in terms of fictitious mean and superimposed flutuating componets according to Renolds, i.e.

$$u = \bar{u} + u' \qquad v = \bar{v} + v'$$
$$\rho = \bar{\rho} + \rho' \qquad c = \bar{c} + c' \tag{5.6}$$

and the boundary layer assumptions, i.e. $v << u$, and $\partial(\quad)/\partial\varphi <<$ $\partial(\quad)/\partial r$ are invoked to yield the following set of equations.

Continuity equation of mass

$$\frac{\partial\overline{u}}{\partial s} + \frac{1}{r}\frac{\partial(r\overline{v})}{\partial r} = 0 \tag{5.7}$$

Y - momentum equation

$$(\overline{u}\frac{\partial\overline{u}}{\partial s} + \overline{v}\frac{\partial\overline{u}}{\partial r})sin\theta_1cos\theta_2 = -q_1\Phi - \frac{1}{r}\frac{\partial(r\overline{u'v'})}{\partial r}sin\theta_1cos\theta_2 \tag{5.8}$$

Z - momentum equation

$$(\overline{u}\frac{\partial\overline{u}}{\partial s} + \overline{v}\frac{\partial\overline{u}}{\partial r})sin\theta_2 = \frac{\rho_a - \overline{\rho}}{\rho_o}g - q_1\frac{cos\theta_2}{r_2} - \frac{1}{r}\frac{\partial(r\overline{u'v'})}{\partial r}sin\theta_2 \tag{5.9}$$

Continuity equation of scalar

$$\overline{u}\frac{\partial\overline{c}}{\partial s} + \overline{v}\frac{\partial\overline{c}}{\partial r} + \frac{1}{r}\frac{\partial(r\overline{v'c'})}{\partial r} = 0; \tag{5.10}$$

in which,

$$q_1 = \overline{u^2} - \frac{r}{4}[\frac{\partial\overline{v^2}}{\partial r} + \frac{\partial\overline{v'^2}}{\partial r}]$$

$$\Phi = \frac{cos\theta_1cos\theta_2}{r_1} - \frac{sin\theta_1sin\theta_2}{r_2}; \quad r_1 = (\frac{d\theta_1}{ds})^{-1}; \quad r_2 = (\frac{d\theta_2}{ds})^{-1};$$

The terms of $\overline{u'v'}, \overline{v'c'}$ and $\overline{v'^2}$ involving the ambient turbulence are not appeared in the control volume method.

93

Basic Assumptions

(1) Ambient Velocity and Density Distributions

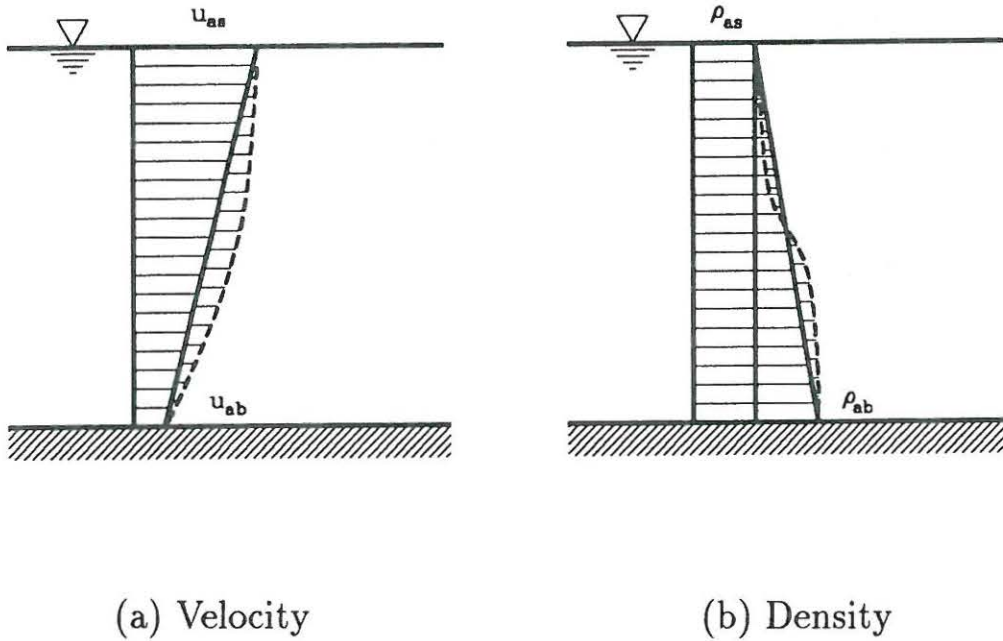The distributions of the ambient velocity and density are sketched in Fig.5.1 and assumed to be fomulated as

(a) Velocity   (b) Density

Figure 5.1: Ambient Velocity and Density Distribution Assumptions

$$u_a(z) = u_{ab} + k_1(u_{as} - u_{ab})\frac{z}{H_a} + k_2(u_{as} - u_{ab})(\frac{z}{H_a})^{1/2} \qquad (5.11)$$

$$\rho_a(z) = \rho_{as} + (\rho_{ab} - \rho_{as})(1 - z/Ha) + (\rho_{ab} - \rho_{as})\, exp\{-\frac{z^2}{Ha}\}(5.12)$$

in which,u_{as} and u_{ab} are surface and bottom ambient velocities; k_1 and k_2 are ambient velocity distribution coefficents; ρ_{as} and ρ_{ab} are ambient surface and bottom densities and H_a is ambient water depth. The

94

reason for this assumption is that Eqs. (5.11) and (5.12) can represent three basic patterns of the ambient velocity and density distributions, i.e. uniform, linear and specified curve distributions.

(2) Similarity Profile Assumption

It is assumed that the flow is fully turbulent after the zone of flow establishmen and the profiles of velocity, $u(s,r)$ concentration, $c(s,r)$, and density deficicency, $\Delta\rho(s,r)$ are self-similar at all cross sections normal to the jet trajectory and to be Gaussian:

$$u(s,r) = u_a(s)cos\theta + u_m(s)\, exp\{-\frac{r^2}{b^2}\} \tag{5.13}$$

$$c(s,r) = c_m(s)\, exp\{-\frac{r^2}{\lambda^2 b^2}\} \tag{5.14}$$

$$\Delta\rho(s,r) = \Delta\rho_m(s)\, exp\{-\frac{r^2}{\lambda^2 b^2}\} \tag{5.15}$$

in which, $u_a(s)$:   ambient velocity;

$u(s,r)$:   jet velocity;

θ :   angle between jet axis and y direction;

$c(s,r)$:   concentration;

s,r :   axial and transverse coordinates;

$\Delta\rho(s,r)$:   density difference between ambient and jet fluids;

b :   characteristic half-width of jet;

λ :   spreading ratio between density and velocity profiles;

$u_m(s)$:   centerline excess velocity;

$c_m(s)$:   centerline excess concentration;

$\Delta\rho_m(s)$:   centerline excess density.

As a matter of fact, the self-similar Gaussain profile assumption is

valid only for jets and plumes in a quiescent ambient. For buoyant jets in a crossflow, the flow tends to roll up into two counter-rotating vortices, see discussion in Chapter. 3. Section. 3.2.2. In spite of this, reasonable gross predictions are still obtained by introducing the Gaussain profiles, probally because the integration of the governing equation over the jet cross section effectively averages out the asymmetry of the paris of the vortices.

The integral form govering equations for turbulent buoyant jets and plumes in flowing ambient fluid with density stratification can be derivated by two methods, i.e. control volume method and differential method. The control volume method applys the principles of conservation of mass, density deficiency and momentum to a slice of jet (control volume), and obtain a set of equations which can be integrated and subsequently solved numerically. The differential method is based on the basic three-dimentional differential equations of fluid mechanics, to be integrated with the aid of some assumptions. Comparing to the two methods that the control volume method is simple and direct therefore it is commenly employed by previous investigators such as Abraham (1963), Fan and Brooks (1966), etc. However the differential method enable the mathematical model to include the background turbulence,better understand the entrainment hypothesis and the gross drag force assumption and to be able to predict the three-dimentional jet in a flowing ambient, but unforturnely this method needs tedious mathematical procedures.

In the following two subsections, integral models for a round turbulent buoyant jet in a stratified flowing environment with two-dimensional and three-dimensional trajectories are developed by means of the control volume method and the differential method, respectively.

5.1.1 Integral Equations for Jet with 2-D Trajectory

Considering a turbulent buoyant round jet with two-dimensional trajectory in a non-uniform density flowing environmet corresponding to a turbulent buoyant jet released from an ocean outfall or a gas from an industrial chimney as shown in Fig. 5.2.
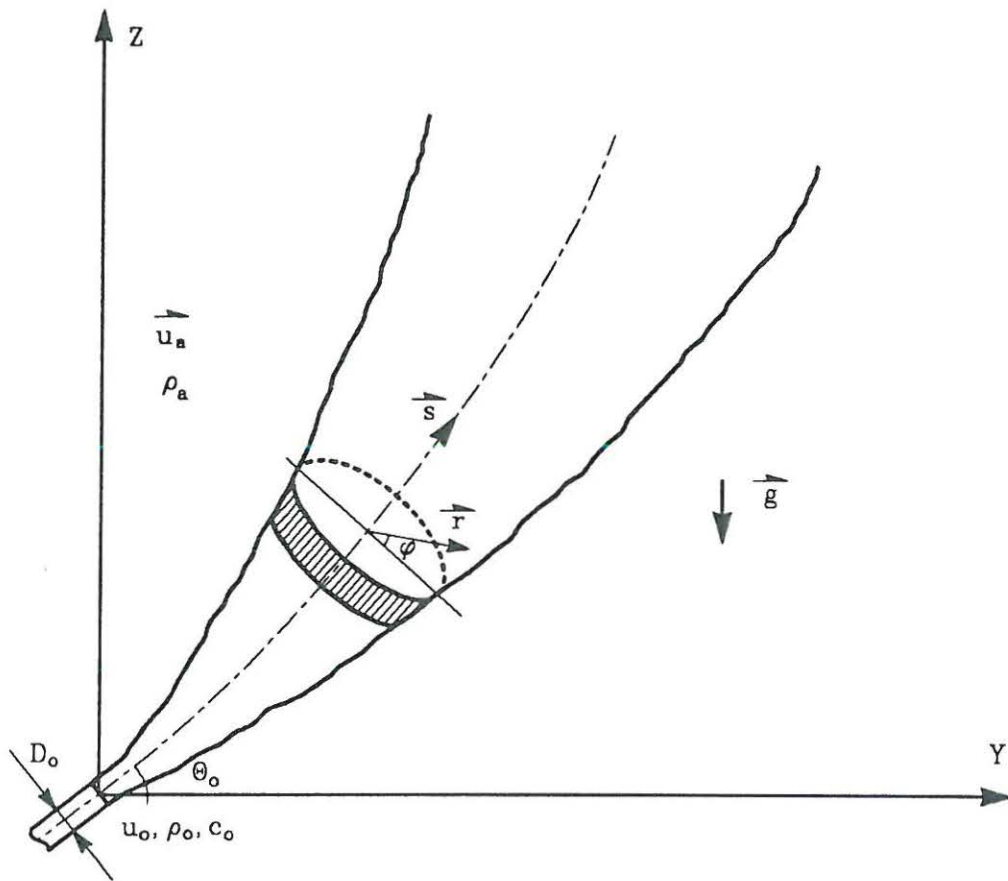

Figure 5.2: A Turbulent Buoyant Jet in Stratified Flowing Environment with 2-D Trajectory

Basic Integral Parameters

The integral parameters such as momentum flux M, volume flux Q and buoyancy flux B can be integrated as

$$Q = \int_A [u_a(s)cos\theta + u_m(s)exp\{-\frac{r^2}{b^2}\}]dA \tag{5.16}$$

$$M = \int_A \rho[u_a(s)cos\theta + u_m(s)exp\{-\frac{r^2}{b^2}\}]^2 \, dA \tag{5.17}$$

$$B = \int_A \Delta\rho[u_a(s)cos\theta + u_m(s)exp\{-\frac{r^2}{b^2}\}]dA \tag{5.18}$$

Basic Equations

By applying the principle of conservation of mass, momentum, concentration and density deficiency, for a control volume shown in Fig. 5.3, the basic equations can be written as follows.

Continuity equation of mass

$$\frac{dQ}{ds} = Q_e \tag{5.19}$$

in which, Q_e is the total entrainmet including turbulent entrainment and convective mass flux from the ambient flow into the jet fluid.

Y - momentum equation

$$\frac{d}{ds}[M cos\theta] = F_D sin\theta + \rho_a u_a Q_e \tag{5.20}$$

in which, F_D is the gross drag force due to the ambient current; $\rho_a u_a Q_e$ is the entrained momentum.

98
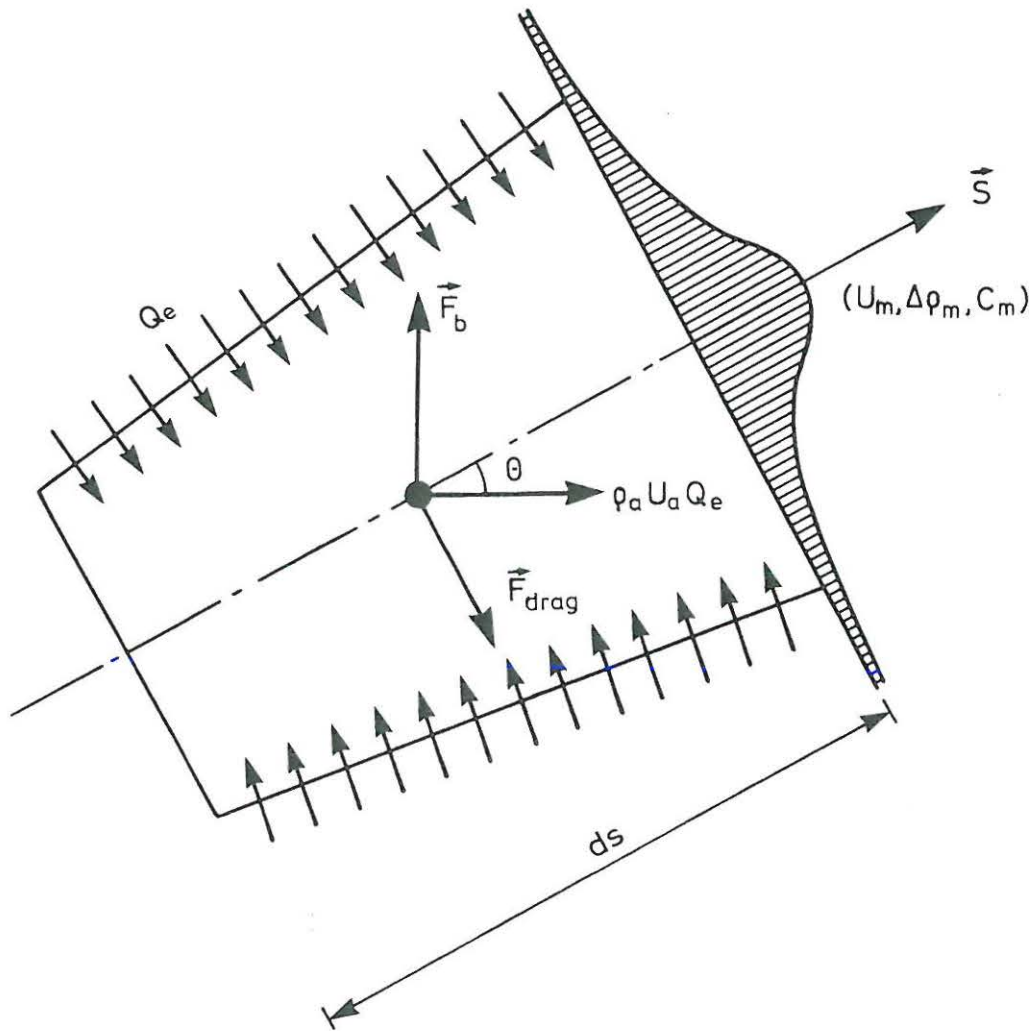
Figure 5.3: The Definition Sketch of the Basic Equations

99

Z - momentum equation

$$\frac{d}{ds}[M sin\theta] = F_B - F_D cos\theta \tag{5.21}$$

in which, $F_B = \int_A \Delta\rho g dA$, is the total buoyancy force acting on the control volume.

Density deficiency conservation

$$\frac{d}{ds}[u(\rho_o - \rho)dA] = Q_e(\rho_o - \rho_a) \tag{5.22}$$

Continuity equation of scalar

$$\frac{d}{ds}[u(c_o - c)dA] = Q_e(c_o - c_a) \tag{5.23}$$

By substituting the profile assumptions into Eqs. (5.19) - (5.23) then integrating them with respect to φ and r yields,

Continuity equation of mass

$$\frac{d}{ds}[\pi b^2(2u_a cos\theta + u_m)] = Q_e \tag{5.24}$$

Y - momentum equation

$$\frac{d}{ds}[\pi\rho_a b^2(2u_a cos\theta + u_m)^2 cos\theta] = 2F_D sin\theta + 2\rho_a u_a Q_e \tag{5.25}$$

Z - momentum equation

$$\frac{d}{ds}[\pi\rho_a b^2(2u_a cos\theta + u_m)^2 sin\theta] = 2F_B - 2F_D cos\theta \tag{5.26}$$

100

Density deficiency conservation

$$\frac{d}{ds}[b^2(u_m + (1+\lambda^2)u_a cos\theta)\Delta\rho_m] = -\frac{1+\lambda^2}{\lambda^2}\frac{d\rho_a}{ds}[b^2(u_m + u_a cos\theta)] \quad (5.27)$$

Continuity equation of scalar

$$\frac{d}{ds}[b^2(u_m + (1+\lambda^2)u_a cos\theta)c_m] = -\frac{1+\lambda^2}{\lambda^2}\frac{dc_a}{ds}[b^2(u_m + u_a cos\theta)] \quad (5.28)$$

Geometric equations

$$\frac{dy}{ds} = cos\theta \quad (5.29)$$

$$\frac{dz}{ds} = sin\theta \quad (5.30)$$

5.1.2 Integral Equations for Jet with 3-D Trajectory

The integral model for a round turbulent buoyant jet with three-dimensional path in a flowing ambient, sketched in Fig. 5.4, can be deriviated by considering the basic partial differential equations, Hirst (1972) and Schatzmann (1978).
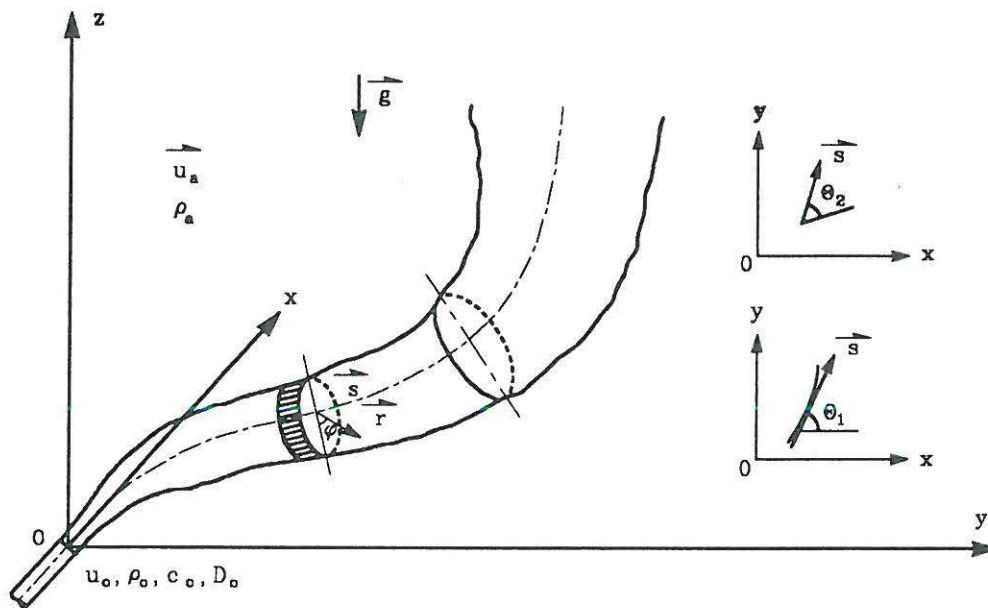
Figure 5.4: Schematic Diagram for Turbulent Buoyant Jet in Flowing Environment with 3-D Trajectory

Integral Forms of the Basic Equations

In order to further simplify the problem the basic equations (5.7) - (5.10) are integrated with respect to $\varphi[0, 2\pi]$ and $r = [0, (\sqrt{2}b, \infty)]$ by substi-

tuting the Gaussian profile assumptions. It should be emphasised that the ambient turbulence terms have been neglected due to no sufficent available laboratory data exist showing the effects of these terms on the jet development, however, it should be kept in mind that the ambient turbulence can be readily handled in case sufficent information available. The following set of ordinary differential equations are obtained:

Continuity equation of mass

$$\frac{d}{ds}[b^2(2u_a cos\theta + u_m)] = 2Q_e \tag{5.31}$$

S - momentum equation

$$\frac{d}{ds}[b^2(u_m + 2u_a cos\theta)^2 sin\theta_1 cos\theta_2]$$
$$= 4Q_e u_a \rho_a sin\theta_1 cos\theta_2 - 2b^2\lambda^2 g sin\theta_2 \frac{\Delta\rho_m}{\rho_o} \tag{5.32}$$

Continuity equation of scalar

$$\frac{d}{ds}[b^2(u_m + (1 + \lambda^2)u_a sin\theta_1 cos\theta_2)c_m]$$
$$= -\frac{1 + \lambda^2}{\lambda^2}\frac{dc_a}{ds}[b^2(u_m + 2u_a sin\theta_1 cos\theta_2)] \tag{5.33}$$

Density deficiency conservation

$$\frac{d}{ds}[b^2(u_m + (1 + \lambda^2)u_a sin\theta_1 cos\theta_2)\Delta\rho_m]$$
$$= -\frac{1 + \lambda^2}{\lambda^2}\frac{d\rho_a}{ds}[b^2(u_m + 2u_a sin\theta_1 cos\theta_2)] \tag{5.34}$$

103

θ_1 - equation

$$\frac{d\theta_1}{ds} = \frac{u_a Q_e cos\theta_1}{[b^2(u_m + 2u_a sin\theta_1 cos\theta_2)^2 - Q_e^2]cos\theta_2} \tag{5.35}$$

θ_2 - equation

$$\frac{d\theta_2}{ds} = \frac{\lambda^2 b^2(\Delta\rho_m/\rho_o)gcos\theta_2 - 2u_a Q_e sin\theta_1 sin\theta_2}{2[b^2(u_m + 2u_a sin\theta_1 cos\theta_2)^2 - Q_e^2]} \tag{5.36}$$

Geometric equations

$$\frac{dx}{ds} = cos\theta_1 cos\theta_2 \tag{5.37}$$

$$\frac{dy}{ds} = sin\theta_1 cos\theta_2 \tag{5.38}$$

$$\frac{dz}{ds} = sin\theta_2 \tag{5.39}$$

5.1.3 Entrainment and Drag Force Hypotheses

In order to achieve closure in Eqs. (5.31)-(5.36) an entrainment function and a gross drag force expression must be specified. The hypotheses for the entrainment and drag force and the proposed functions will be presented and discussed as follows.

Entrainment Hypothesis

Entrainment is a physical phenomenon that fluid from a laminar or low turbulent region into a turbulent or hight turbulent region. For a turbulent buoyant jet in a flowing ambient, it is the ambient flow (with lower turbulence) into the jet region (with higher turbulence) (see Fig. 3.4). Since the entrainment is closely related to turbulence and largely determined by the turbulence structure within the jet, particularly near the edges, consequently it is one of the most complex problem in fluid mechanics.

As shown in Fig. 3.4 that the jet flow and the ambient fluid are formated a vortex pairs at the jet edges where the entrainment occurs. It is still beyon our knowlge on turbulence properties to describe the entrainment in detailed, although it is well known that the most characteristic feature of turbulence is its non-determinstic/ramdom and chaotic eddy motion. Fl. B. Pedersen (1980).

However, a great effort has been devoted to the bulk entrainment by relating the entrainment velocity, u_e to the jet centerline velocity, u_m i.e. $u_e = \alpha u_m$, where α is the well known entrainment coeffient which was firstly suggested by Morton, Taylor and Turner (1956) for a plume in a stagnant ambient water.

(1) In Stagnant Receiving Water

In stagnant receiving water the turbulet entrainment coeffient was originally assumed as a universal constant, for examples,

$$\text{For jet} \begin{cases} \alpha = 0.057 & (round\ jet) \\ \alpha = 0.068 & (slot\ jet) \end{cases} \Bigg\} Albertson(1950)$$

$$\text{For plume} \begin{cases} \alpha = 0.082 & (round\ plume) & Rouse\ et\ al(1952) \\ \alpha = 0.057 & (slot\ plume) & Lee\ \&\ Emmons(1951) \end{cases}$$

Later, It was found that the entrainment coefficent is not an universal contant but depends on the local characters of the jet flow, Hirst(1971), List and Imberger(1973),

$$\alpha = 0.057 + \frac{0.083}{F_l^2} \qquad List\ and\ Imberger\ (1973)$$

$$\alpha = 0.057 + \frac{0.97}{F_l^2} sin\theta \qquad Hirst\ (1971)$$

in which, F_l is the local densimetrical Froude number, defined as $F_l = u_m / \sqrt{\Delta\rho_m/\rho_a gb}$.

Gu and Stefan(1988) derived the expression for the entrainment coefficent, from the basic equations in the integral model (water continuty and x-momentum equations), using hydrostatic pressure assumption.

$$\alpha_r = (-\lambda^2 + \frac{3\lambda^2}{2+\lambda^2})sin\theta R_{il} + 6I_r \qquad (\ ruond\ jet\ )$$

$$\alpha_s = (-\sqrt{\frac{\pi}{2}} + \sqrt{\frac{3\pi^2}{4+4\lambda^2}})sin\theta R_{il} + 2\sqrt{3}I_s \qquad (\ slot\ jet\ )$$

in which, R_{il} : Richarson number, defined as $R_{il} = \Delta\rho_m g 2b / \rho_o u_m^2$; $2b$ = jet diameter; I_r: shear-stress integral, defined as

$$I_r = \frac{1}{u_m^3 b} \int_o^\infty u \frac{\partial[r(\overline{u'v'})]}{\partial r} dr$$

106

$$I_s = \frac{1}{u_m^3} \int_o^\infty u \frac{\partial[r(\overline{u'v'})]}{\partial y} dy$$

I_r was determined from experimental data, Hirst(1971) suggested $I_r = 0.0095$ and recommended by Koh and Brooks(1975), $I_s = 0.0182$, from laborotaory experiments.

(2) In Flowing Receiving Water

In flowing receiving environment the entrainment function should be depended on the following factors, (i) local mean jet parameters, u_m and b; (ii) local buoyancy within the jet, F_l; (iii) jet orientation, θ_1 and θ_2; (iv) ambient velocity, u_a and (v) ambient turbulence.

An entrainment hypothesis suggested by Fan(1967), considering the iterms (i), (iii) and (iv).

$$Q_e = 2\pi \alpha b \sqrt{u_a^2 sin^2\theta + u_m^2} \tag{5.40}$$

in which, $\alpha = 0.4 \sim 0.5$;

Hoult et al (1969) developed an entrainment function for the prediction of vertical buoyant jets in a crossflowing environment by assuming that there are basically two entrainments; one is due to the difference between the plume velocity and ambient velocity component parallel to the plume and the other owing to the ambient velocity component normal to the plume.

$$Q_e = \alpha_1 b \mid u_m - u_a cos\theta \mid +\alpha_2 b u_a sin\theta \tag{5.41}$$

in which, $\alpha_1 = 0.057, \alpha_2 = 0.97$:

A combination of the above entrainment hypothesis provides an entrainment function which satisfies the items (i) - (iv) by neglecting the ambient turbulence, Hirst (1972).

$$Q_e = \frac{\alpha_1 + \alpha_2 sin\theta_2}{F_l^2}[b \mid u_m - u_a sin\theta_1 cos\theta_2 \mid$$
$$+\alpha_3 u_a b\sqrt{1 - sin^2\theta_1 cos^2\theta_2}] \tag{5.42}$$

in which, $\alpha_3 = 0.90$; $F_l^2 = u_m^2/(\rho_a - \rho_m)/\rho_o bg$

In fact, the entrainment rate Q_e above is not the turbulent entrainment as that in stagnant water but is the total entrainment including both turbulent entrainment and convective mass flux which can not be caused by turbulence. Recently, a generalized entrainment function has been proposed by Lee and Cheung (1990) by separating the entrainment into shear entrainment and forced entrainment. The shear entrainment is assumed as

$$Q_{es} = 2\pi\alpha b \mid u_m - u_a cos\theta_1 cos\theta_2 \mid \tag{5.43}$$

in which, the entrainment coeffiicent is a function of local densimetrical Froude number, jet orientation and excess and ambient velocities. The forced entrainment formulation is taken as the ambient flow intercepted by the so called windward side of the buoyant jet. The formulation yields:

$$Q_{ef} = u_a[2b\sqrt{1 - cos^2\theta_1 cos^2\theta_2} + \pi b\Delta b cos\theta_1 cos\theta_2$$
$$+\frac{\pi b^2}{2}\Delta(cos\theta_1 cos\theta_2)] \tag{5.44}$$

The Eq. (5.44) includes three contributions: the first term represents the forced entrainment due to the projected jet area normal to the cross flow; the second and the third terms are a correction for the growth of jet radius and the curvature of the jet trajectory which are not appeared in the previous entrainment functions.

Drag Force Hypothesis

The pressure gradient terms $\partial p_d/\partial s, \partial p_d/\partial r, \partial p_d/\partial \varphi$ appeared in the derivation of the basic equations are not known. The fact is that the pressure field around a bent-over jet in a flowing fluid is so complex that it seems to be impossible to find a general function, therefore it become necessary to arbitrarily set $\partial p_d/\partial s = \partial p_d/\partial r = \partial p_d/\partial \varphi = 0$. The error arising from this simplification will be partially compensated for by introducing an empirical function for the pressure force per jet unit length Δs. Regarding the jet as a solid body, the gross drag force can be defined, Fan(1967)

$$F_D = \int_{-b}^{b} \frac{1}{2} c_D \rho_a u_a sin^2\theta db \tag{5.45}$$

in which c_D is the drag coefficent needed to be determined empirically.

5.1.4 Initial Conditions

The initial conditions at the begining of the zone of flow establishment are:

$$
\begin{cases}
u_m = u_o \\
b = b_o \\
\theta_1 = \theta_{1o} \\
\theta_2 = \theta_{2o} \\
\Delta\rho_m = \Delta\rho_o \\
c_m = c_o
\end{cases}
$$

The initial conditions at the end of the zone of flow establishment can be obtained by considering the conservation equations of mass, density deficiency and concentration.

Mass conservation

$$
\int_A [u_a(s)\cos\theta + u(s,r)]dA] = \frac{\pi D_o^2}{4}u_o \tag{5.46}
$$

Density deficiency conservation

$$
\int_A \Delta\rho_m[u_a(s)\cos\theta + u(s,r)]dA = \frac{\pi D_o^2}{4}u_o\Delta\rho_o \tag{5.47}
$$

Concentration conservation

$$
\int_A c_m[u_a(s)\cos\theta + u(s,r)]dA = \frac{\pi D_o^2}{4}u_o c_o \tag{5.48}
$$

By solving Eqs.(5.46) $\sim$ (5.48), the initial conditions at the end of zone of flow establishment are determinted as

$$\begin{cases} u_m = u_o \\ b_m = \dfrac{\sqrt{2}}{2} \dfrac{\sqrt{u_o(2u_a cos\theta + u_o)}}{2u_a cos\theta + u_a} b_o \\ \theta_1 = \theta_{1o} \\ \theta_2 = \theta_{2o} \\ \Delta\rho_m = \dfrac{2u_a cos\theta + u_o}{2\lambda u_a cos\theta + \frac{\lambda^2}{1+\lambda^2} u_o} \Delta\rho_o \\ c_m = \dfrac{2u_a cos\theta + u_o}{2\lambda u_a cos\theta + \frac{\lambda^2}{1+\lambda^2} u_o} c_o \end{cases}$$

The initial discharging angles are still assumed to be the same as the orientation outlet discharging angles although they are changed depending on the velocity ratio between the jet and ambient, it is believed to be unimportant in practical problems.

5.1.5 Solution Technique

Thus, nine first order, ordinary differential equations are available for the nine unknowns: $u_m, \Delta\rho_m, c_m, b, \theta_1, \theta_2$, x, y, and z, but dx, dy and dz can be determined by θ_1, θ_2 and ds directly, therefore, there are only six unknowns remained to be solved. After derivation and manipulations of Eqs.(5.31) to (5.36) yields:

$$\frac{du_m}{ds} = f_1(u_m, b, \theta_1, \theta_2, \Delta\rho_m, c_m) \tag{5.49}$$

$$\frac{db}{ds} = f_2(u_m, b, \theta_1, \theta_2, \Delta\rho_m, c_m) \tag{5.50}$$

$$\frac{d\theta_1}{ds} = f_3(u_m, b, \theta_1, \theta_2, \Delta\rho_m, c_m) \tag{5.51}$$

$$\frac{d\theta_2}{ds} = f_4(u_m, b, \theta_1, \theta_2, \Delta\rho_m, c_m) \tag{5.52}$$

$$\frac{dc_m}{ds} = f_5(u_m, b, \theta_1, \theta_2, \Delta\rho_m, c_m) \tag{5.53}$$

$$\frac{d\Delta\rho_m}{ds} = f_6(u_m, b, \theta_1, \theta_2, \Delta\rho_m, c_m) \tag{5.54}$$

A fourth order Runge-Kutta integration method is employed to solve the Eqs. (5.49) - (5.54) with small increments of Δs along the jet trajectory. Take u_m for example,

$$u_m(s + \Delta s) = u_m(s) + \frac{1}{6}(K_{11} + 2K_{12} + 2K_{13} + K_{14})$$

where

$$K_{11} = \Delta s f_1(u_{mi}, b_i, \theta_{1i}, \theta_{2i}, \Delta\rho_{mi}, c_{mi})$$

$$K_{12} = \Delta s f_1(u_{mi} + \frac{K_{11}}{2}, b_i + \frac{K_{21}}{2}, \theta_{1i} + \frac{K_{31}}{2}, \theta_{2i} + \frac{K_{41}}{2}, \Delta\rho_i + \frac{K_{51}}{2}, c_{mi} + \frac{K_{61}}{2})$$

$$K_{13} = \Delta s f_1(u_{mi} + \frac{K_{12}}{2}, b_i + \frac{K_{22}}{2}, \theta_{1i} + \frac{K_{32}}{2}, \theta_{2i} + \frac{K_{42}}{2}, \Delta\rho_i + \frac{K_{52}}{2}, c_{mi} + \frac{K_{62}}{2})$$

$$K_{14} = \Delta s f_1(u_{mi} + \frac{K_{13}}{2}, b_i + \frac{K_{23}}{2}, \theta_{1i} + \frac{K_{33}}{2}, \theta_{2i} + \frac{K_{43}}{2}, \Delta\rho_i + \frac{K_{53}}{2}, c_{mi} + \frac{K_{63}}{2})$$

subcript i indicates values at s. Similarly, $K_{21}, K_{31}, K_{41}, K_{51}, K_{61},$ ..... etc. are simultaneously and similarly obtained from the functions f_2, f_3, f_4, f_5 and f_6.

The interval Δs should be small to maintain stability since Runge-Kutta method is based on a truncated Taylor series with $O(\Delta s^5)$.

5.2 The Turbulence Model

5.2.1 Introduction

The integral models are difficult to be extended to more complex turbulent buoyant flows such as jets discharged into an arbitarily stratified environment, into a heighly turbulent ambient flow and into a receiving environment with complex buondary configurations and water-air interface. In such general flows it seems to be almost impossible to prescribe the shapes of the concentration and velocity profiles and to establish the entrainment function in relation to the local jet mean parameters and the ambient turbulence characteristics. Therefore, the turbulence models become increasingly popular to simulate and predict the turbulent buoyant jets in flowing ambients.

Turbulence models of various levels of complexity have been suggested and practiced, such as the Prandlt mixing length hypothesis, one equation model, two equation model and multiple equation model. A number of review articles of the availabe models has been published, for examples, Reynolds(1970),Launder and Spalding(1972), Rodi(1984), Markatos (1985), Lakshminarayara(1986) and Ferziger(1987) as well as ASCE Task Committee(1988).

The well-known $k - \varepsilon$ model based on Launder and Spalding are adopted here to predict the turbulent buoyant jets in flowing ambients.

5.2.2 Reynolds Equation and Reynolds Stress

The Reynolds equations for a turbulent flow are written as

Continuity equation of mass

$$\frac{\partial \rho}{\partial t} + \frac{\partial (\rho u_i)}{\partial x_i} = 0 \tag{5.55}$$

114

Momentun equation

$$\frac{\partial u_i}{\partial t} + u_j \frac{\partial u_i}{\partial x_j} = -\frac{1}{\rho}\frac{\partial P}{\partial x_i} + \frac{1}{\rho}\frac{\partial(-\rho\overline{u_i'u_j'})}{\partial x_j} + g_i\frac{\Delta\rho}{\rho} \tag{5.56}$$

Continuity equation of scalar

$$\frac{\partial \Phi}{\partial t} + u_j \frac{\partial \Phi}{\partial x_j} = \frac{1}{\rho}\frac{\partial(-\rho\overline{u_i'\varphi'})}{\partial x_j} + S_\phi \tag{5.57}$$

in which, $-\rho\overline{u_i'u_j'}$ and $-\rho\overline{u_i'\varphi'}$ are Reynolds stress and scalar "Reynolds stress", respectively. For enviromental hydraulic problem, most of the situations are hight Renolds number flows, the molecular diffusion terms $\mu\frac{\partial u_i}{\partial x_j}$ and $\lambda\frac{\partial \Phi}{\partial x_i}$ are negligible in comparison with the corresponding Reynolds stresess, $-\rho\overline{u_i'u_j'}$ and $-\rho\overline{u_i'\varphi'}$. therefore the molecular diffusion terms are not included in Eqs.(5.56) and (5.57).

5.2.3 The $k-\varepsilon$ Turbulence Model

Most of the present applicable turbulence models are established on the concepts of eddy viscosity, μ_t and dispersion coefficent Γ_t. Boussineq eddy viscosity links the Reynolds stress and time-averager velocity gradient as

$$-\overline{u_i'u_j'} = \mu_t(\frac{\partial u_i}{\partial x_j} + \frac{\partial u_j}{\partial x_i}) - \frac{2}{3}k\delta_{ij} \tag{5.58}$$

in which, μ_t is the turbulent eddy viscosity which is not a property of fluid but strongly depended on the turbulence. k is the kinetic energy and δ_{ij} is the Kronecker delta. similarly, the scalar Reynolds fluxes, $\overline{u_i'\varphi'}$ is approximated

$$-\overline{u_i'\varphi'} = \Gamma_t\frac{\partial \Phi}{\partial x_i}; \qquad \Gamma_t = \frac{\mu_t}{\sigma_t} \tag{5.59}$$

Γ_t : turbulent dispersion coefficent, similar to μ_t, is a local property of turbulence. σ_t: Prandtl number.

Obviously, it is not sufficent to establish a turbulence model by introducing Eq.(5.58) only because μ_t is a turbulence property as a funtion of space and time. The $k - \varepsilon$ model, Launder and Spalding (1974), makes the turbulence viscosity, μ_t dependent on two parameters, for which two differential equations are solved. The expression for μ_t is

$$\mu_t = c_\mu \rho \frac{k^2}{\varepsilon} \tag{5.60}$$

where c_μ is a constant. The kinetic energy, k and the dissipation rate, ε are definded as

$$k = \frac{1}{2}\overline{u_i' u_j'}; \qquad \varepsilon = \nu_t \overline{\frac{\partial u_i}{\partial x_j} \frac{\partial u_i}{\partial x_j}} \tag{5.61}$$

The governing equations for k and ε are written as

k - equation

$$\frac{\partial k}{\partial t} + u_i \frac{\partial k}{\partial x_i} = \frac{\partial}{\partial x_i}(\frac{\mu_t}{\sigma_k}\frac{\partial k}{\partial x_i}) + P + G - \varepsilon \tag{5.62}$$

ε - equation

$$\frac{\partial \varepsilon}{\partial t} + u_i \frac{\partial \varepsilon}{\partial x_i} = \frac{\partial}{\partial x_i}(\frac{\mu_t}{\sigma_\varepsilon}\frac{\partial \varepsilon}{\partial x_i}) + c_{1\varepsilon}\frac{\varepsilon}{k}(P + G)(1 + c_{3\varepsilon}R_f) - c_{2\varepsilon}\frac{\varepsilon^2}{k} \tag{5.63}$$

in which,

$$P = \mu_t(\frac{\partial u_i}{\partial x_j} + \frac{\partial u_j}{\partial x_i})\frac{\partial u_i}{\partial x_j}$$

116

$$G = \beta g_i \frac{\mu_t}{\sigma_t} \frac{\partial \Phi}{\partial x_i}$$

where, R_f : is the flux Richarsen number, β is the volumentic expension coefficent. The $k - \varepsilon$ turbulence model contains six empirical constants $c_\mu, c_{1\varepsilon}, c_{2\varepsilon}, c_{3\varepsilon}, \sigma_k, \sigma_\varepsilon$, and σ_t needed to be determined empirically.

5.3 Predictions and Disscusions

5.3.1 Integral Model Predictions and Comparisons to Experimental Data

The integral model has been employed to simulate the turbulent buoyant jets and plumes in flowing ambients. The predictions are presented and compared with the laboratory experimental data in terms of jet trajectories, centerline velocities and concentration decaies and the trace contours. The comparisons include horizontal buoyant jets in coflowing currents and vertical jets in crossflowing ambients. The constants of the spreading ratio between the concentration and velocity profiles, λ, the gross drag force coefficent, c_D and the entrainment coefficents, α_1, α_2 and α_3 in the integral model are taken the values as shown in Table. 5.1.

Table 5.1: The Values of Constants in the Integral Model

λ	c_D	α_1	α_2	α_3
1.16	1.00	0.057	0.97	0.9 - 0.5

Trajectories and Geometries

The predicted jet trajectories for horizontal jets in coflowing environments are shown in Fig. 5.5 and compared to the experimental data by the present studies. The simulated jet trajectories for vertical jets in crossflowing ambients are demonstrated in Fig.5.6 in comparison with the laboratory data reported by Fan (1967). It shows that the predictions of jet trajectories and geometries agree satisfactorily with the avairable data.
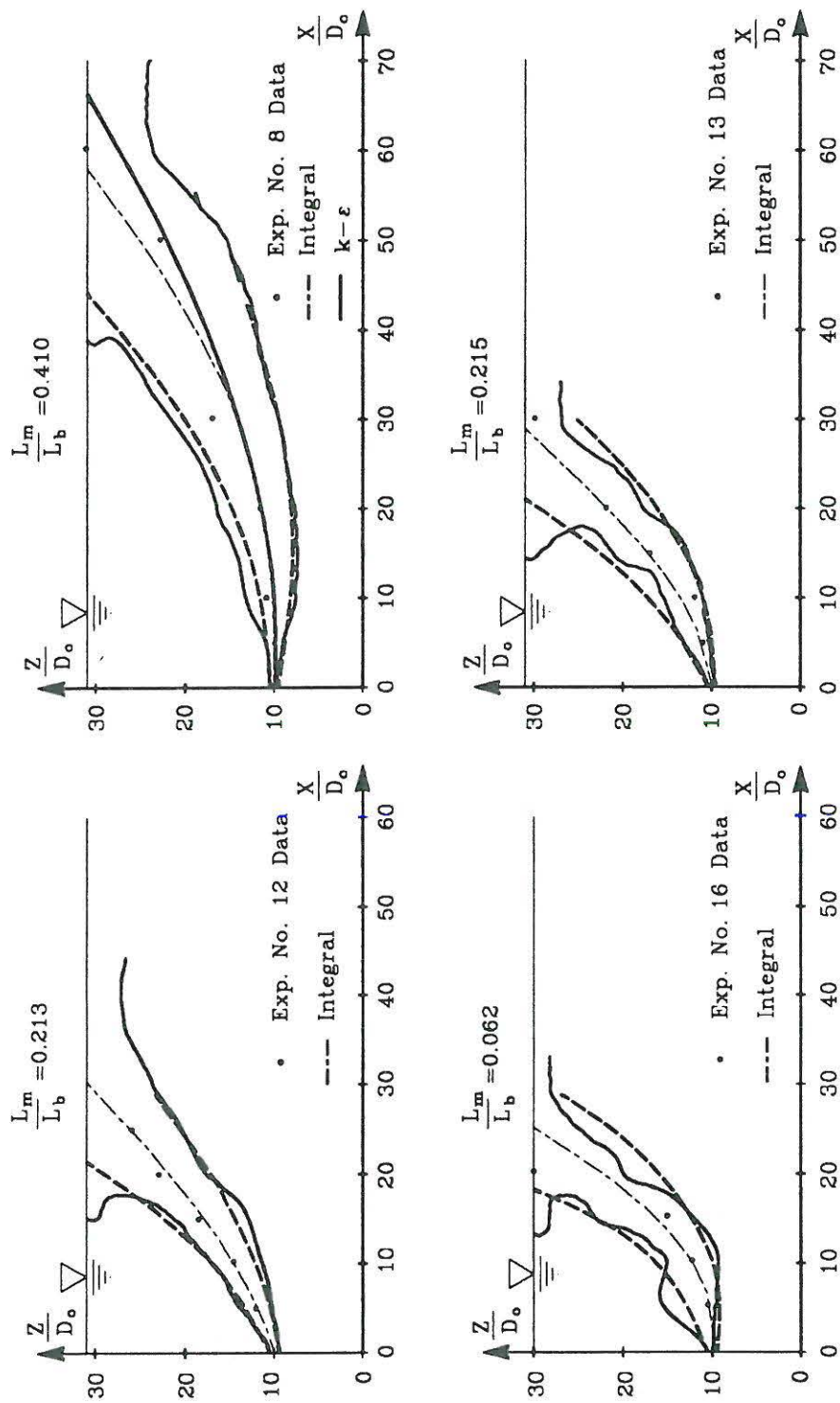
Figure 5.5: (a) Prediction and Comparison of Horizontal Jet Trajectories and Geometries in Coflowing Ambients

119
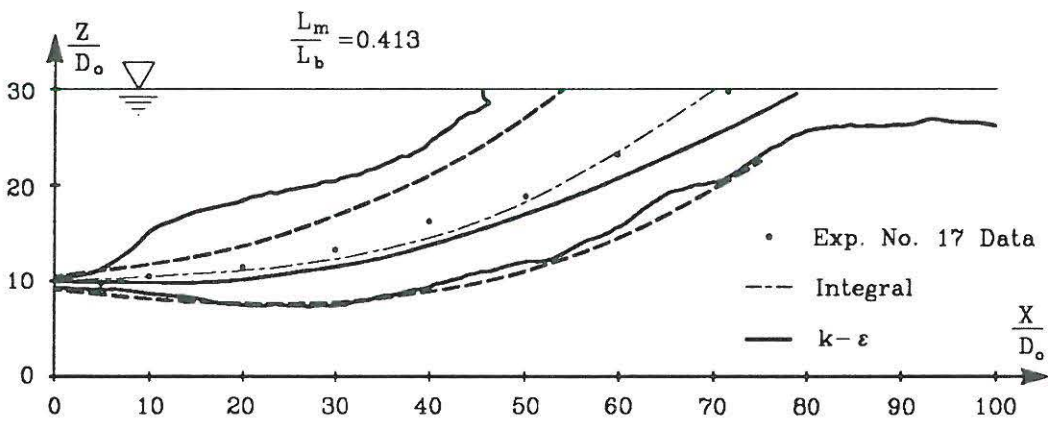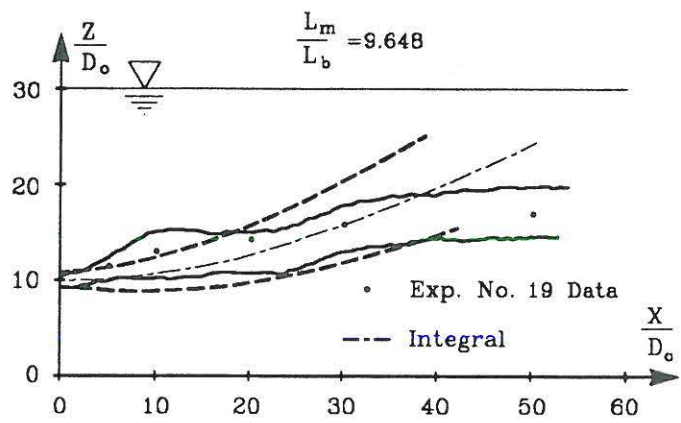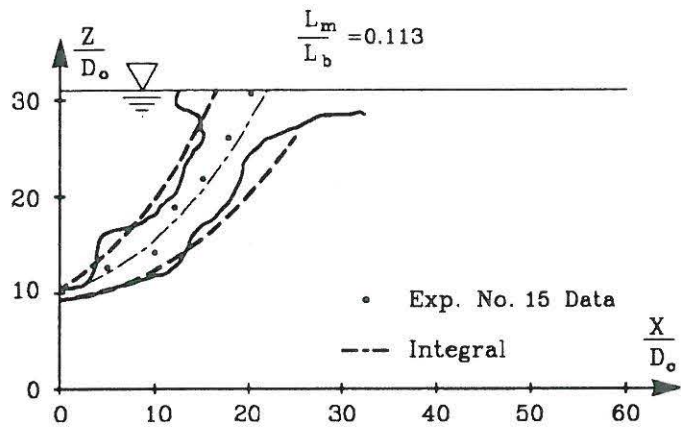
Figure 5.5: (b) Prediction and Comparison of Horizontal Jet Trajectories and Geometries in Coflowing Ambients
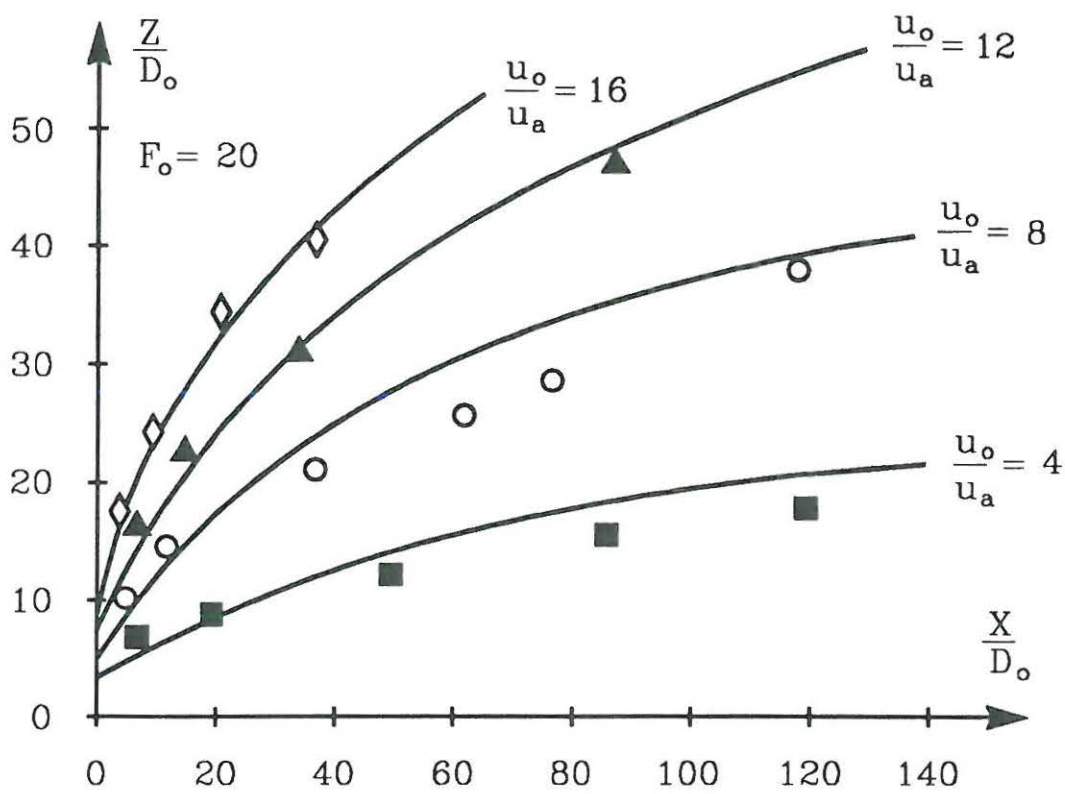
120

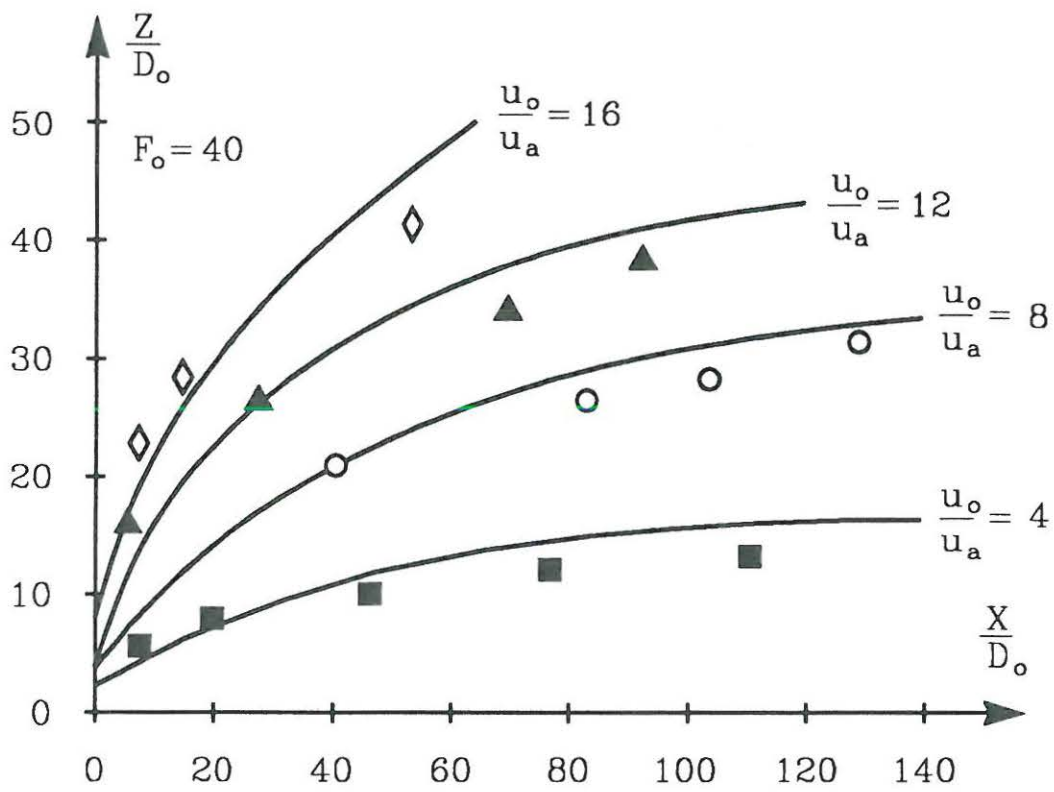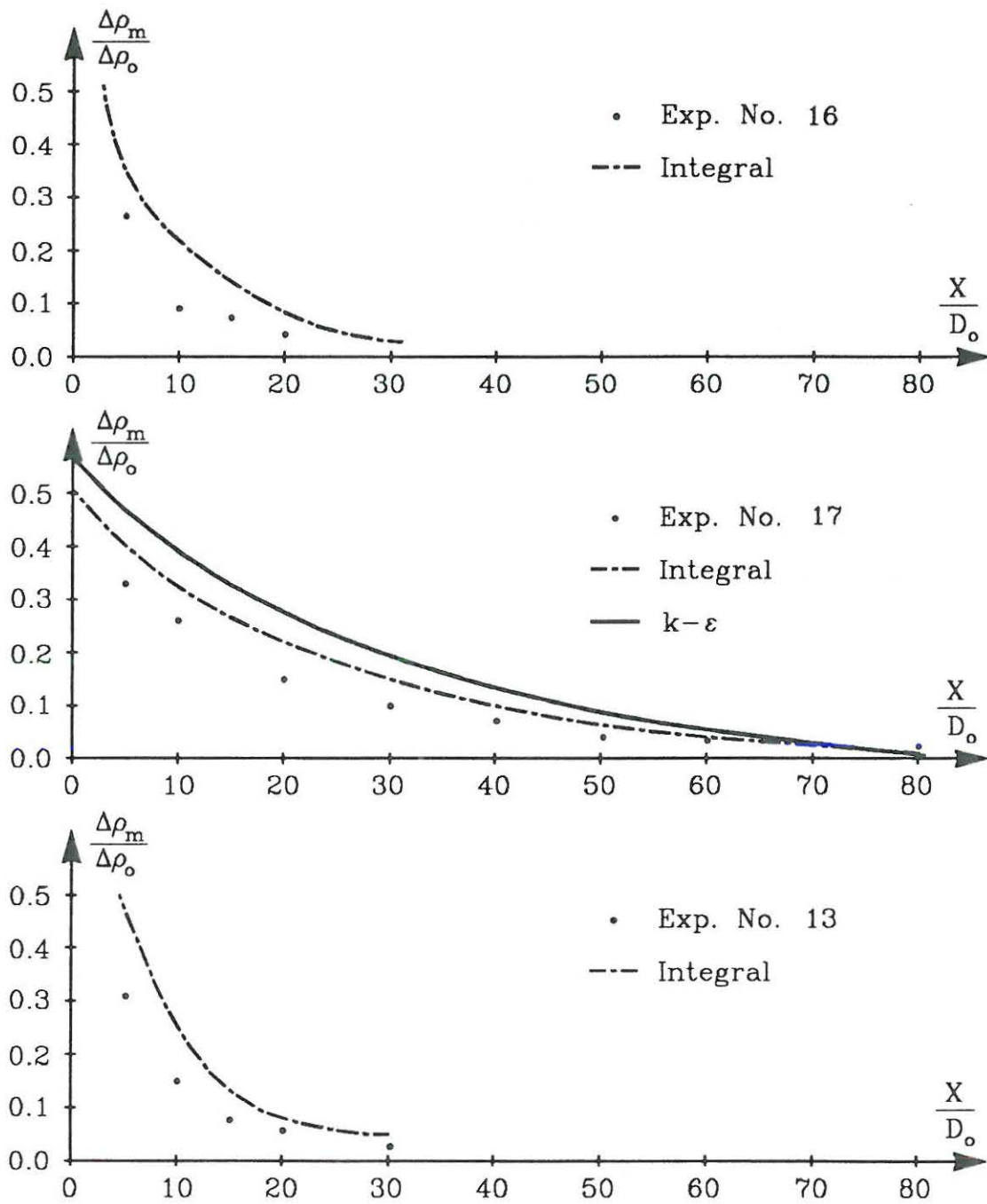Figure 5.6: (a) Prediction and Comparison of Vertical Jet Trajectories in Crossflowing Ambients (Fan's Data)

Figure 5.6 (b) Prediction and Comparison of Vertical Jet Trajectories in Crossflowing Ambients (Fan's Data)

Centerline Density Deficiencies and Concentrations

The predicted jet centerline density deficiencies for horizontal jets in coflowing ambients are plotted in Fig. 5.7 and compared to the experimental data showing that the prediction are in good agreement with the data, with erros in the order of 10 - 20 %. The centerline concentrations for vertical jets in crossflowing environments are simulated and plotted in Fig. 5.8, and compared to the well documented data reported by Fan (1967), with the initial densimetrical Froude number, $F_{\Delta o} = 10$ and 20, and the velocity ratio $K = u_o/u_a = 4 - 16$. It demonstrats that the predictions agreen favaorably well with the laboratory data.

Centerline Velocities

The predicted centerline velocity for horizontal jets in coflowing ambients are shown in Fig. 5.9 and compared with the measurements. It appears that reasonably well simulated results can be obtained by using the mathematical model.

Figure 5.7: (a) Prediction and Comparision of Horizontal Jet Centerline Density Deficiency in Coflowing Ambients

124
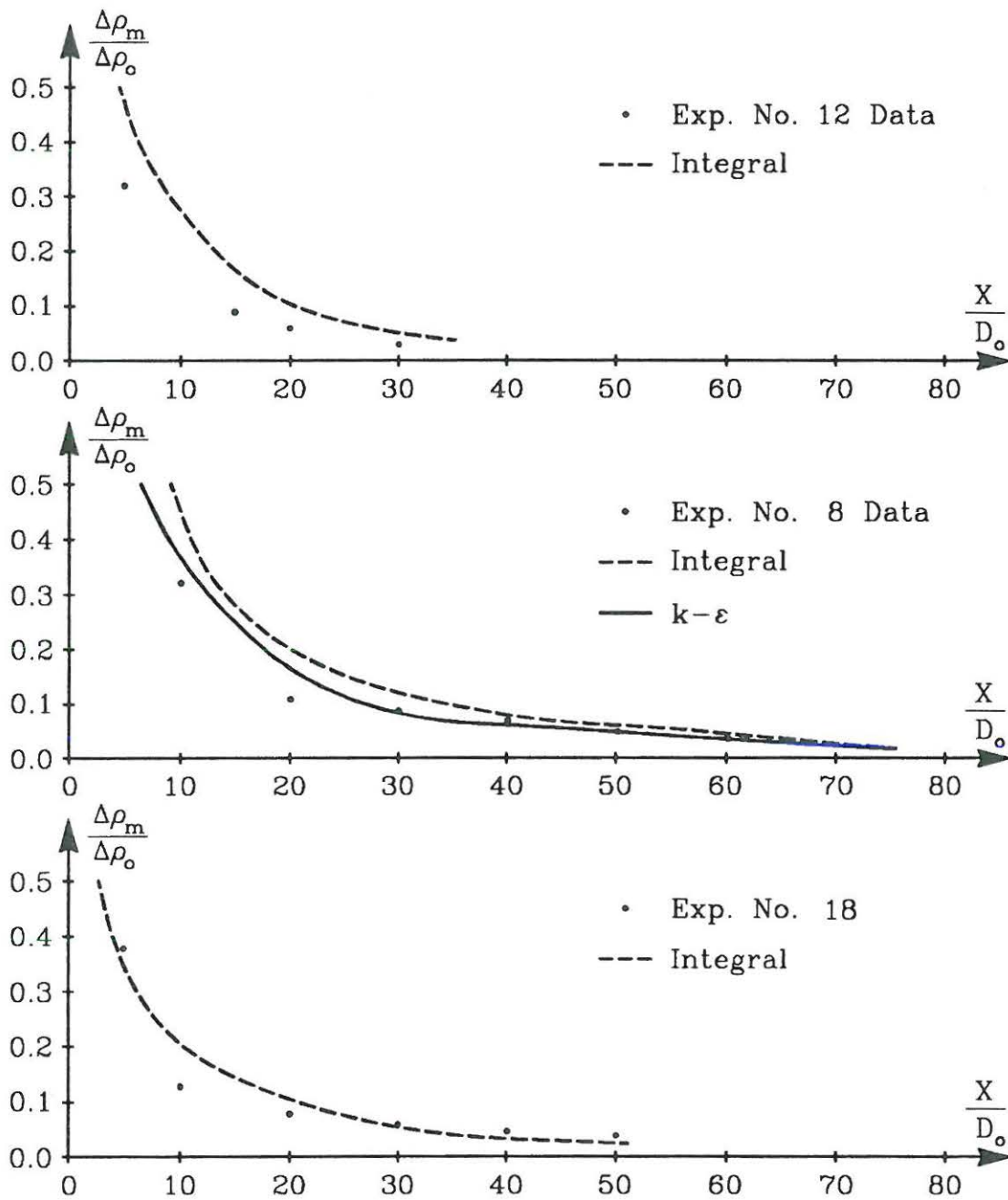
Figure 5.7: (b) Prediction and Comparision of Horizontal Jet Centerline Density Deficiency in Coflowing Ambients

Figure 5.7: (c) Prediction and Comparision of Horizontal Jet Centerline Density Deficiency in Coflowing Ambients
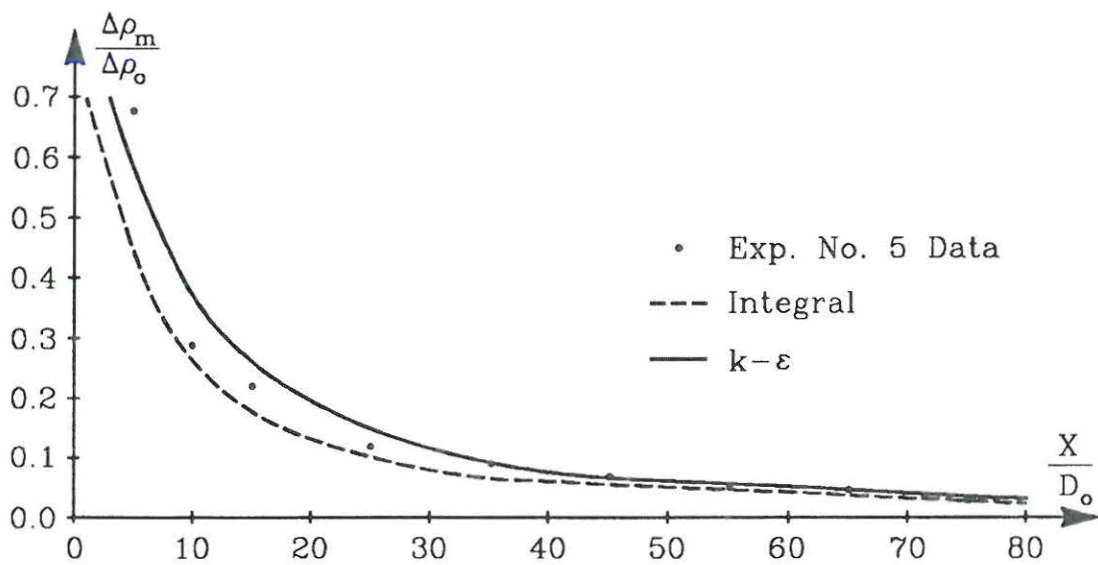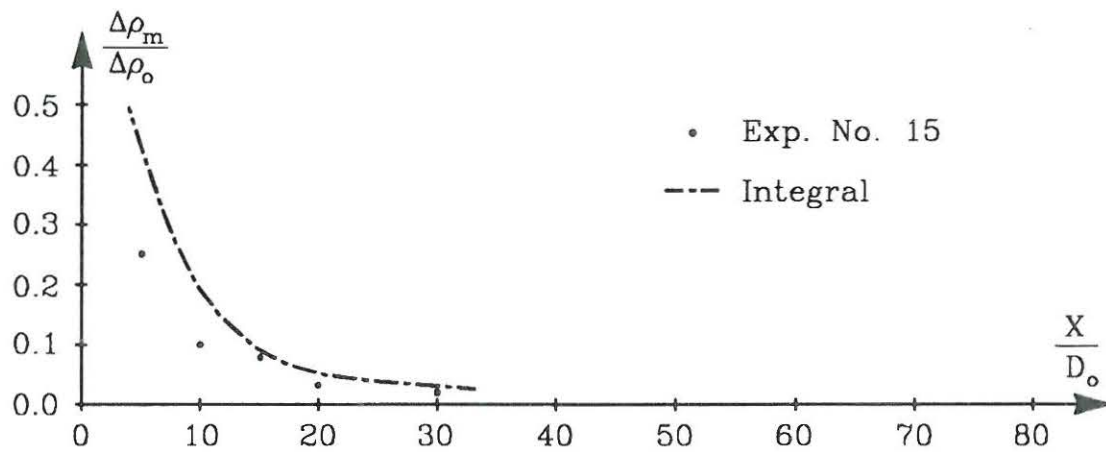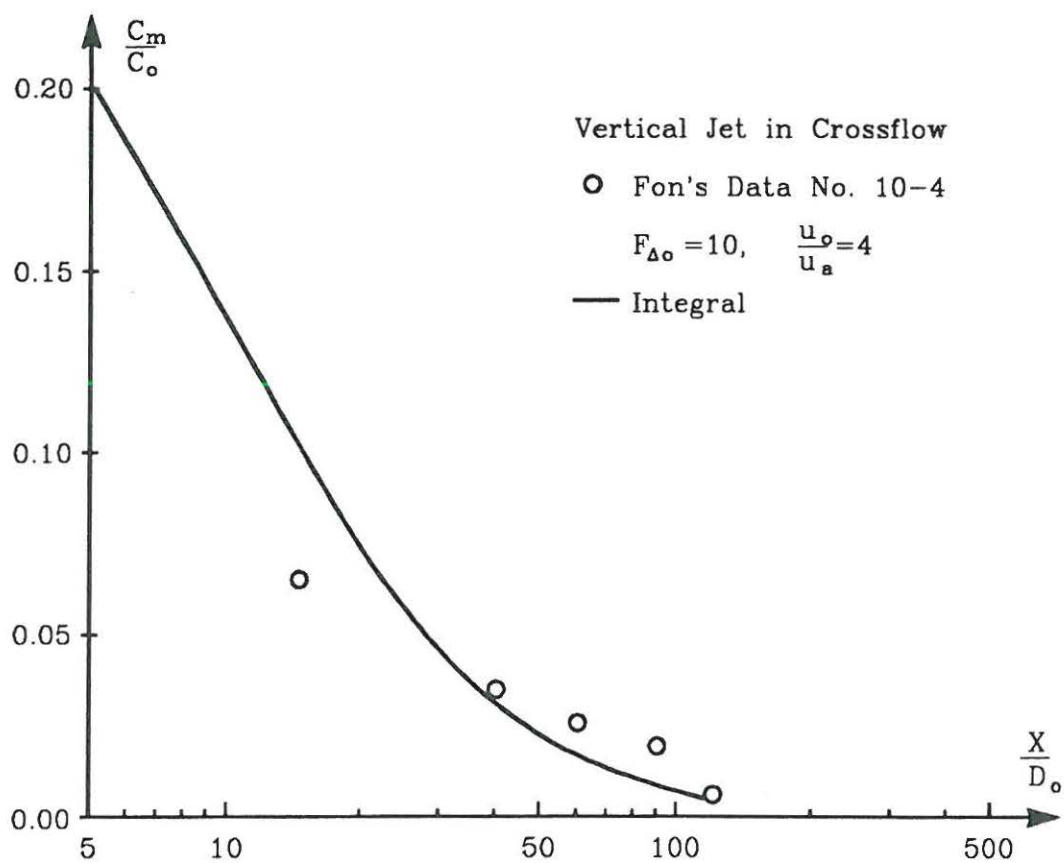
126

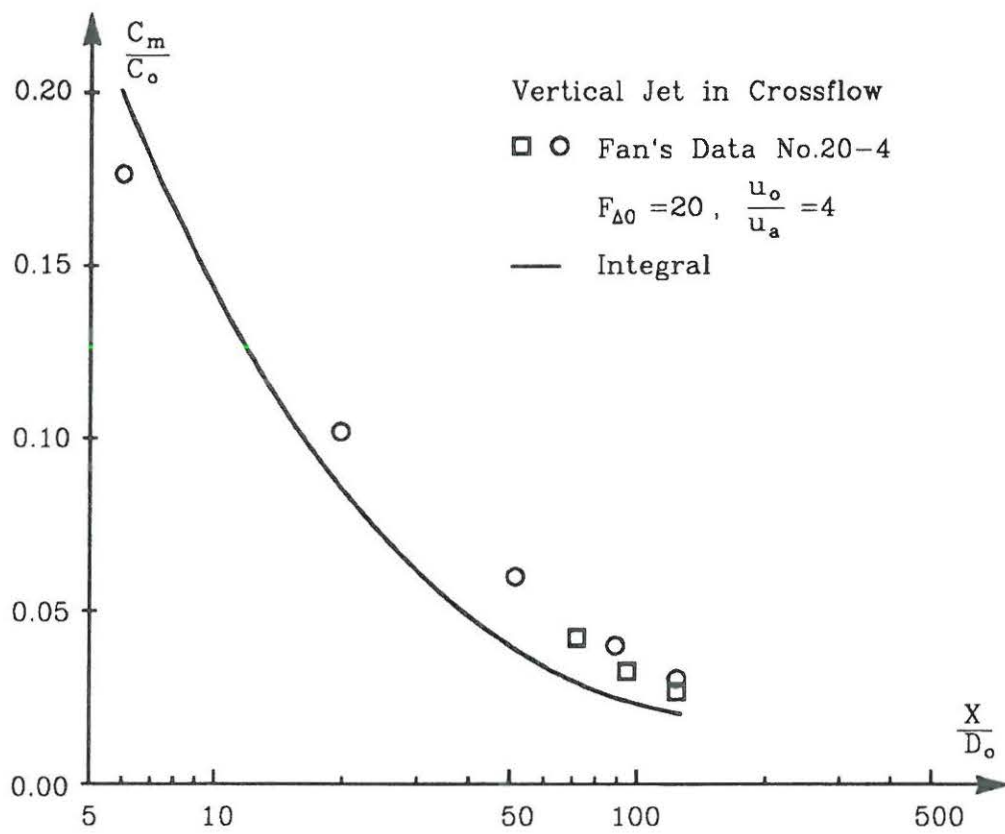Figure 5.8: (a) Prediction and Comparision of Vertical Jet Centerline Concentration in Crossflowing Ambients

127

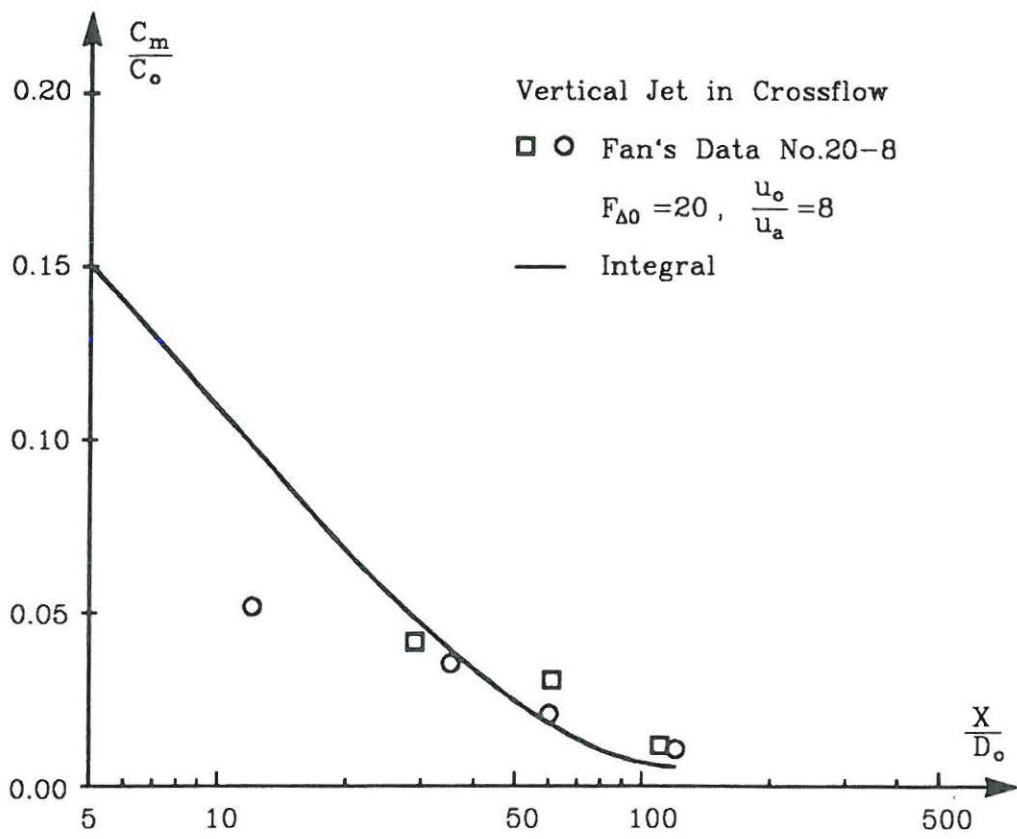Figure 5.8: (b) Prediction and Comparision of Vertical Jet Centerline Concentration in Crossflowing Ambients

128

Figure 5.8: (c) Prediction and Comparision of Vertical Jet Centerline Concentration in Crossflowing Ambients
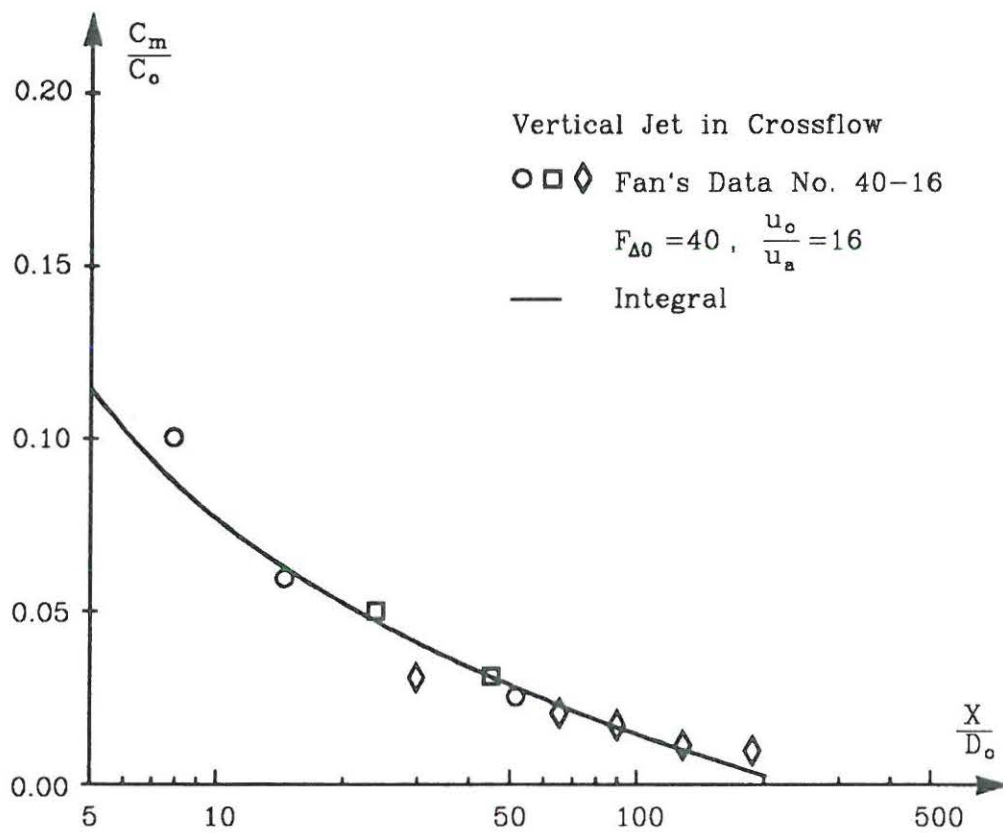
129

Figure 5.8: (d) Prediction and Comparision of Vertical Jet Centerline Concentration in Crossflowing Ambients
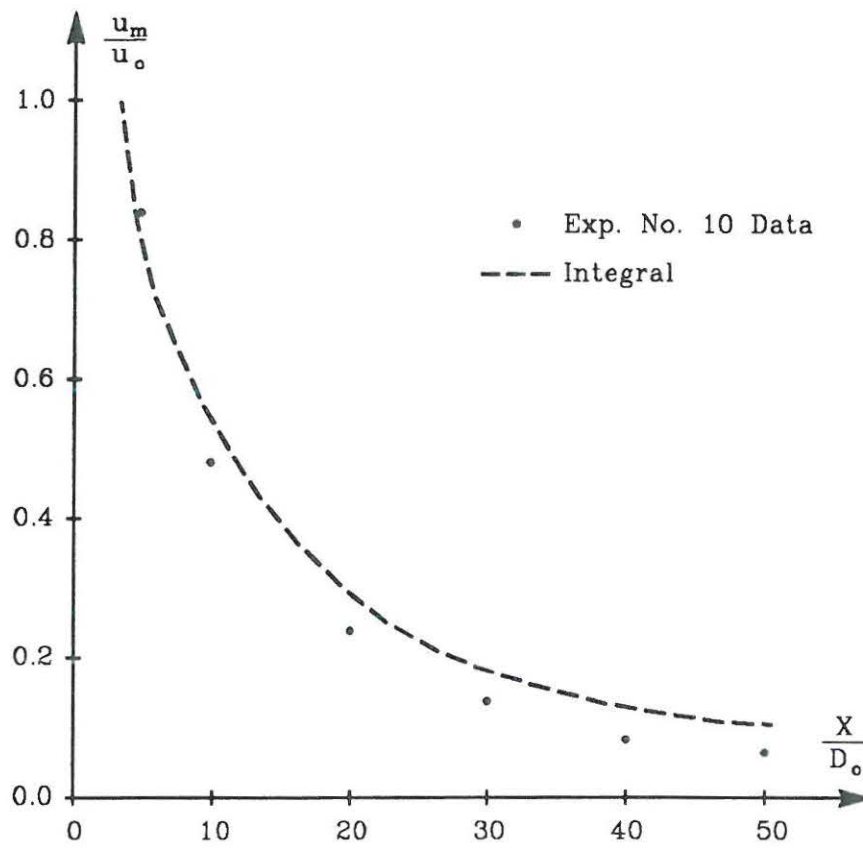
130

Figure 5.9: (a) Prediction and Comparision of Horizontal Jet Centerline Velocities in Coflowing Ambients
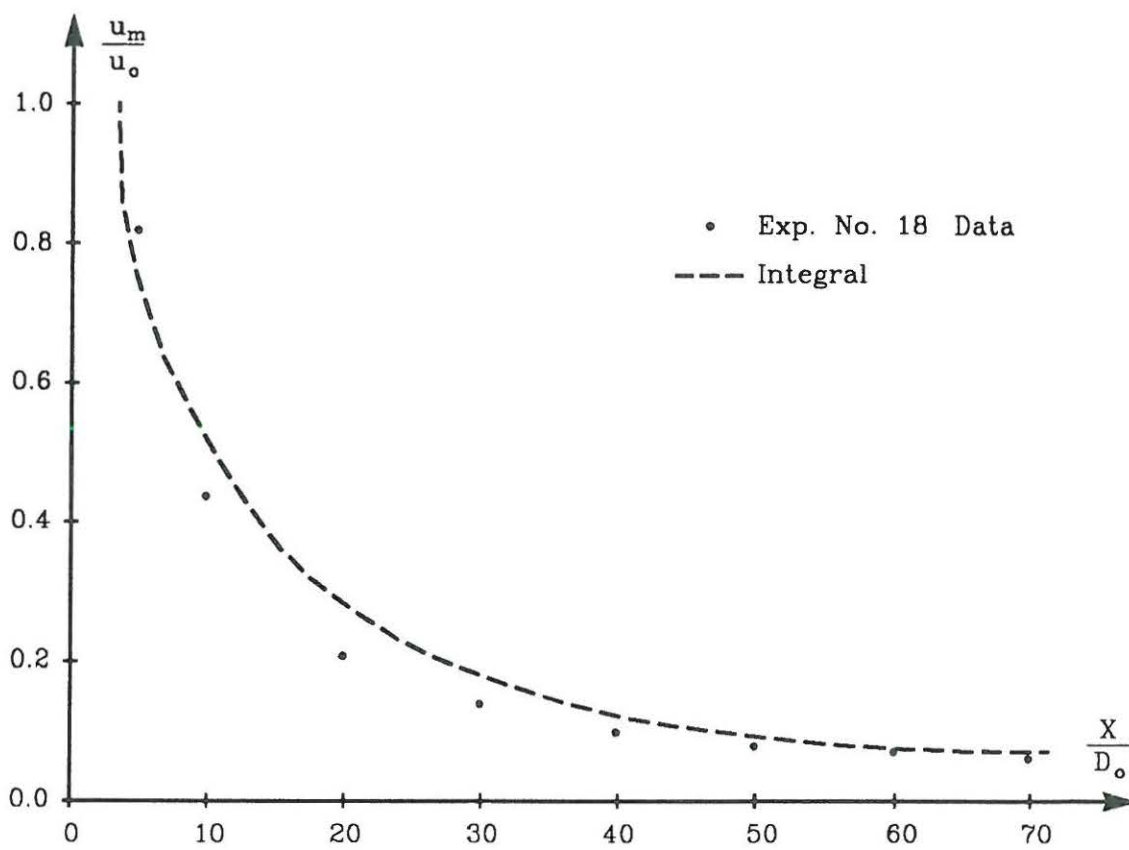
131

Figure 5.9: (b) Prediction and Comparision of Horizontal Jet Centerline Velocities in Coflowing Ambients

5.3.2 $k - \varepsilon$ Model Predictions Compared to Experimental Data

The $k - \varepsilon$ turbulence model based on Launder and Spalding (1974) has been used to predict the turbulent buoyant jets in flowing ambients.

The governing equations for velocity u, v, and w, turbulence properties k and ε and the scalar variables φ are solved by using the programme packege PHONICS developed by the Cham Ltd, U.K. with the variables defined on a staggered grid system. Variations of density are found from a temperature equation and an equation of state. The buondary conditions are prescribed at the walls, upstream, outlet and surface, that is, Walls: u, v, w, k and ε wall functions and $\partial \varphi / \partial n = 0$; Upstream: prescribed by log law; Surface: rigid lid approximation; outlet: $k_o = 0.01 u_o^2$; $\varepsilon_o = k^{3/2} / D_o$.

The predictions were carried out by using the standard $k - \varepsilon$ model since the densimetrical Froude numbers in the runs were not so low as to require a buoyancy extention of the $k - \varepsilon$ model. McGuirk and Spalding (1975). The empirical constants of $c_\mu, c_{1\varepsilon}, c_{2\varepsilon}, \sigma_k, \sigma_\varepsilon$, and σ_t employed in the $k - \varepsilon$ turbulence model are listed in Table. 5.2.

Table 5.2: The Values of Coffients in the $k - \varepsilon$ Model

c_μ	$c_{1\varepsilon}$	$c_{2\varepsilon}$	σ_k	σ_ε	σ_t
0.09	1.44	1.92	1.00	1.30	0.70

Examples of Predictions Compared to Experimental Data

Different cases have been run by using the $k - \varepsilon$ turbulence model. Three Examples of the simulations are presented in comparison with the integral model prediction and the experimental data. In general, It apears

133

that the $k - \varepsilon$ turbulence model is capable of predicting the turbulent buoyant jets in flowing environments with reasonably well results.

Example 1: Horizontal Buoyant Jet in Coflow; Exp. No. 7

The discharging and ambient conditions in Exp. No. 7 are:

$$u_a = 1.7 cm/s; \qquad T_a = 21.0C; \qquad H_a = 30.0cm;$$

$$u_o = 78.6 cm/s; \qquad T_o = 40.0C; \qquad D_o = 1.0cm;$$

The $k - \varepsilon$ turbulence model's predictions for experiment no. 7 are shown in Fig. 5.10. It is shown that the calculated jet trajectory is somewhat longer than the measurement. The predicted jet centerline excess velocity and density deficiency are presented in Fig.5.10 (c) and (d). In addition, a flow pattern predicted by the $k - \varepsilon$ model is demonstrated in Fig. 5.10 (b).
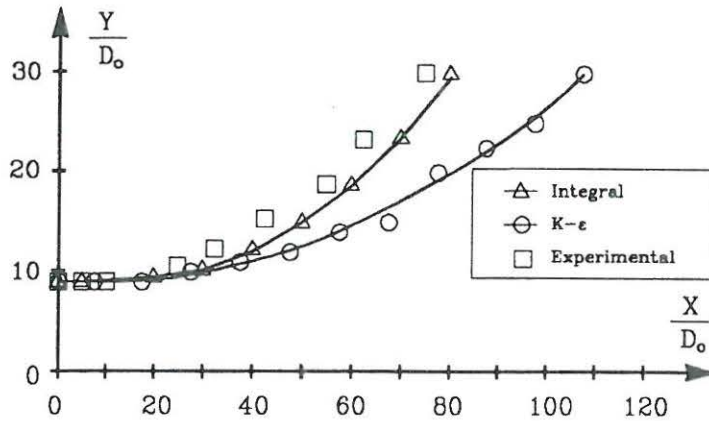
Example 2: Horizontal Buoyant Jet in Coflow; Exp. No. 8

The discharging and ambient conditions in Exp. No. 8 are:

$$u_a = 1.7 cm/s; \qquad T_a = 20.6C; \qquad H_a = 30.0cm;$$

$$u_o = 40.0 cm/s; \qquad T_o = 40.9C; \qquad D_o = 1.0cm;$$

The predicted jet trajectory is shown in Fig. 5.5 (a) and compared with the experimental data. It seems that satisfactory calculations have been obtained. The calculated jet centerline density deficiency by the $k - \varepsilon$ model is presented in Fig. 5.7 (b) in association with the laboratory measuremnets, showing a reasonable prediction.

(a) Jet Trajectory

Figure 5.10: (A) $k - \varepsilon$ model Prediction and Comparison of Exp. No. 7

Example 3: Horizontal Buoyant Jet in Coflow; Exp. No. 17

The discharging and ambient conditions in Exp. No. 17 are:

$$u_a = 1.7cm/s; \qquad T_a = 21.0C; \qquad H_a = 30.0cm;$$

$$u_o = 78.6cm/s; \qquad T_o = 40.0C; \qquad D_o = 1.0cm;$$

The predictions by the $k - \varepsilon$ model of experiment no. 17 on the jet trajectory and centerline density deficiency are plotted in Fig. 5.5 (b) and Fig. 5.7 (a), respectively. It appears that the predictions agree with the experimental data reasonably well.

It is indicated in Figs. 5.7.(a), 5.7.(b) and 5.10 that the $k - \varepsilon$ Model's Predictions of the centerline velocity and density deficiency are somewhat over-estimated, which seems to be a consequence of the lower entrainment coefficient predicted by the $k - \varepsilon$ Model, see Larsen, Petersen and Chen

135

(1990) for explanation. As a result, the trajectories given by the $k - \varepsilon$ Model are also longer than the integral model's predictions, refer to Figs. 5.5.(a), 5.5.(c) and 5.10.(A).
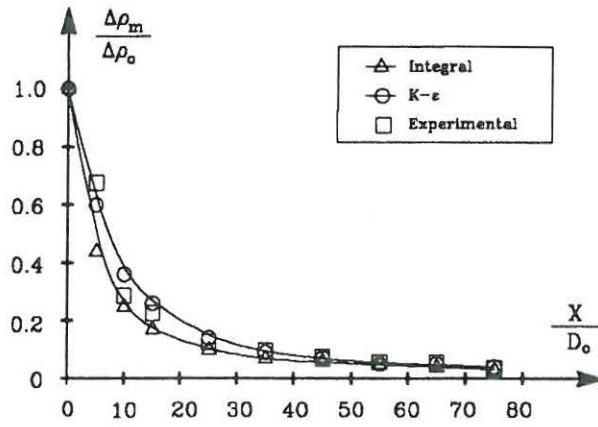
(b) Jet Centerline Density Deficiency
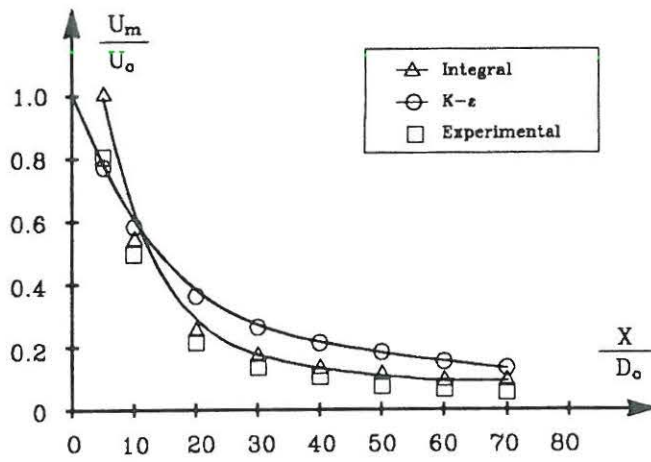
(c) Jet Centerline Velocity

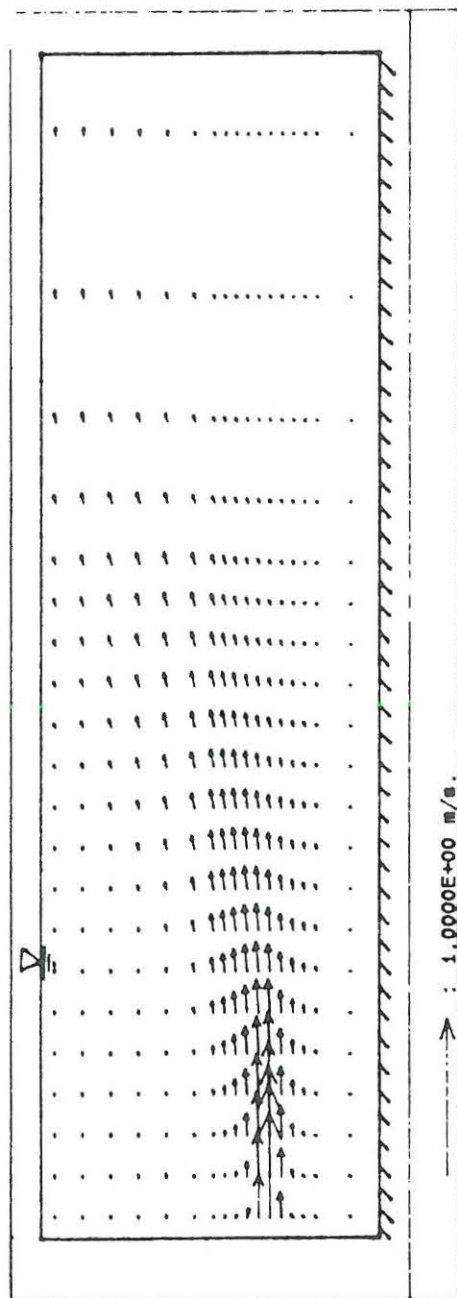Figure 5.10: (B) $k - \varepsilon$ model Prediction and Comparison of Exp. No. 7

Figure 5.10: (C) $k - \varepsilon$ model Predicted Flow Pattern of Exp. No. 7

5.3.3 Disscusion of Entrainment Function

The entrainment function used herein is proposed by Hirst (1972) and stated in Eq.(5.42). It is assumed that the total entrainment rate Q_e is contributed by the shear-induced entrainment and the forced entrainment due to the cross flow by taking the effect of the local buoyancy, the jet trajectory and the jet width into account.

The three coefficents α_1, α_2 and α_3 in Eq.(5.42) are needed to be determined and one could adjust the three coefficents in a way to make the predictions optimized. However this process is highly subjective and nonunique. The other way to solve the problem is to define the first two constants α_1 and α_2 at fixed values based on available experimental data and to adjust the third coefficent α_3 by fitting the experimental results, which has been used herein.

The entrainment coefficents in the integral model are taken the values as shown in Table 5.1. It seems to be difficult to use a constant α_3 to predict the wide range of flow conditions reported here and certainly this is a limitation of the integral model.

It is perhaps interesting to investigate the reasons for the varying coefficent in the entrainment funtion in order to better understand the different terms in the different stages. The first term in Eq.(5.42) can be rewritten as

$$b \mid u_m - u_a sin\theta_1 cos\theta_2 \mid \tag{5.64}$$

representing the shear entrainment due to the velocity difference between the jet velocity and the ambient velocity component parallel to the jet trajectory. It is fair to beleived that in the jet stage, especially in the vinicity of the orifice, u_m dominates the entrainment and the effect of the ambient velocity u_a is comparatively smaller due to the fact that $u_m \gg u_a$ in the near field.

139

The second term in Eq.(5.42) can be rewritten as

$$bu_a\sqrt{1 - sin^2\theta_1 cos^2\theta_2} \tag{5.65}$$

which represents the forced entrainment due to the projected plume area normal to the cross flow. It has been demonstrated by Lee and Cheung (1990) that the forced entrainment should include three contributions as indicated in Eq.(5.44) and rewritten herein for the sake of convinence

$$2bu_a\sqrt{1 - sin^2\theta_1 cos^2\theta_2} + u_a\pi b\Delta b cos\theta_1 cos\theta_2$$
$$+\frac{\pi b^2 u_a}{2}\Delta(cos\theta_1 cos\theta_2) \tag{5.66}$$

The first term represents the forced entrainment due to the projected plume area normal to the cross flow; the second is a correction due to the growth of plume radius; and the third is a correction due to the curvature of the trajectory.

The importance of each term in Eq.(5.66) may be comparied quantitaviely by estimating the order of magnitude of them. In order to simplify the disscusion a jet with two-dimensional trajectory is considered.

For a jet with two-dimensional trajectory ($\theta_1 = 0$) the forced entrainment function can be written as

$$\underbrace{2bu_a\sqrt{1 - cos^2\theta_2}}_{(1)} + \underbrace{u_a\pi b\Delta b cos\theta_2}_{(2)} + \underbrace{\frac{\pi b^2 u_a}{2}\Delta(cos\theta_2)}_{(3)} \tag{5.67}$$

Typically, the orders of the magnitude of each individual variable for a buoyant jet in a flowing ambient are approximately as

140

$$o(b) \approx 10^{-1} \sim 10^1 \ m; \quad o(u_a) \approx 0 \sim 10^0 \ m/s;$$

$$o(cos\theta) \approx 0 \sim 10^0; \quad o(\Delta b) \approx 10^{-2} \sim 10^0 \ m;$$

$$o(\Delta cos\theta) \approx 0 \sim 10^0;$$

subsequently, the orders of magnitude of term (1), (2) and (3) are estimated as

$$Term(1): \quad o(2bu_a\sqrt{1 - cos^2\theta_2}) \approx 0 \sim 2 \times 10^2$$

$$Term(2): \quad o(\pi bu_a\Delta bcos\theta_2) \approx 0 \sim 3.14 \times 10^3$$

$$Term(3): \quad o(\frac{\pi b^2 u_a}{2}\Delta(cos\theta_2)) \approx 0 \sim 5 \times 10^3$$

Frome the estimation of the order of magnitude of each term in the forced entrainment function, it may be concluded that the three contributions are approximately equally important and none of them can be neglected.

It can be seen that the forced entrainment hypothesis proposed by Hirst includes only the first contribution. As pointed out by Frick (1984) that many previous investigators have typically neglected at least one of the three terms; this may be the reason variable entrainment coefficents were required to fit the model predictions to experimental data.

Obviously, one of the solutions to the varying entrainment coefficents may be that all the three contributions in the forced entrainment formular should be included in the model.

141

Chapter 6

Conclusions

Turbulent buoyant jets and plumes in flowing environments have been studied theoretically and experimentally.

1. The turbulent buoyant jets and plumes in flowing ambients are characterized by volume, momentum and buoyancy fluxes and length scales, defined as:

$$Volume\ flux: \qquad Q = \int_A u_o dA$$

$$Momentum\ flux: \qquad M = \int_A u_o^2 dA$$

$$Buoyancy\ flux: \qquad B = \int_A u_o \frac{\Delta \rho}{\rho_a} dA$$

$$Volume\ length\ scale: \qquad L_q = \frac{Q}{M^{1/2}}$$

$$Momentum\ length\ scale: L_m = \frac{M^{3/4}}{B^{1/2}} \quad or \quad L_m = \frac{M^{1/2}}{u_a}$$

$$Buoyancy\ length\ scale: \qquad L_b = \frac{B}{u_a^3}$$

142

2. The basic physical processes for a submerged turbulent buoyant jet released from sea outfall can be divided into four primary stages, namely, zone of flow establishment, stage of jet, stage of intermediate and stage of plume. The stability criteria for upstream wedge introduced by the submerged turbulent buoyant jet can be established by applying the Bernoulli equations for a two-layer flow system and by considering the front velocity driven by the buoyancy force for a three-dimensional problem as described in Chapter 3.

3. It has been found from the experiments that the length of the zone of flow establishment of buoyant jet is shorter than that of pure momentum jet.

4. Comprehensive laboratory experiments have been conducted and the experimental data on jet trajectories and dilutions have been analyzed using dimensionless variables. It has been found that the jet trajectories and dilutions can be successfully correlated using the momentum and buoyancy fluxes and length scales and follow different power laws with various constants, depending upon the types and regimes of the flows. The relations for jet trajectories and dilutions for horizontal buoyant jets in coflows, vertical buoyant jets in crossflows and horizontal buoyant jets in perpendicular crossflows are summarized in Tables 4.5 $\sim$ 4.6.

5. From the experimental results, the flow regimes for a submerged buoyant jet in a homogeneous flowing ambient can be identified with respect to the upstream wedge, i.e. stable upstream wedge ($F_{\Delta s} < 0.3 \sim 0.4$); unstable upstream wedge ($0.4 < F_{\Delta s} < 1.0$); and no upstream wedge ($F_{\Delta s} > 1.0$).

6. The surface plume height can be determined from the stability analysis of the upstream wedge Eq. (3.33) and the relation between the plume width and height may be derivated from the conservation equation of the mass in the intermediate zone as shown in Eq.(3.38). The experimental data on the plume

heights and widths are plotted in Fig. 4.17 ~ 4.18.

7. It has been demonstrated that the dilution within the intermediate zone is of minor importance with the order of 1 ~ 2 times from section A_1 to A_2 in Fig. 3.5.

8. Integral models for turbulent buoyant jets and plumes in flowing ambients with two-dimensional and three-dimensional trajectories have been developed. Mathematical modelling on the buoyant jets in flowing currents using the integral model have been carried out and compared with available experimental data. It has been found that variable entrainment coefficent is required to predict the wide range of flow conditions reported here; it is believed that all the three contributions in the forced entrainment function are equally important and none of them can be neglected.

9. Turbulence model ($k - \varepsilon$) has been adopted to predict turbulent buoyant jets in flowing ambients. The predictions have been made and compared to the experimental measurements. It seems that the turbulence model predicts the turbulent buoyant jets in flowing environments well but needs to be further improved and modified.

144

List of Figures

146

List of Tables

147

LIST OF SYMBOLS

A	:	area;
B	:	buoyancy flux or plume width;
C_i	:	constants; $i = 1, 2, ...n$;
D_o	:	diameter of nozzle;
F_Δ	:	densimetric Froude number;
$F_{\Delta o}$	:	initial densimetric Froude number;
$F_{\Delta s}$	:	surface plume densimetric Froude number;
F_B	:	buoyancy force;
F_D	:	drag force due to ambient current;
F_l	:	local densimetrical Froude number;
H_a	:	ambient water depth;
H_p	:	surface plume height;
I_r	:	integrated turbulence parameter for round jet;
I_s	:	integrated turbulence parameter for slot jet;
I_r	:	unit vector in r direction;
I_s	:	unit vector in s direction;
I_φ	:	unit vector in φ direction;
K	:	time constant in the temperature measurement;
K_{ij}	:	coefficents in Runge-Kutta method;
M	:	momentun flux;
P	:	shear production;
P_d	:	pressure term;
P_{rt}	:	Prandtl number;
Q	:	volume flux;
Q_e	:	entrainment rate;
Q_{ef}	:	forced entrainment rate;
Q_{es}	:	shear entrainment rate;
Q_o	:	outlet discharge;

148

R	:	jet radiurs;
R_e	:	Renolds number;
R_f	:	flux Richarson number;
R_i	:	Richarson number;
R_{il}	:	local Richarson number;
S	:	dilution or salinity;
S_o	:	initial dilution;
T	:	temperature;
T_a	:	ambient water temperature;
T_o	:	initial water temperature;
T_1	:	ambient water temperature before the measuring step;
T_2	:	ambient water temperature after the measuring step;
U	:	velocity in x-direction;
V	:	velocity in y-direction;
$\vec{V}$	:	velocity vector;
W	:	velocity in z-direction;
X	:	coordinate in x-direction;
X_m	:	location of the minimum suface dilution;
Y	:	coordinate in y-direction;
Z	:	coordinate in z-direction;
b	:	width of jet;
b_i	:	width of jet;
b'	:	width of jet core;
c	:	concentration;
c_a	:	ambient concentration;
c_m	:	jet centerline excess concentration;
c_{mi}	:	jet centerline excess concentration;
c_D	:	drag force coefficent;
c_o	:	initial concentration;
c_μ	:	constant in $k - \varepsilon$ model;
$c_{i\varepsilon}$	:	constant in $k - \varepsilon$ model; i=1,2,3;

149

c'	:	concentration fluctuation;
$\bar{c}$	:	mean concentration;
d	:	plume height;
exp	:	e exponential funtion;
f_i	:	functions; i=1,2,3,....n;
g	:	gravitational acceleration;
g'	:	reduced gravitational acceleration; $g' = \Delta\rho/\rho_a g$;
h	:	ambient water depth under the surface plume;
i	:	exponent in dilution coorelation;
j	:	exponent in dilution coorelation;
k	:	turbulent kinetic energy;
k	:	exponent in dilution coorelation;
l	:	exponent in dilution coorelation;
k_1	:	ambient velocity distribution coeffient;
k_2	:	ambient velocity distribution coeffient;
L_b	:	buoyancy length scale;
L_m	:	momentun length scale;
L_q	:	volume length scale;
m	:	exponents in trajectory correlations;
n	:	exponents in trajectory correlations;
p	:	exponents in trajectory correlations;
q	:	exponents in dilution correlations;
r	:	exponents in dilution correlations;
r	:	r coordinate;
r_i	:	radius of curvature; i=1,2;
s	:	coordinate along jet trajectory;
t	:	time;
u	:	velocity in x-direction;
u_a	:	ambient velocity;
u_{ab}	:	bottom ambient velocity;
u_{as}	:	surface ambient velocity;

u_f	:	front velocity;
u_m	:	jet centerline excess velocity;
u_{mi}	:	jet centerline excess velocity at s_i location;
u_o	:	initial jet velocity;
u', v', w'	:	velocity fluctuations;
$\overline{u}$	:	mean velocity in x-direction;
v	:	velocity in y-direction;
$\overline{v}$	:	mean velocity in y-direction;
$\overline{u'v'}, \overline{u'w'}$	:	Renolds stresses;
w	:	velocity in z-direction;
w_g	:	velocity in gravity direction;
$\overline{w}$	:	mean velocity in z-direction;
x	:	coordinate in x-direction;
y	:	coordinate in y-direction;
z	:	coordinate in z-direction;
α	:	entrainment coefficent;
α_i	:	coefficents in entrainment functions; i=1,2,3;
α_r	:	entrainment coefficent for round jet;
α_s	:	entrainment coefficent for slot jet;
β	:	angle in surface plume spreading;
ε	:	turbulent dissipation rate;
ε_m	:	eddy diffusivity for momentum;
ε_n	:	eddy diffusivity for heat;
η	:	surface excess water lever;
θ	:	angle between jet trajectory and y-direction;
θ_i	:	jet angles; i=1,2;
θ_o	:	initial jet discharging angle with refered to y direction;
λ	:	spreading ratio between density and velocity profiles;
μ_t	:	turbulent eddy viscosity;
ν_o	:	viscosity of discharged fluid;
ρ	:	water density;
ρ_a	:	ambient water density;

ρ_{ab}	:	ambient water density at the bottom;
ρ_{as}	:	ambient water density on the surface;
ρ_o	:	initial water density;
Δs	:	space step increasment along jet centerline;
$\Delta \rho$	:	water density deficit;
$\Delta \rho_o$	:	initial water density deficit; $\Delta \rho_o = \rho_a - \rho_o$;
$\Delta \rho_m$	:	Jet centerline excess density deficit;
σ_t	:	Prandtl number;
σ_k	:	Prandtl number;
σ_ε	:	Prandtl number;
φ	:	coordinate in φ direction;
φ'	:	fluctuation of scalar;
Γ_t	:	turbulent dispersion coefficent;
Φ	:	variable of scalars;

subscripts

a	:	ambient value;
b	:	value at bottom;
m	:	centerline value;
o	:	initial value;
s	:	value at surface;

superscripts

-	:	averaged value
'	:	fluctuation

152

REFERENCES

1. Abraham, G. (1963), Jet Diffusion in Stagnant Ambient Fliud, Delft Hy. Lab. pub.No. 29, 183 pp.

2. Abraham, G. (1970), The Flow of Round Buoyant Jets issuing vertically into ambient fluid flowing in a horizontal direction. Proc. of 5th Water Pollution Conf., July-August, 1970, III-15/1 - III-15/7. pub.No. 29, 183 pp.

3. Agg, A.R. (1978), Initial Dilution, Investigations of Sewage Discharges to Some British Coastal Waters, Ch. 6, Tech. Report 99, Water Research Center, Dec.

4. Albertson, M.L., Dai, Y.B., Jensen, R.A. and Rouse, H. (1950), Diffusion of Submerged Jets, Trans. ASCE 115:639-97.

5. ASCE Task Committee (1988), Turbulence Modelling of Surface Water Flow and Transport: Part I,II,III,IV and V, Vol.114, No.9, Sept. J. of Hy. Eng.

6. Ayoub, G.M. (1971), Dispersion of Buoyant Jets in a flowing Ambient Fluid, Ph.D thesis presented to Imperial College, Uni. of London, England.

7. Bennett, N.J. (1981), Initial Dilution: A Practical Study on the Hastings Long Sea Outfalls, Proc. of the Inst. of Civil Eng., Part I, Vol.70, 1981, pp.113-122.

8. Bennett, N.J. (1983), Design of Sea Outfalls - The Lower Limit Concept of Initial Dilution, Tech. Note 354, Proc. of the Inst. of Civil Eng., Part II, Vol.75, pp.113-121.

9. Brooks,N.H. (1973), Dispersion in Hydrologyic and Coastal Environments, Enviro. Prot. Agency Rep. 660/3-73-010, 136

pp. also W.M Keck. Lab. Rep. KH-R-29, Calif. Inst. of Tech.

10. Brooks, N.H. (1980), Synthesis of Stratified Flow Phenomen for Design of outfalls, Second Inter. Symp. on Stratified Flows, Vol.2 pp 809-831, June, Norway.

11. Brooks, N.H. and Koh, R.C.Y. (1965), Discharge of Sewage effluent from a line source into a stratified ocean. XI Congr., IAHR, Paper No. 2.19.

12. Chen, C.J. and Rodi, W. (1975), A Mathematical Model for Stratified Turbulent Flows and Its Application to Buoyant Jets. 16th Congress of IAHR.

13. Chen, C.J. and Rodi, W. (1980), Vertical Turbulent Buoyant Jets: A review of experimental data, Pergamon Press, Oxford.

14. Chen, H.B., Schrøder, H., Pertesen, H.M. and Kongborg, K. (1989), The combination of Near and Far Field Mathematical Modelling of Waster Water Discharges into Receiving Water Bodies, XXIII Congress of IAHR, D-423-428, Aug. 21-25, 1989, Ottawa, Canada.

15. Chen, H.B., Larsen, T. and Petersen, O. (1991), Turbulent Buoyant Jets in Flowing Ambients, to be presented in the International Symposim on Environmental Hydraulics, to be held in Hong Kong, Dec. 16-18.

16. Chu, V.H. (1979), L.N.Fan's DATA on Buoyant Jets in Cross-flow, J. of Hy. Div. ASCE, Vol.105, No. HY5, May, 1979.

17. Chu, V.H. and Goldberg, M.B. (1974), Buoyant Forced-Plumes in Cross Flow, J. of Hy. Div. ASCE, Vol.100, No. HY9, pp1203-1214.

18. Fan, L-N. (1967), Turbulent Buoyant Jets into Stratified or Flowing Ambient Fluids. Calif. Inst. of Tech. June, Report No. KH-R-15.

19. Fan, L-N. and Brooks, N.H. (1966), Discussion of Paper "Horizontal Jets in Stagnant Fluid of Other Density", by G. Abraham, J. of Hy. Div. ASCE 92(2):423-429.

20. Fan, L-N. and Brooks, N.H. (1969), Numerical Solutions of Turbulent Buoyant Jets Problems, W.M Keck. Lab. Rep. KH-R-18, Calif. Inst. of Tech. 104 pp.

21. Fisher et al, (1979), Mixing in the Inland and Coastal Waters, Academic Press, New York.

22. Frick, W.E. (1984), None-empirical Closure of the Plume Equations, Atmos. Envir., 18(4), pp 653-662.

23. Gu, R. and Stefan, H.G. (1988), Analysis of Turbulent Buoyant Jet in Density- stratified Water, J. of Hy. Div. ASCE, Vol. 114, No.4 Aug.

24. Hansen, A.J. and Jensen, P. (1981), Hydrographical and Hydraulic Marine Outfall Design, WHO Coures, Copenhagen.

25. Hirst, E. (1971), Analysis of Round, Turbulent, Buoyant Jets Discharged to Flowing Stratified Ambients, Report 4685, Oak Ridge National Lab.

26. Hirst, E. (1971), Buoyant Jets Discharged into Quiescent Stratified Ambients, J. of Geophysical Research, Vol.76, pp.30.

27. Hirst, E. (1972), Buoyant Jets with three-dimensional Trajectories, J. of Hy. Div. ASCE, Vol.98, No. HY11, pp.1999-2014.

28. Holley, E.R. and Jirka, G.H. (1985), Mixing and Solute Transport in Rivers, Report E-85, U.S Army Engr. Waterways Experiment Station, Vicksburg, Miss.

29. Hoult, D.P., Fay, J.A. and Forney, L.F. (1969), A Theory of Plume rise Compared with Filed Observations, J. of Air Pollution Control Assoc. No.19, pp.585-590.

30. Jirka, G.H. (1982), Turbulent Buoyant Jets in Shallow Fluid Layers, Turbulent Buoyant Jets and Plumes, Edited by W. Rodi, Pergamon Press.

31. Jirka, G.H., Abraham, G. and Harleman, D.R.F. (1975), An Assesment of Techniques for Hydrothermal Prediction, Rep. No. 203, Ralph Parsons Lab. MIT. Cambridge, Mass.

32. Knudsen, M. and Wood, J.R. (1988), Buoyant Horizontal Jets in an Ambient, Flow, Research Report 88-7, Dept. of Civil Eng. Univ. of Canterbury, Canterbury, New Zealand.

33. Koh, and Brooks,N.H. (1975), Fluid mechanics of Waste Water disposal in the Ocean. Ann. Rev. of Fluid Mech. 7:187-211.

34. Larsen, T., Petersen, O. and Chen, H.B. (1990), Numerical Experiment on Turbulent Buoyant Jets in Flowing Ambient, Proc. of the Eigth International Conference on Computational Methods in Water Resources, Venice, Italy, June 11-15.

35. Lakshminarayana, B. (1986), Turbulence Modelling for Complex Shear Flows, Presented as Paper 85-1652 at the AIAA 18th Fluid Dynamics, Plasmadynamics and Lasers Conf., Cincinnati, OH, July 16-18.

36. Launder, B.E. and Spalding, D.B. (1972), Lecture in Mathematical Models of Turbulence, Academic Press, London, New York.

37. Launder, B.E. and Spalding, D.B. (1974), The Numerical Computation of Turbulent Flows, Computer Methods in Appl. Mech. and Eng. 269-289.

38. Lee, J.H-W. and Cheung, V. (1990), Generalized Lagrangian Model for Buoyant Jets in Current, J. of Environ. Eng. ASCE, Vol.116, No.6, Nov./Dec.

39. Lee, S.L. and Emmons, H.W. (1951), A Study of Thermal Convection above a line fire, J. of Fluid Mech. 11:353-68 (1 plate).

40. Lee J.H.W. and Nevill-Jones, P. (1987), Initial Dilution of Horizontal Jet in Crossflow, J. of Hy. Div. Vol.113, No.5, May.

41. List, E.J. (1982), Mechanics of Turbulent Buoyant Jets and Plumes Turbulent Buoyant Jets and Plumes, Edited by W. Rodi, Pergamon Press.

42. List, E.J. and Imberger, J. (1973), Turbulent Entrainment in Buoyant Jets, J. of Hy. Div., ASCE, 99, pp.1461-1474.

43. Markattos, N.C. (1986), The Mathmetical Modelling of Turbulet Flows Appl. Math. Modelling, Vol. 10, June.

44. McGuirk and Spalding, D.B. (1975), Mathematical Modelling of Thermal Pollution in Rivers, Procc. of Int. Conf. on Math. Models for Environ. Problems, Southampto, Sept.

45. Morton, B., Taylor, G.I. and Turner, J.S. (1956), Turbulent Gravitational Convectained and Instantaneous Sources, Proc. R. Soc. London. Ser. A234:1-23.

46. Pedersen, Fl. B. (1980), A Monograph on Turbulent Entrainment and Friction in Two-Layer Stratifited Flow, Series Paper No. 25, April, 1980, ISVA, Tech. Univ. of Denmark.

47. Petersen, O. (1987), Dilution of Buoyant Surface Plumes, Nov. 1987, Hydraulic and Coastal Eng. Lab., Univ. of Aalborg, Denmark.

48. Priestly, C.H.B. (1956), A Working Theory of the Bent-Over Plumes of Hot Gas, Quarterly J. of Royal Meteorological Society, Vol.82, pp. 165-176.

49. Rawn, A.M. and Palmer, H.K. (1930), Predeterming the Extent of Field in Sea Water, Trans. ASCE 94:1036.

50. Rawn, A.M., Bowerman, and Brook, N.H. (1961), Diffusers for Disposal of Sewage in Sea Water, Tran. ASCE 126(III):344-388.

51. Renolds, W.C. (1970), Computation of Turbulent Flows, State-of-the -art, Dept. of Mech. Eng., Stanford Univ., Report MD-27.

52. Robert, C.Y. and Brooks, N.H. (1975), Fluid Mechanics of Waste-Water Disposal in the Ocean.

53. Rodi, W. (1984), Turbulent Models and Their Applications in Hydraulics State-of-the-art paper, IAHR Section on Fundamentals of Division II, Experimental and Math. Fluid Dynamics.

54. Rouse, H., Yih, C.S. and Humphreys, H.W. (1952), Measurements of Entrainment by Axisymmetrical Turbulent Jets, J. Of Fluid Mech. 11:21-32.

55. Schatzmann, M. (1978), The Integral Equations for Round Buoyant Jets in Stratified Flows. J. Applied Math. and Physics (ZAMP), 29, pp. 608-630.

56. Schrøder, H. (1990), " Vandforurening ", edited by Harremöes, P. (in danish).

57. Scorer, R.S. (1958), Natural Aerodynamics, Pergamon Press, Inc., London, England.

58. Weast, R. (1977), CRC Handbook of Chemistry and Physics, the 58th Edition, CRC Press, Inc. 18901 Cranwood Parkway, Cleveland, Ohio 44128.

59. Wright, S.J. (1977), Mean Behavior of Buoyant Jets in a Crossflow, J of Hy. Div, ASCE, 103, Hy5, pp.499-513.